TECHNISCHE UNIVERSITÄT DARMSTADT

Identification and impact of Topoisomerase II β induced DNA double-strand breaks in Glioblastoma multiforme: NMDA-receptor signaling pathway as target structure

Vom Fachbereich Biologie
der Technischen Universität Darmstadt
zur Erlangung des Grades
Doctor rerum naturalium
genehmigte Dissertation

von
Henrik Lutz
geboren am 06.11.1988
in Büdingen

Erstgutachter: Prof. Dr. Bodo Laube
Zweitgutachter: Prof. Dr. Gerhard Thiel

Tag der Einreichung: 02.05.2019
Tag der mündlichen Prüfung: 04.07.2019

Darmstadt 2019

Lutz, Henrik: Identification and impact of Topoisomerase II β induced DNA double-strand breaks in Glioblastoma multiforme: NMDA-receptor signaling pathway as target structure
Darmstadt, Technische Universität Darmstadt,
Jahr der Veröffentlichung der Dissertation auf TUprints: 2019
URN: urn:nbn:de:tuda-tuprints-86783
Tag der mündlichen Prüfung: 04.07.2019

Ehrenwörtliche Erklärung

Ich erkläre hiermit ehrenwörtlich, dass ich die vorliegende Arbeit entsprechend den Regeln guter wissenschaftlicher Praxis selbstständig und ohne unzulässige Hilfe Dritter angefertigt habe.

Sämtliche aus fremden Quellen direkt oder indirekt übernommenen Gedanken sowie sämtliche von Anderen direkt oder indirekt übernommenen Daten, Techniken und Materialien sind als solche kenntlich gemacht. Die Arbeit wurde bisher bei keiner anderen Hochschule zu Prüfungszwecken eingereicht.

Darmstadt, den …….

…….

Contents

1. Summary

Glioblastoma multiforme (GBM) is a highly lethal and incurable cancer of the central nervous system and current therapies are challenged by GBMs invasive growth and chemo-radioresistance. Ca^{2+}-permeable N-Methyl-D-aspartate receptors (NMDARs) are important for synaptic transmission of excitatory neurons and essentially regulate the plasticity of our brain via activation of several NMDAR-dependent signaling pathways. However, NMDARs have been shown to contribute to GBMs malignancy by promoting growth, survival and migration. Although the impact of NMDARs on GBM has been clearly demonstrated, the particular signaling pathways used by GBM are poorly known. The identification of the NMDAR signaling pathways used by GBM cells might therefore help to develop NMDAR-targeted cancer therapies which highly impact GBM cells but do not disrupt synaptic transmission in neurons.

The NMDAR-dependent expression of early-response genes (ERGs) upon neuronal activity is essential for synaptic plasticity and the formation of long term memory. The expression of ERGs depends on NMDAR-induced DNA-double strand breaks (DSBs) in the transcriptional start site of these genes. Some neuronal ERGs encode for proto-oncogenes like *cFos*, suggesting that GBM cells might hijack NMDAR signaling pathways to promote proto-oncogenes expression.

In order to investigate the impact of NMDAR-dependent ERG expression in GBM cells we intended to identify the hallmark of this NMDAR signaling pathway: The induction of NMDAR-dependent and Topoisomerase II β (Top2β) mediated DSBs in GBM cells.

For this task we validated the expression of NMDARs and functional Ca^{2+} signaling in the LN229 GBM cell line, which revealed functional NMDAR signaling in LN229 cells. Immunofluorescence staining of the DSB marker 53BP1 showed that NMDARs activation induces DSBs in a subpopulation of GBM cells and that DSB induction depends on Top2β activity, which demonstrates an analogues NMDAR signaling pathway in GBM cells and neurons.

Analysis of ERG expression revealed that NMDARs, the cAMP-responsive element binding transcription factor (CREB) and Top2β all contribute to the expression of cFos and the brain-derived neurotrophic factor (BDNF) in GBM cells. Inhibition of Top2β or NMDARs also impaired the expression of cFos in a primary GBM cell line. In a clonogenic survival assay knock-down of Top2β with siRNAs and inhibition of NMDARs decreased LN229 cells resistance to X-rays. Additionally, a newly discovered interplay of NMDAR signaling and IR damage response on the expression of BDNF and cFos might explain the high impact of NMDAR inhibition on radiosensitivity. Interestingly, inhibition of DNA-dependent protein kinase indicates that NMDAR-mediated transcription involves factors required in DSB repair, suggesting an important role for DNA repair in NMDAR-mediated transcriptional regulation.

The results presented in this work demonstrate a functional Top2β-dependent NMDAR signaling pathway in GBM cells. The radiosensitizing effect of Top2β and NMDAR inhibition reveals that targeting NMDAR-dependent and Top2β-mediated ERG expression might be a promising strategy for GBM therapy.

2. Zusammenfassung

Glioblastoma multiforme (GBM) ist ein hoch letaler und unheilbarer Krebs des zentralen Nervensystems und sein invasives Wachstum und die Chemo-Radioresistenz stellen eine Herausforderung für die derzeitigen Therapien gegen GBM dar. Ca^{2+}-permeable N-Methyl-D-Aspartat Rezeptoren (NMDARs) sind wichtig für die synaptische Übertragung von exzitatorischen Neuronen und regulieren im Wesentlichen die Plastizität unseres Gehirns durch Aktivierung verschiedener NMDAR-abhängiger Signalwege. Es hat sich jedoch gezeigt, dass NMDARs durch die Förderung von Wachstum, Überleben und Migration zur Malignität von GBM beitragen. Obwohl die Auswirkungen von NMDARs auf GBM eindeutig nachgewiesen wurden, sind die von GBM verwendeten Signalwege im Einzelnen nur wenig bekannt. Die Identifizierung der von GBM-Zellen genutzten NMDAR-Signalwege, könnte daher dabei helfen NMDAR-gerichtete Krebstherapien zu entwickeln, welche stark auf GBM-Zellen wirken, aber die synaptische Übertragung von Neuronen nicht unterbrechen.

Die NMDAR-abhängige Expression von *early response genes* (ERGs) in Folge von neuronaler Aktivität ist essentiell für die synaptische Plastizität und die Bildung von Langzeitgedächtnis. Die Expression von ERGs hängt von NMDAR-induzierten DNA-Doppelstrangbrüchen (DSBs) in der transkriptionellen Startstelle dieser Gene ab. Einige neuronale ERGs kodieren für Protoonkogene wie *cFos*, was darauf hindeutet, dass GBM-Zellen NMDAR Signalwege missbrauchen könnten, um die Expression von Protoonkogenen zu fördern.

Um die Auswirkungen der NMDAR-abhängigen ERG-Expression in GBM-Zellen zu untersuchen, wollten wir das besondere Kennzeichen dieses NMDAR-Signalwegs identifizieren: Die Induktion von NMDAR-abhängigen und Topoisomerase II β (Top2β) vermittelten DSBs in GBM-Zellen.

Für diese Aufgabe haben wir die Expression von NMDARs und funktionelle Ca^{2+}-Signale in der LN229 GBM-Zelllinie validiert, was eine funktionelle NMDAR-Signalweiterleitung in LN229-Zellen ergab. Die Immunfluoreszenzfärbung des DSB-Markers 53BP1 zeigte die Aktivierung von NMDARs-induzierten DSBs in einer Subpopulation von GBM-Zellen und dass die DSB Induktion von der Top2β-Aktivität abhängt, was einen analogen NMDAR-Signalweg in GBM-Zellen und Neuronen zeigt.

Die Analyse der ERG-Expression ergab, dass NMDARs, cAMP-*responsive element binding transcription factor* (CREB) und Top2β alle zur Expression von cFos und dem *brain-derived neurotrophic factor* (BDNF) in GBM-Zellen beitragen. Die Inhibition von Top2β oder NMDARs beeinträchtigte auch die Expression von cFos in einer primären GBM-Zelllinie. In einem klonogenen Überlebensassay verringerte der Knock-down von Top2β mittels siRNAs und die Inhibition von NMDARs die Resistenz von LN229-Zellen gegen Röntgenstrahlen. Zusätzlich könnte ein neu entdecktes Zusammenspiel von NMDAR-Signalweiterleitung und IR-Schadensantwort auf die Expression von BDNF und cFos den hohen Einfluss der NMDAR-Inhibition auf die Strahlungsempfindlichkeit erklären. Interessanterweise

zeigt die Inhibition der DNA-abhängigen Proteinkinase, dass die NMDAR-vermittelte Transkription Faktoren beinhaltet, welche für die DSB-Reparatur erforderlich sind, was auf eine wichtige Rolle der DNA-Reparatur für die NMDAR-vermittelten Transkriptionsregulation hinweist.

Die in dieser Arbeit vorgestellten Ergebnisse zeigen einen funktionellen Top2β-abhängigen NMDAR-Signalweg in GBM-Zellen. Die radiosensibilisierende Wirkung durch die Inhibition von Top2β und NMDAR zeigt, dass die gezielte Inhibition der NMDAR-abhängigen und Top2β-vermittelten ERG-Expression eine vielversprechende Strategie für die GBM-Therapie sein könnte.

3. Introduction

3.1. Glioblastoma multiforme: Characteristics and treatment

Glioblastoma multiforme (GBM) is an incurable cancer and the most common primary brain tumor in adults with an annual incidence rate of 3.2 per 100 000 in the USA. GBMs aggressive growth and poor prognosis classifies it as a WHO grade IV tumor [1, 2]. The median survival of GBM patients is 3 months, which is prolonged to 14.6 months by the current standard therapy consisting of surgical resection, chemotherapy with temozolomide (TMZ) and radiotherapy. However, current therapies are not curative and less than 5% of the patients survive longer than 5 years [3, 4].

Primary GBMs are marked by typical genetic alteration such as epidermal growth factor receptor (EGFR) overexpression, pleiotrophin mutation and loss of chromosome 10, whereas isocitrate dehydrogenase 1 (IDH1) mutations, tumor suppressor TP53 mutations and chromosome 19q loss are more common in secondary GBMs [2]. However, therapeutic targeting of pathways correlated with these typical mutations gave no striking progress for therapy by now [5-7]. Despite typical genetic alteration and resistances, GBM tumors are in fact highly heterogeneous. Surgical multisampling revealed several subclones within a single tumor. Single cell analysis demonstrated that subclones use different signaling pathways and have variable tumorigenety [8]. GBMs heterogeneity is based on different characteristics of subpopulations inside the tumor with variable expression patterns and resistances [8, 9], which makes GBM´s inhomogeneity a major challenge for therapeutic approaches.

The failure to cure or at least control GBM growth is due to the tumors invasive growth as well as high chemo- and radioresistance [10-12]. High radioresistance is characteristic for GBM. During radiotherapy, GBMs are exposed to ionizing radiation (IR), which is capable to detach electrons form atoms or molecules and potentially damages all cellular structures of tumor cells. The main cytotoxic effect of IR depends on the induction of DNA damage or precisely DNA double-strand breaks (DSBs), which in high number induce apoptosis, necrosis or senescence [13]. In conventional GBM radiotherapy the tumor is irradiated with 60 Gy X-rays within 6 weeks applied in 2 Gy fractions, which improves the overall survival of GBM patients but is not curative [14]. GBMs resistance to IR is promoted by an improved DNA damage response. GBM cells show a high DNA repair capacity, induction of cell cycle checkpoints, which stop cell cycle progression for DNA damage repair as well as expression of anti-apoptotic factors [9, 10, 13, 15].

Additional to IR, chemotherapy with TMZ is used to treat GBM. The toxic effect of TMZ on cells depends on the alkylation of nucleobases during replication. The alkylation causes mismatch of DNA base pairs, which results in the formation of DSBs and eventually induces cell death [16]. However, GBM cells have been shown to express O_6-methylguanine DNA methyltransferase (MGMT), a repair protein which mediates resistance towards TMZ [17]. In addition, ATP binding cassette transporters

actively clear chemotherapeutic drugs from the cytosol, further promoting chemoresistance in GBM cells [18].

Beside the strong chemo-and radioresistance GBM treatment is complicated by the typically high invasive growth of GBMs. Even radical resection fails to remove all tumor cells and remaining cells with high tumorigenicity cause fast recurrence of GBM tumors [3]. Because of their highly tumorigenic nature, such cells have been described as tumor initiating cells (TICs) [19, 20]. These TICs represent a subpopulation of cells which play a key role in new therapeutic strategies. Unfortunately, the highly invasive tumorigenic subpopulations of GBM cells exhibit especially high resistances towards radiation and chemotherapeutics [10, 21].

3.1.1. GBM heterogeneity and development

The highly invasive and proliferating TICs can generate cancer cells with different properties and induce tumors which faithfully represent the phenotype of the initial tumor. The proliferation capacity of TICs and the ability to produce GBM cancer cells with different phenotypes led to the terminus of "glioma stem cells" (GSC) which are thought to primarily initiate GBM (**Figure 1a**) [19]. The most favored theory by now is, that GBM stem cells develop through malignant transformation of neural stem cells (NSCs) [19, 22]. In the adult brain, NSCs can be found in so called stem cells niches in the subventricular zone of the lateral ventricle and the subgranular zone of the dentate gyrus [23]. Inside these stem cell niches, NSCs have ability to self-renewal and differentiate which gives rise to progenitor cells. These progenitor cells leave the stem cell niche and differentiate into neurons, astrocytes or oligodendrocytes, the three primary cell types of the central nervous system (CNS) [23]. In mice, it has been shown, that NSCs which carry driver mutations of GBM radially migrate from NSC niches and produce malignant gliomas at distance brain regions [24]. Interestingly, GBM cells have been divided into subpopulations which exhibit expression patterns of neurons, astrocytes and oligodendrocytes [25, 26], including expression of typical marker proteins like oligodendrocyte marker O4 or astrocyte associated glial fibrillary acidic protein (GFAP) [10, 27].

To study TICs *in vitro*, GBM samples can be dissociated and cultured under serum free conditions with the stem cell mitogens epidermal growth factor (EGF) and fibroblast growth factor 2 (FGF2). These culture conditions cause most GBM cells to die, but TICs keep proliferating and form non-adherent spheres, providing a cell culture model enriched in TICs [28]. Upon removal of stem cell mitogens, the sphere culture again produces GBM cells with different phenotypes (**Figure 1b**) [19]. This proposes that GSCs might have the capacity to "differentiate" into heterogeneous GBM cell types, which reflect a partial phenotype of normal brain cells and provide an explanation for the characteristic diversity of GBM tumors.

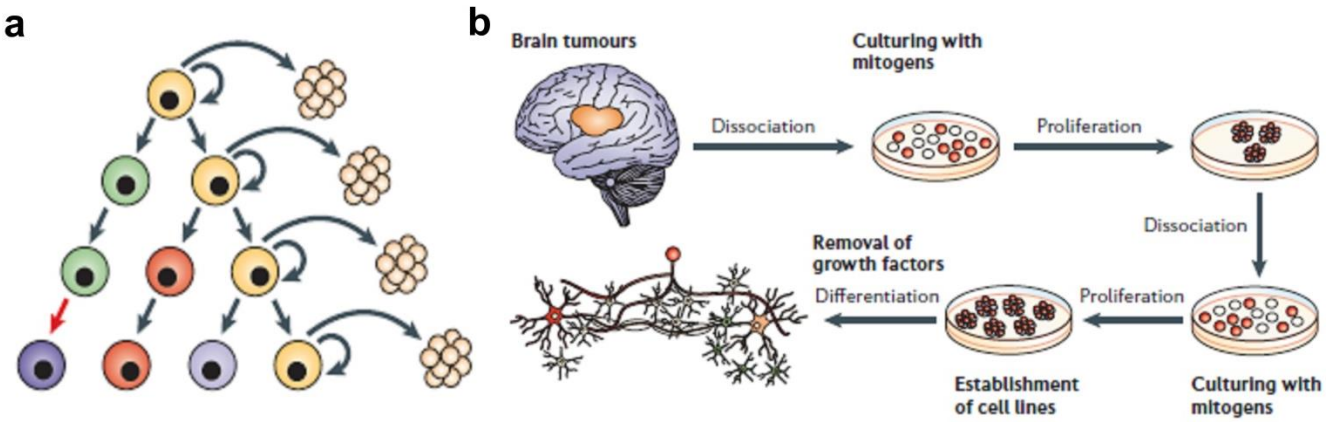

Figure 1: Hierarchical organization of GBM. (a) GBM tumors exhibit a subpopulation of self-renewing and dividing cells (yellow), who produce cancer cell with different phenotypes (green, red, purple), which lost the ability for self-renewal. The dividing subpopulation is highly tumorigenic. **(b)** Dissociated GBM samples form spheroids enriched in TICs when cultured with EGF and FGF2. When GBM spheres are dissociated they keep growing in sphere cultures. Upon growth factor depletion GBM spheres again produce cancer cells with different phenotypes (adopted from Vescovi *et al* [19]).

3.1.2. The role of glutamate in GBM

A specific characteristic of GBM is the active secretion of glutamate (Glu) which accumulates to high concentration ($\sim$250 μM) in the tumors vicinity [29-31]. Glu is a metabolite which is educt and product of many reactions throughout the body, but essentially Glu is the most common excitatory neurotransmitter in the mammalian brain [32]. The physiological activation of glutamate receptors (GluRs) by Glu is besides neuronal signal transmission a key signal for synapses modulation and therefore needed for fundamental cognitive functions such as memory and learning [33, 34]. Pathological activation of GluR in GBM patients interferes normal GluRs signaling and can additionally induce seizures, which cause significant morbidity for patients [35]. On the cellular level, persistent and high concentrations of Glu secreted by GBM tumors induce excitotoxicity in nearby neurons as a result of prolonged GluR activation, causing neuronal tissue to die and providing accruing space for GBM growth [30].

The excitotoxic Glu release of the tumor is mainly mediated via system X^-_c, a cystine/glutamate exchanger, highly expressed in GBM cells [36, 37]. Additionally, GBM cells have low expression of the excitatory amino acid transporters (EAAT) and especially EAAT2, which is responsible for Glu uptake in the brain for example by astrocytes. It has been demonstrated that several primary GBMs as well as GBM cell lines show low expression of EAAT2 and consequently highly decreased Glu uptake compared to astrocytes [36, 38]. This high Glu secretion- low Glu uptake mechanism of GBMs further increases the accumulation of Glu in the tumor vicinity.

The cystine, which is transported into the cell upon Glu release by system $X^-_{c,}$ is used by GBM cells to synthesize glutathione (GSH), a radical scavenger which has been shown to promote growth of GBM cells [39]. The physiological role of cystine in cell growth raised the question, if Glu release has a direct effect on GBM cells or is a byproduct of cystine uptake. The specific effect of Glu on GBMs was shown by Lyons *et al*. in 2007. They used sulfasalazine (SAS) to inhibit the system X^-_c in GBM cells, which decreased secretion of Glu in a dose-dependent manner. It has been demonstrated that SAS treatment and inhibition of GluRs comparably reduce growth and invasion of GBM cells *in vitro,* indicating a direct effect of Glu on GBM signaling and migration. [39, 40]. Hence, GBM-mediated Glu release not only acts on surrounding neurons but also on GBM in an autocrine way.

Glu operates via Ca^{2+} conducting GluRs in GBM cells

As known from neurons glutamatergic signaling can be transmitted via GluRs. Dependent on the intracellular signal transduction GluRs are divided into two types: Metabotropic glutamate receptors (mGluRs) and ionotropic glutamate receptors (iGluRs), which are both expressed in GBM cells [41]. However, especially Ca^{2+} signaling has been shown to be important in GBM cells [42] and Ca^{2+} conducting iGluRs are known to promote proliferation and migration in neuronal cells [43]. Accordingly, it was supposed, that Glu-mediated growth and migration in GBM depends on the activation of Ca^{2+} conducting iGluRs [40].

iGluRs are divided into three groups which are defined by their specific agonist: kainate-receptors, α-amino-3-hydroxy-5-methyl-4-isoxazolepropionic acid receptors (AMPARs) and N-Methyl-D-aspartate-receptors (NMDARs). The role of kainate-receptors on GBM has been neglected, since kainat-receptors typically have very limited permeability for Ca^{2+} [44]. AMPARs show a similar low Ca^{2+} permeability in neurons. The high expression of the AMPAR subunit GluA2, which assembles to Ca^{2+}-impermeable AMPARs, causes the low Ca^{2+}-permeability of neuronal AMPARs. Interestingly, GBM cells have been reported to lack the AMPAR subunit GluA2, resulting in the expression of Ca^{2+} permeable AMPARs in GBM [40, 45] and blockage of AMPARs slowed the migration of GBM cells [46].

Anyhow, the iGluRs with the highest conductance for Ca^{2+} are NMDARs. In contrast to fast desensitizing AMPARs, NMDARs allow a prolonged influx of Ca^{2+} upon activation, which is known to be essential for downstream genomic regulation in neurons [43]. The expression of NMDARs has been reported not only in GBM cells but in many other cancers as well [47-54], indicating that NMDAR expression may be implicated in the signaling of various cancers types.

3.2. N-Methyl-D-aspartate-receptor: Structure and function

NMDARs play a key role in synaptic transmission and therefore are highly expressed throughout the brain. All known NMDARs are heterotetrameric assemblies, which are composed of two essential GluN1 subunits and varying contributions of two GluN2A-D subunits or GluN3A-B subunits [43, 44, 55]. In the brain, GluN1 mostly assembles with GluN2A or GluN2B. The assembled channel pore is selective for cations with high permeability for Ca^{2+} and lower permeability for Na^{+} and K^{+}. An unique property which distinguishes NMDARs from other iGluRs is that channel opening needs binding of two different ligands [56]. The fist ligand is glycine (Gly) or D-serine, which binds to the GluN1 subunit while the second ligand Glu binds to GluN2 subunits [43]. In order to activate synaptic NMDARs the transient release of Glu is sufficient, while the extracellular Gly concentration is constantly high enough to activate NMDARs [43, 57].

Each NMDAR subunit consists of four domains: The extracellular amino-terminal domain (ATD) plays an important role in receptor assembly and binds allosteric modulators like ifenprodil. The agonist binding domain (ABD) consists of two polypeptide sequences (S1 and S2 **Figure 2b**). These sequences form two lobes (upper lobe D1, lower lobe D2 **Figure 2b**) with a cleft in between, in which the ligand binds. The transmembrane domain (TMD) consists of three transmembrane helices (M1, M3 and M4) and the reentrance loop (M2). They form the channel pore which is the target of channel blockers like MK801. The intracellular carboxyl-terminal domain (CTD) binds scaffold and signaling proteins which are associated with NMDARs, like PSD-95 and calmodulin [43]. In addition, the CTD is subject to phosphorylation modulating NMDARs trafficking and currents [58].

GluN2A/B subunits are typical for synaptic NMDARs in the forebrain with slightly different properties than GluN2C/D containing NMDARs. GluN2A/B ligand affinity, for example, is relatively low with a concentration for half maximal activation (EC_{50}) of $\sim 2\,\mu$M Glu [59] while GluN2C/D have a higher affinity for Glu but a lower open probability. NMDARs containing GluN2B and especially GluN2A have a higher open probability, resulting in an increased Ca^{2+} conductance [43]. These GluN2A/B containing receptors also show the highest sensitivity for Mg^{2+} blockage [60], which is a characteristic property of NMDARs.

At the resting membrane potential of neurons (~-70 mV), the channel pore of NMDARs is blocked by Mg^{2+}. This block relieves as the membrane depolarizes and can be removed by depolarization of membrane potential to ~-20 mV. To overcome this ion-block, NMDARs are expressed together with AMPARs at synapses. Upon presynaptic Glu release, AMPAR activation first depolarizes the membrane, which resolves the Mg^{2+} block in NMDARs. Then NMDARs channel open, allowing Ca^{2+} to enter the cell [43]. The highly increased intracellular Ca^{2+} concentration is a second messenger signal for further neuronal signaling as gene activation and subsequently physiological adaptions. In neurons, NMDAR-mediated Ca^{2+} influx regulates a vast number of genes [61], promoting survival, migration,

proliferation and synaptic plasticity [34, 43, 62-64], which makes NMDAR activation indispensable for neurons.

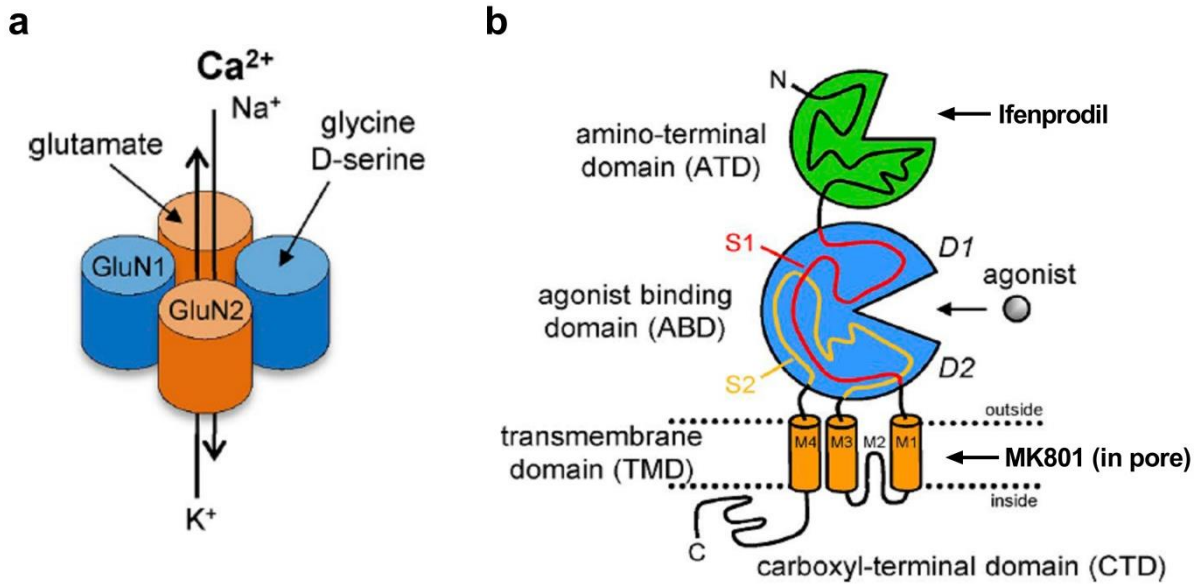

Figure 2: Assembly and structure of NMDARs. (a) NMDARs are tetramers classically consisting of two GluN1 subunits, which bind glycine and D-serine (blue) and two GluN2 subunits, which bind Glu (orange). Both agonists must bind for channel opening, allowing the channel pore to conduct cations like Ca^{2+}, Na^{+} and K^{+}. **(b)** NMDAR subunits have four major domains: The amino-terminal domain (green), which binds allosteric modulators of the channel like ifenprodil. The agonist binding domain (blue) consists of the polypeptide sequence between ATD and M1 transmembrane domain (upper lobe, S1) and the polypeptide sequence between M3 and M4 transmembrane domains (lower lobe, S2). The agonist-binding site is located in the cleft between the two lobes. The transmembrane domain (orange) builds the channel pore through the membrane and consists of three transmembrane helices (M1, M2, and M4) and a membrane reentrance loop (M2). The channel pore is the target of channel blockers like MK801. The intracellular carboxyl-terminal domain binds scaffold and signaling proteins (Figure adopted from Hansen *et al.* [43]).

3.2.1. The role of NMDARs in cancer

The function of NMDARs in synaptic transmission has been investigated for a long time, but NMDAR expression is not restricted to neurons. In fact, NMDAR can be found in cells and tissues from all germ layers including pancreatic islet cells, bone cells, epithelial cells, keratinocytes, the urogenital tract and the cardiovascular system [65-70], demonstrating the importance of NMDAR signaling beyond synaptic transmission. Based on these findings, it is not surprising that primary brain tumors are not the only cancers which express NMDARs. A broad variety of cancer types have been reported to express NMDARs [47, 48]. In addition, Glu secretion has been demonstrated in other tumors beside GBM [31, 50, 71], providing the base for a functional signaling circuit.

In 2001, Rzeski *et al.* reported that MK801, a specific NMDAR inhibitor, limits the growth of several human cancer cell lines including neuroblastoma, thyroid carcinoma, colon adenocarcinoma, breast carcinoma and lung carcinoma *in vitro* and thus suggested functional NMDAR expression in many

cancers [72]. Subsequent works confirmed the expression of NMDARs in several cancer cell lines as well the anti-proliferative effect of NMDAR inhibitors [49, 52-54, 73]. Additionally, the potential therapeutic value of NMDAR inhibition was demonstrated when the *in vivo* growth of tumor xenografts in mice was limited for small-cell lung cancer and breast cancer cell lines upon MK801 treatment [52, 53]. Immunohistological staining proposed a correlation of NMDAR expression and high tumor grade in breast and prostate cancer [49, 53] as well as in glioma [50], suggesting that NMDAR expression might support tumor malignancy.

qPCR profiling of 13 cancer cell lines revealed that all tested cell lines expressed mRNAs coding for NMDAR subunits and only three cell lines lacked expression of the essential GluN1. NMDAR subunits were differently expressed in the cell lines. While GluN2B and GluN2C subunits were transcribed in all cell lines the GluN2A was missing in a neuroblastoma (SK-NA-S) and thyroid carcinoma (FTC 238) [47]. The varying NMDAR composition might define the role of NMDARs in cancer cells. For example, increased proliferation upon NMDAR activation has been reported in the GluN2B deficient gastric cancer cell line MKN45. The authors could show the ability of GluN2A containing NMDARs to promote proliferation by knocking down GluN2A with siRNA [54]. Furthermore, GluN2B is thought to be a tumor suppressor which is epigenetically downregulated in human esophageal cancer [74]. On the other hand, the GluN2B specific antagonist ifenprodil was equally potent to reduce the viability of small-cell lung cancer cells (H345 and H82) as MK801, which demonstrates the impact of the GluN2B subunit on proliferation in the tested cell lines [52]. Ifenprodil also decreased the proliferation and migration of LN229 GBM cells [73], which is in line with the observations of Li and Hanahan, who claimed that GluN2B promotes migration and invasion in several cancers including GBM. Invasion of tumor cells into healthy tissue displays a major problem for therapies. GBM patients with tumors expressing the GluN2B subunit and consequently higher invasiveness indeed had a significantly decreased survival [50, 75]. The bivalent role of GluN2B in different cancers shows that NMDAR subunit composition does not solely define the effect of NMDAR activation in cancer and that cancerous NMDAR signaling is complex.

The fact that NMDAR signaling has various effects in different cells is also demonstrated by the paradox role of Glu in GBM tumors. On the one hand, activation of NMDARs with pathological concentration of Glu leads to epilepsy and neuronal cell death in GBM patients via the activation of NMDARs and AMPARs. At the same time, Glu activates NMDARs in GBM cells and promotes survival, proliferation and migration (**Figure 3**) [50, 73, 76]. This shows that NMDARs do not have a distinct function but can promote opposing cellular effects.

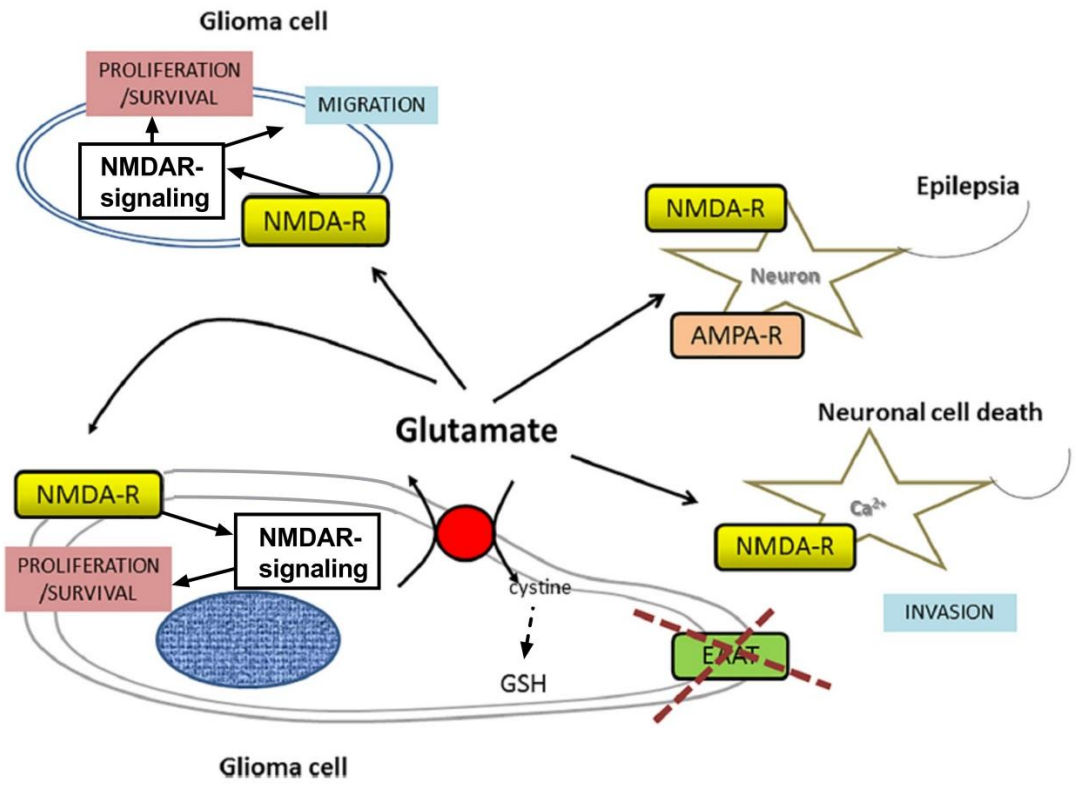

Figure 3: Pathological release of Glu by GBM effects neurons and GBM cells via NMDARs. GBM cells secrete Glu via the cystine/glutamate exchanger system X_c^-. Cystine is used for glutathione (GSH) synthesis and Glu accumulates in the extracellular space, because reuptake of Glu via EAAT transporters is downregulated in GBM cells. Glu acts autocrine and paracrine on GBM cells and neurons. Uncontrolled activation of NMDARs and AMPARs in neurons leads to epilepsy and neuronal cell death through excitotoxicity. NMDAR signaling promotes proliferation, survival and migration/invasion in GBM cells upon NMDAR activation (Figure adapted and changed from Lefranc *et al.* 2018 [76]).

3.2.2. NMDAR signaling in neurons and cancer

The effect of NMDAR activation depends on intracellular signaling

NMDAR-mediated Ca^{2+}-influx can induce both, neuronal survival and death. While the activity of synaptic NMDARs is known to promote survival, the activation of extrasynaptic NMDARs primarily promotes apoptosis, indicating that the receptors localization defines the effect of NMDAR activation.
Ca^{2+}-induced apoptosis in neurons depends on the cytosolic concentration of Ca^{2+} [77]. Extensive accumulation of cytosolic Ca^{2+} leads to the depolarization of the mitochondrial membrane due to Ca^{2+}-uptake into the mitochondria. This Ca^{2+} overload induces swelling of mitochondria which results in rupture of the outer membrane and release of apoptotic factors like cytochrome c and apoptosis inducing factor (AIF) [78].
The induction of apoptosis is a direct result of high Ca^{2+}-influx upon NMDAR activation, while activation of other signaling pathways, like the ERK1/2 or CaMKIV pathway, depend on the connection of receptor and intracellular proteins [79]. At the synapse, NMDARs are bound to scaffold proteins of

the postsynaptic density, including membrane-associated guanylate kinases (MAGUK) like PSD-95 and guanylate kinase-associated protein (GKAP) which are known to bind intracellular signal transducing proteins [80, 81]. The proximity of NMDARs and signaling proteins then allows activation of preferential signaling pathways and also effective buffering of intracellular Ca^{2+} [79].

In newborn rats, the GluN2B subunit is highly expressed in the forebrain. During the first weeks of life, the expression of the GluN2B slowly declines, while the expression of the GluN2A subunit increases, indicating that GluN2B expression is especially important for brain development [82, 83]. The observation led to the propose that GluN2A subunits mainly mediate synaptic NMDAR signaling in mature neurons, while GluN2B subunits were thought to promote extrasynaptic signaling [82, 84]. Anyhow, GluN2A and GluN2B are both located at synapses and therefore contribute to synaptic signaling in neurons, promoting survival and synaptic plasticity [83, 85].

Neuronal survival upon synaptic NMDARs activation is mainly mediated by cAMP response element-binding protein (CREB). CREB activation in turn is known to be regulated by two different signaling pathways upon NMDAR activation: The Ca^{2+}/calmodulin kinase IV (CaMKIV) pathway and the extracellular signal-regulated kinases (ERK) pathway. CaMKIV is activated upon binding of Ca^{2+}/calmodulin and phosphorylates CREB at Ser133 and also the CREB cofactor CREB-binding protein (CBP). Both phosphorylations lead to the activation of CREB, allowing it to promote transcription (**Figure 4Aa/Ac)** [79]. CaMKIV-mediated CREB activation is a fast but short-lasting process and mediates fast response to NMDAR signaling. Longer lasting activation of CREB is mediated by the ERK1/2 [86]. In order to promote ERK1/2-dependent CREB phosphorylation, Ca^{2+}/calmodulin activates the Ras-specific GDP/GTP exchange factor RasGRF1 which activates Ras. Activated Ras-GTP binds to Raf which triggers downstream kinases, resulting in the activation of ERK1/2 (**Figure 4Ab**). Additionally, Ca^{2+}/calmodulin activates calcineurin, a phosphatase which dephosphorylates transducer of regulated CREB activity (TORC). The dephosphorylated form of TORC is imported into the nucleus where assists CREB-dependent gene regulation (**Figure 4Ad**) [79].

Activation of extrasynaptic NMDARs in turn hinders CREB activation by inhibiting ERK1/2 (**Figure 4Ae**). In addition, extrasynaptic NMDARs mediate dephosphorylation of CREB via the juxtasynaptic attractor of caldendrin on dendritic boutons protein (Jacob), which is translocated into the nucleus upon activation of extrasynaptic NMDARs (**Figure 4Af**) [79].

NMDAR-mediated survival not only depends on the expression of survival factor but also on the inhibition of apoptotic factors. In this case, Ca^{2+}/calmodulin activates phosphoinositide-3-kinase (PI3K) [87] which subsequently results in the phosphorylation of Akt. Then Akt phosphorylates factor forkhead box protein O 1 and 3 (FOXO1/3), which triggers the transcription of apoptotic factors like Bim, Fasl and Txnip. Upon phosphorylation FOXO1/3 is translocated into the cytoplasm which disrupts its activity. Contrary, activation of extrasynaptic NMDARs mediates the nuclear import of FOXO1/3 (**Figure 4Bb**), which in turn can be inhibited by synaptic NMDARs (**Figure 4Bc**) [79]. Additionally,

Akt has been reported to activate CREB as well, which further emphasizes the central role of CREB activation for NMDAR-mediated survival in neurons [88].

Taken together NMDAR activation is an important initiating signal of varying cellular pathways depending on the intracellular signaling in neurons.

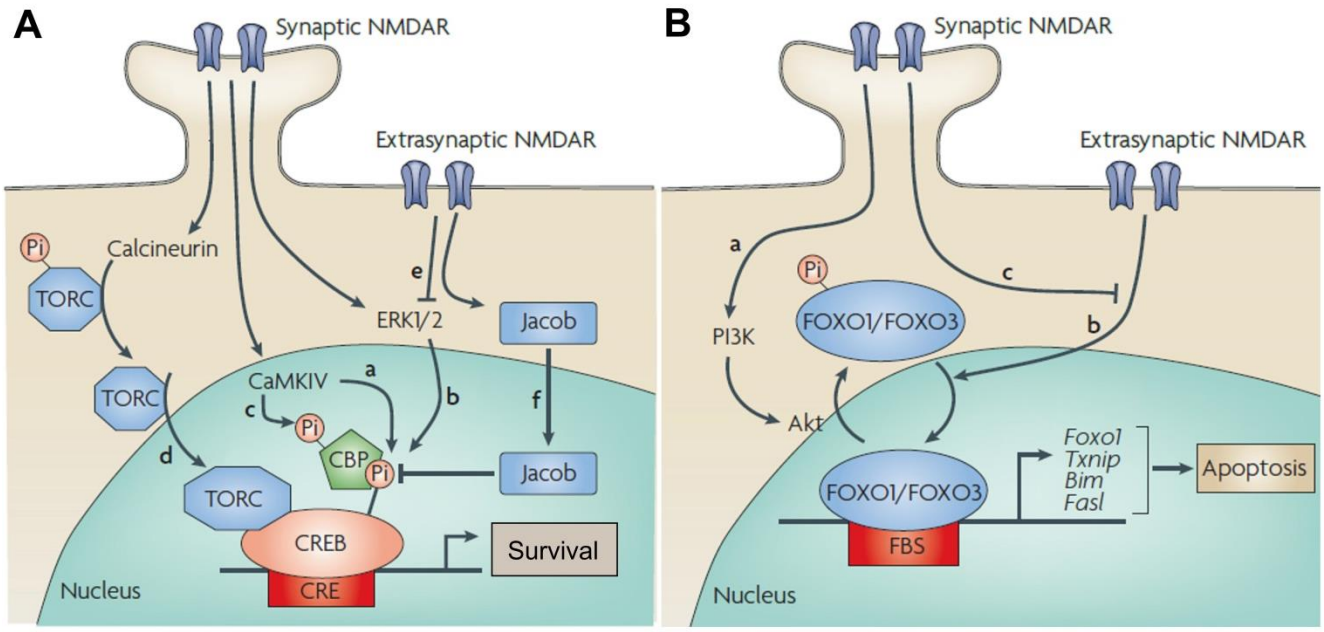

Figure 4: Opposing effects of synaptic and extrasynaptic NMDARs via differential signaling. (A) Activity of synaptic NMDARs leads to the activation of CaMKIV and ERK1/2, which both phosphorylate CREB at Ser133 **(Aa/Ab)**. CaMKIV also phosphorylates CBP, a cofactor of CREB, at Ser301 **(Ac)**. Both phosphorylations activate CREB which initiates the transcription of pro-survival genes. Additionally, Ca^{2+}-influx upon activation of synaptic NMDARs mediates the nuclear transport of TORC via dephosphorylation by calcineurin **(Ad)**, which is an important step in CREB activation. Activation of extrasynaptic NMDARs inhibits ERK1/2 **(Ae)** and mediates the nuclear translocation of Jacob **(Af)**, which promotes CREB dephosphorylation. **(B)** Synaptic NMDARs can activate the PI3K/Akt pathway, which induces the export of FOXO1/3 via phosphorylation **(Ba)**. FOXO promotes the transcription of pro-apoptotic factors like Foxo1, Txnip, Bim and Fasl. Activation of extrasynaptic NMDARs mediates the nuclear import of FOXO1/3 **(Bb)**, which can be inhibited by synaptic NMDAR activity **(Bc)** (adopted form Hardingham and Bading 2010 [79]).

Cancer cells use neuronal NMDAR signaling pathways

Compared to neurons, NMDAR signaling pathways in cancer cells are less well investigated. In one case, Li *et al.* could show that NMDAR-mediated invasion of the murine pancreatic neuroendocrine tumor cell line bTC-B6 depends on the expression of the synaptic protein GKAP. They revealed that GKAP high expressing cancer cell lines showed increased invasion and increased sensitivity to the NMDA blocker MK801. They further demonstrated that GKAP knock down decreased the response of bTC-B6 cells to NMDA in a fluorescent calcium indicator assay, indicating that expression of synaptic proteins is important for NMDAR signaling in cancer cells [75].

Other authors reported that CREB is involved in NMDAR-mediated signaling in cancer cells. Previous results from our workgroup could demonstrate that NMDAR-expressing LN229 GBM cells show increased CREB phosphorylation upon Glu treatment [73]. In lung adenocarcinoma cells (A549), blockage of NMDARs with MK801 inhibits the phosphorylation of CREB at Ser133. Inhibition of NMDARs also decreased the phosphorylated form of MEK and ERK but not CaMKII and Akt, demonstrating that CREB activation is mediated by the ERK pathway in A549 cells [89]. Li and Hanahan demonstrated that MK801 treatment reduces the amount of phosphorylated CREB in murine βTC-3 cancer cells as well. They found that NMDAR signaling is propagated via the ERK and CaMKII signaling pathways and emphasized the dominant of the GluN2B subunit [50]. The fact that CaMKII binds to the GluN2B subunit [90] and the role of GluN2B and CaMKII in the migration of several cancers and neuros suggest that NMDAR promoted migration might depend on GluN2B-mediated activation of CaMKII [50, 63, 91-93].

Although the number of studies is limited, it has been clearly shown that several cancers use NMDAR-dependent CREB activation to promote survival and growth [50, 89]. In addition, high CREB expression was observed in many cancers including melanoma, breast cancer and glioblastoma, where it has been correlated with cancer survival and poor prognosis [94-97]. A prominent gene, which is typically regulated upon NMDAR activation and CREB phosphorylation, is *cFos*. *cFos* is a proto-oncogene, which is highly expressed in many cancers where it promotes tumor progression and radioresistance [98-102] and which is expressed upon NMDAR activation in the A549 cancer cell line [89].

The role of CREB and NMDARs in varying cancer types made both proteins to proposed targets for cancer therapy [48, 94], suggesting that NMDAR-mediated CREB signaling might play a regulative role in the progress of different cancer types.

3.3. The induction of DSBs is needed for NMDAR-dependent and CREB-mediated gene expression

In neurons, activation of synaptic NMDARs leads to the expression of early response genes (ERGs). ERGs are rapidly expressed dependent on CREB activation and encode for transcription factors including cFos, cJun and Egr1 [103, 104]. The expression of ERGs is mediated by the DNA-dependent RNA polymerase II (PolII) and the expression level peaks around 30 min after stimulus and then declines [105]. In 2010, Kim *et al.* could show that CREB and PolII are both bound to the transcription start site (TSS) of early response genes before stimulus induction. Their results indicate that the pre-binding of transcription factor and RNA polymerase enables a faster start of transcription upon activation of synaptic receptors. Furthermore, they showed that CBP is not localized at TSS in

unstimulated cells, proposing that the binding of CBP to CREB is the initiating step of ERG expression [106].

In 2015, Madabhushi *et al.* expanded the mechanism of NMDAR-dependent and CREB-mediated expression of early response genes. They noticed that the expression of ERGs increased and persisted in active neurons when topoisomerase II (Top2) was inhibited with etoposide [104]. Top2 unwinds DNA by inducing a single DSB followed by subsequent religation of the DNA damage, and therefore has an important role in removing topological tension inside the DNA during replication and transcription [107]. Etoposide inhibits Top2-mediated religation, inducing persisting DSBs at sites of Top2 activity. In subsequent experiments Madabhushi and colleges found that topoisomerase II β (Top2β) induces DSBs inside the TSS of ERGs upon NMDAR activation, which are essential to start PolII-dependent transcription of ERGs. The induction of DSBs at the specific TSS even was sufficient to induce gene transcription without activation of NMDARs, indicating that Top2β-mediated induction of DSBs is a key step in NMDAR-mediated gene regulation (see **Figure 5**).

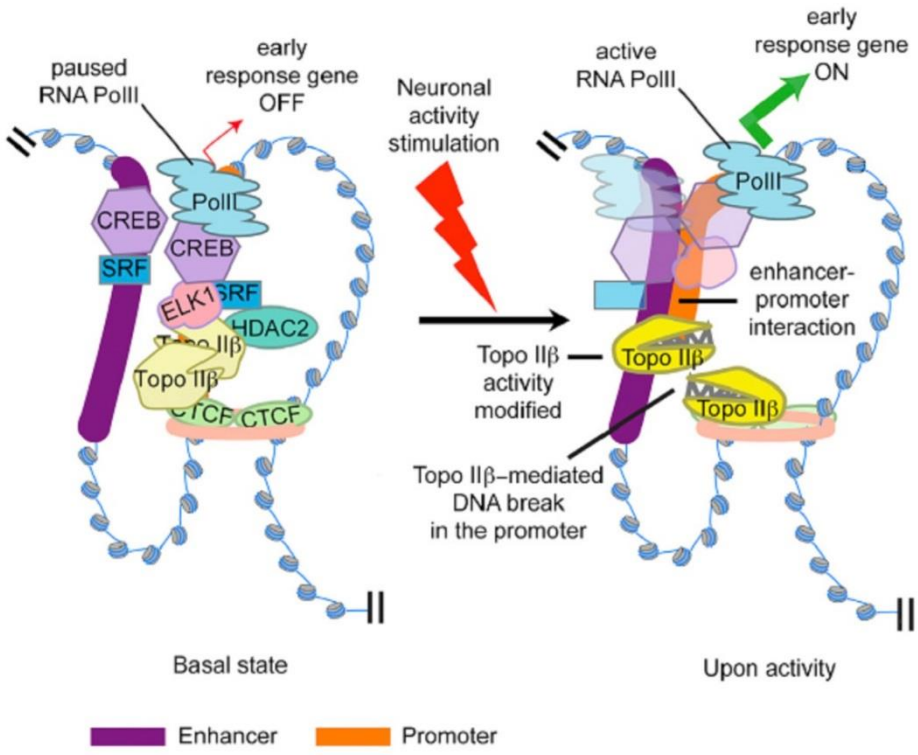

Figure 5: Top2β-mediated DSBs govern NMDAR and CREB-dependent gene transcription. In absence of neuronal activity, CREB and serum response factor (SRF) are bound to promoter and enhancer region of ERGs. The transcription activator ELK1 as well as PolII are also pre-bound to the promoter. The transcriptional repressor CTCF binds close the TSS and holds the expression of EGRs inactive together with histone deacetylase 2 (HDAC), which is bound to the promoter. Top2β binds close the CTCF binding sites. Upon neuronal activity, histone deacetylase 2 is released by activated calcineurin activity and increased Top2β activity induces a DSB into the promoter region of the ERG. This DSB relieves topological tension of the DNA, which enables enhancer-promoter interaction, allowing the pausing PolII to start gene transcription (Adopted from Madabhushi *et al.* [104]).

Furthermore it has been shown that inhibition of non-homologues end joining (NHEJ), which is the main DSB repair mechanism, led to prolonged expression of ERGs upon NMDAR activation. This indicates that ERG inactivation relies on the repair of regulatory DSBs by NHEJ and not by Top2β [104].

Based on these findings they extended the model of NMDAR-mediated gene regulation of ERGs in neurons described by West and Greenberg [108]. Without stimulation CREB and several regulatory factors are already bound to the TSS and PolII rests at the promoter. Top2β is bound near the transcriptional repressor CTCF. Upon NMDAR stimulation, Top2β get activated and induces DSBs into the TSS of ERGs including *cFos*, *Npas4* and *EGR*, but not in the TSS of late-response genes like *BDNF* and *Homer1*. This reduces topological constrains inside the DNA and allows promoter-enhancer interaction, which allows the resting PolII to start gene transcription (**Figure 5**) [104].

3.3.1. Topoisomerase II β: Function and role in transcription

DNA topoisomerases are enzymes that solve topological problems inside the DNA which result from strand separation during replication and transcription. The genome of human cells encodes for six different topoisomerases called Top1, Top1mt, Top2α, Top2β, Top3α and Top3β. Topoisomerases of subgroup one and three are type I topoisomerases, which means they resolve supercoiled DNA structure through induction of a single-strand DNA break, unwinding of DNA and subsequent religation. The activity of type I topoisomerases is essential during replicational and transcriptional elongation [109].

Top2α and Top2β are type II topoisomerases. Although, both types of topoisomerases use transient covalent linkage of a Tyr residue to the phosphate backbone of DNA in order to unwind the DNA, type II topoisomerases induces breakage of both DNA strands within four base pairs, resulting in a DSB. The complete break of DNA allows the passage of one DNA strand through another, which is needed to solve DNA knots and catenanes [109]. For this, Top2 homodimers bind two DNA strands, called G and T segment. The G segment is cleaved and upon hydrolysis of ATP the T segment is transported through the break. ATP is also needed to religate the G segment. Finally, dissociation of ADP allows opening of the C-terminal and the ATPase domain, which releases the T segment from C-terminal domain and Top2 from the DNA (**Figure 6**) [110].

Compounds which inhibit a specific step of Top2´s catalytic cycle are broadly used in cancer therapy [107, 110]. Most important for cancer therapy are Top2 inhibitors which result in the induction of DSBs, so called Top2 poisons [111-113]. Induction of DSBs by Top2 poisons promotes apoptosis or senescence in cancer cell but exposure to Top2 poisons has been associated with young age leukemia [114] and poisoning of Top2β with etoposide increased the incidence of melanoma in mice [115].

Interestingly, Top2β activity upon androgen-receptor activation has also been correlated with genomic rearrangements, which lead to the development of prostate cancer [116]. In this line, Top2β activity was supposed to be both: oncogenic force and potential therapeutic target in cancer [117].

Top2α and Top2β have different physiological roles. The expression of Top2α increases during S/G2-phase and Top2α activity is especially important during chromosome segregation and chromosome condensation, while Top2β shows no cell cycle specific expression and is especially needed during transcription [109, 118].

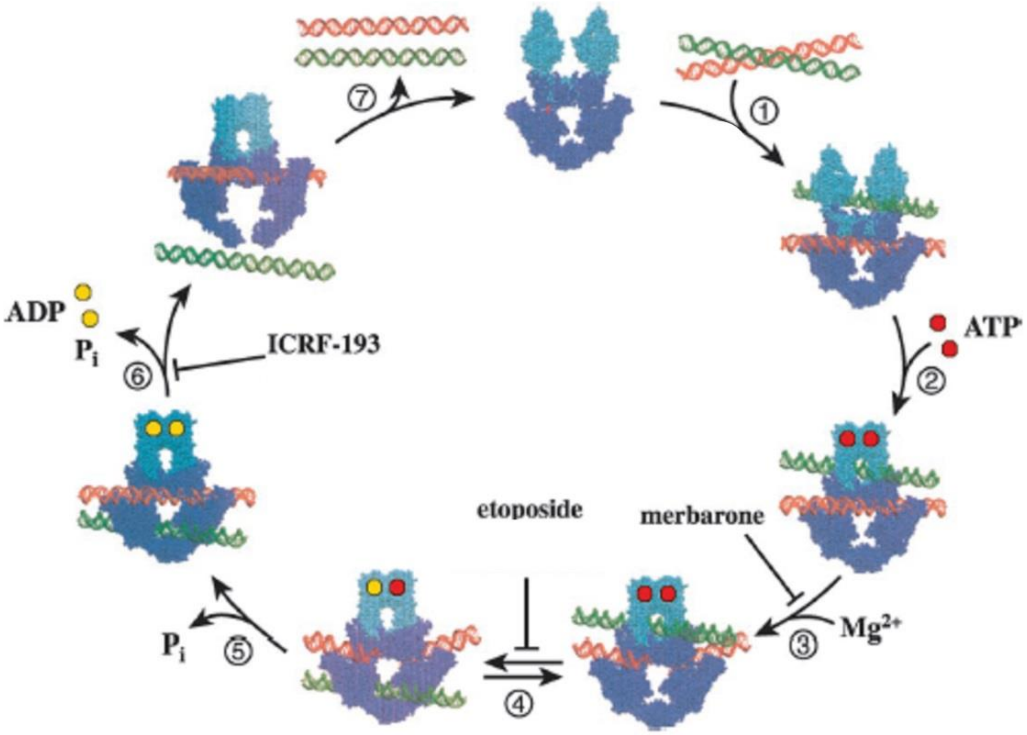

Figure 6: Catalytic cycle and inhibitors of Top2 enzymes. ATPase domain is shown in light blue and the DNA-binding and cleavage core domain and the C-terminal domain are dark blue. (1) First, the core domain binds one DNA double strand (G segment; red) and the ATPase domain binds a second DNA double strand (T segment; green). (2) Two ATP molecules bind to the ATPase domain which forms a closed clamp around the T segment. (3) The cleavage of the G segment is Mg^{2+}-dependent and can be inhibited with merbarone. (4) Hydrolysis of the first ATP supports the passage of T segment through the G segment. This step can be inhibited with etoposide, which traps the enzyme with a broken DNA double strand. (5) Hydrolysis of the second ATP is needed for religation of the G segment. (6) Dissociation of ADP enables the release of the T segment through the C-Terminal gate. This step can be inhibited by ICRF-193, which traps Top2 in an inactive state. (7) Top2 can dissociate from the G segment (adopted and modified from Larsen *et al. [110]*).

Interestingly, Top2β knock out mice have no morphological abnormalities in major organs but die perinatal [119]. qPCR revealed that in mice only a small number of genes (1-4%) were affected by Top2β knock-out during early embryonal development, indicating that Top2β is not generally needed for transcription [120]. Anyhow, Top2β deficient mice show abnormal neural and neuromuscular development, indicated by motor neurons which fail to innervate the diaphragm muscle and missing

sensory projections in the spinal cord as well as mainly suppressed transcription of late developmental genes [119, 120]. In addition, brain specific knock down of Top2β caused abnormal lamination of the cerebral cortex and decreased migration of neurons [121], suggesting that Top2β activity is required for the transcription of specific genes. A mechanism for specific gene regulation by Top2β in neurons, as described in **Figure 5**, was reported later. Here Top2β induces persistent DSBs, which are not religated by Top2β itself [104].

Nevertheless, the induction of regulatory DSBs by Top2β was not primarily discovered in neurons, but was reported earlier in MCF-7 breast cancer cells. Here, Top2β inflicted DSBs are required for the expression of estrogen receptor α regulated genes, which was confirmed by another groups [116, 122, 123]. In addition, glucocorticoid receptor transcriptional activation has been shown to be dependent on Top2β activity as well [124].

By now it is unknown how Top2β activity is regulated in context of transcriptional activation. Several proteins which are part of the DNA damage response are associated with Top2β, including poly(ADPribose)polymerase 1 (PARP1), DNA-dependent protein kinase (DNA-PK) and KU70 [122] as well as the serine/threonine kinase ATM [123]. Inhibition of DNA-PK and ATM decreased the number of DNA breaks upon activation of estrogen receptor α [123], indicating a role of these proteins in the induction of DSBs. But the number of Top2β-induced DSBs has also been reported to be increased upon DNA-PK inhibition, indicating a role in repair [104]. Ribosylation of Top2β by PARP1 decreases its catalytic activity [125] and might therefore play a role in Top2β inactivation [126]. On the other hand, PARP1 deficient cells showed decreased activity and expression of Top2β but not Top2α [127]. In addition, Top2 activity is modulated upon phosphorylation, for example by Casein kinase II [128], but Top2 is phosphorylated by many kinases among different species, including protein kinase A and C, ERK1/2 and CaMK [118]. Taken together, Top2β is involved in the signal transduction pathways of extracellular stimuli and induces regulatory DSBs, which promote transcription but also display a risk for genomic integrity [117].

3.4. Aim of study

Activation of neuronal NMDARs is multifunctional. NMDAR-mediated Ca^{2+} transients regulate a vast variety of genes in neurons which are essential for synaptic plasticity and memory formation and can also promote migration, survival and death [34, 61-63, 79, 129]. The effect of NMDAR activation depends on the expression of intracellular signaling proteins and the coupling of these proteins to the receptor, which allows NMDARs to activate distinct signaling pathways [75, 79]. GBM and other cancer cells hijack NMDAR signaling pathways to drive tumor malignancy by increasing their growth, survival and invasiveness [30, 49, 50, 52, 53, 73]. However, the essential role of NMDARs for neuronal activity limits the benefit of direct NMDAR inhibition in cancer therapy, since the general inhibition of

NMDARs by potent drugs induces severe side effects, including loss of memory and psychosis [130]. Inhibition of particular NMDAR signaling pathways or specific NMDAR subunits, which contribute to NMDAR-mediated malignancy in cancer cells, might be a possible way to target NMDARs in cancer therapy without disrupting synaptic transmission. However, the particular signaling pathways used by cancer cells are poorly investigated.

The finding, that NMDAR activity in cancer cells mediates Ca^{2+}-dependent activation of CaMKII/IV and ERK1/2 and phosphorylation of CREB, suggests similar NMDAR signaling in cancer cells and neurons [50, 73, 89]. In neurons, NMDARs promote strong expression of several ERGs by the induction of Top2β-mediated DSBs [104]. ERGs regulated by Top2β-induced DSBs include proto-oncogenes like *cFos* [100, 104, 105], suggesting that cancer cells might use this particular NMDAR signaling pathway to promote their own survival and growth.

Highly malignant GBM cells use NMDAR activation to promote growth, survival and invasion, which display severe obstructions for successful therapies [50, 73, 75, 131]. In order to identify potential therapeutic targets for GBM therapy inside NMDAR signaling pathways this study aims to investigate the impact of Top2β-dependent NMDAR signaling on GBM cells and therefore analyzed: i) The expression of NMDARs and functional Ca^{2+} signaling in the GBM cell line LN229. ii) NMDAR-dependent induction of DSBs, the expression of the ERG cFos and subsequent expression of BDNF, in special respect of the contribution of GluN2B containing NMDARs in GBM cell lines and primary GBM cells. iii) And the therapeutic implications of Top2β-dependent NMDAR signaling in GBM cells upon irradiation with X-rays.

4. Material and Methods

4.1. Antibodies

Table 1: Primary antibodies

Antibody	Host	Clone number; Manufacturer
Anti-GluN1	rabbit	D65B7; Cell Signaling (Danvers, U.S.A)
Anti-GluN2A	mouse	N327A/38; Abcam (Cambridge, U.K)
Anti-GluN2B	mouse	S59-20; Stress Marq (Victoria, Canada)
Anti-Top2β	mouse	A-12; Santa Cruz (Dallas, U.S.A)
Anti-53BP1	rabbit	H-300; Santa Cruz
Anti-cFos	rabbit	PA1318; BosterBio (Pleasanton, U.S.A)
Anti-GAPDH	rabbit	FL-335; Santa Cruz

Table 2: Secondary antibodies

Antibody	Host	Manufacturer
Anti-rabbit Alexa 488	donkey	Abcam
Anti-rabbit Alexa 594	donkey	Abcam
Anti-mouse Alexa 488	donkey	Abcam
Anti-mouse Alexa 594	goat	Abcam
Anti-rabbit-HRP	?	Chemicon (part of Merck, Darmstadt)
Anti-mouse-HRP	?	Chemicon

4.2. Agonists and inhibitors

Glutamate sodium salt	Sigma-Aldrich (St. Louis, U.S.A.)
Glycine	Carl Roth GmBH (Karlsruhe)
NMDA	Tocris Bioscience (Bristol, U.K.)
AMPA	Tocris Bioscience
(+)-MK801 maleate (Dizocilpine)	Tocris Bioscience
Ifenprodil hemitartrate	Tocris Bioscience
NBQX	Tocris Bioscience
Sulfasalazine	Sigma-Aldrich
NU7441	Tocris Bioscience
ICRF193	Santa Cruz
KG501	Sigma-Aldrich
Merbarone	Sigma-Aldrich

4.3. Solutions

Ca^{2+}-Imaging	
Imaging buffer	140 mM NaCl; 2.8 mM KCl; 1.8 mM $CaCl_2$; 10 mM HEPES; 20 mM Glucose; 10 μM EDTA; pH 7.2
Immunofluorescence staining	
PBG	PBS+0.05% gelatin
Blocking buffer	PBG+5% goat serum+0.5% BSA
Antibody buffer	PBG+5% goat serum
Western Blot	
Lysis buffer	20 mM Tris-HCl (pH 7.5); 150 mM NaCl; 1 mM Na_2EDTA; 1 mM EGTA; 1% Triton; 2.5 mM sodium pyrophosphate; 1 mM b-glycerophosphate; 1 mM Na_3VO_4; 1 μg/ml leupeptin (cell signaling #9803)
4x Loading buffer	240 mM Tris/HCL (pH6.8); 40% glycerol; 8% SDS; 0.04% bromphenol blue
10% SDS gel	33% v/v Rotiphorese (37.5:1); 250 mM Tris-HCl (pH 8.8); 0.01% w/v SDS; 0.01% w/v Ammonium persulfate; 0,001% v/v Tetramethylethylenediamine
SDS-PAGE running-buffer	25 mM Tris; 192 mM glycine, 0.1% SDS
Anode buffer	60 mM Tris; 40 mM 6-Aminocapric acid; 20% Methanol
Cathode buffer	60 mM Tris; 40 mM 6-Aminocapric acid; 0.1% SDS
TBS-T	50 mM Tris; 150 mM NaCl; 0.1% Tween-20
Blocking buffer	5% milk in TBS-T (0.1% Tween-20)
Antibody buffer	1% milk in TBS-T (0.1% Tween-20)
Electrophysiological Measurements:	
External solution	4 mM KCl; 140 mM NaCl; 2 mM, $CaCl_2$ 5 mM D-Glucose; 10 mM HEPES/NaOH; pH 7.4; ~298 mOsmol
Internal solution	50 mM KCl; 10 mM NaCl; 60 mM KF; 20 mM EGTA; 10 mM HEPES/KOH; pH 7.3; ~285 mOsmol

4.4. Cell lines and cell culture

The immortalized human GBM cell lines LN229 and U-87 MG were kindly provided by Prof. Franz Rödel (Frankfurt University Hospital, Frankfurt am Main). Both cell lines are IDH1-wt and were cultured at 37°C under humid atmosphere and 5% CO_2 in T75 flasks (Sarstedt, Nümbrecht) using DMEM (Sigma-Aldrich) including ~400 μM glycine and supplemented with 10% FCS (Sigma-Aldrich), 100 U/ml penicillin/0.1 mg/ml streptomycin (Sigma-Aldrich) and 2 mM L-glutamine (Sigma-Aldrich). LN229 and U-87 MG cells were not used for more than 15 passages.

The primary human GBM cell line G1702 was kindly provided by Prof. Donat Kögel (Frankfurt University Hospital, Frankfurt am Main). The G1702 cell line was established from a biopsy of a male patient and classified as glioblastoma multiforme. The cells are IDH1-wt, ATRX-positive and carry a hypermethylation of the MGMT promoter. The G1702 cells were cultured at 37°C under humid atmosphere and 5% CO_2 in T75 flasks (Sarstedt) as spheres in Neurobasal Medium (Gibco, trade mark of Thermo Fisher Scientific, Waltham, U.S.A.) including ~400 μM glycine and supplemented with 2% B27 (Gibco), 100 U/ml penicillin/0.1 mg/ml streptomycin (Sigma-Aldrich), 2 mM L-glutamine (Sigma-Aldrich), 20 nM EFG (R&D systems, Minneapolis, U.S.A.) and 20 nM FGF2 (Sigma-Aldrich). We received the G1702 at passage 30 and used them not longer than 10 passages.

4.5. Immunofluorescence staining (General Protocol)

$2*10^4$ LN229 cells or $4*10^4$ U-87 MG cells were seeded in μ-slides $VI^{0,4}$ (Ibidi, Planegg) in a total volume of 150 μl/channel. Next day the cells were fixed with 4% PFA in PBS for 15 min at RT, permeabilized with 0.1 % Triton X-100 in PBS and stained with Hoechst 33342 for 10 min at RT. Then cells were blocked for at least 1 h RT and incubated with primary antibodies overnight at 4°C. Next day samples were washed three times with PBG for 10 min, incubated with anti-rabbit/mouse Alexa Fluor 488/594 labeled secondary antibody (1:400) for 1 h at RT and washed three times for 10 min with PBG and twice with PBS.

G1702 cells were stained with the same protocol except following differences: G1702 spheres were dissociated through repeated pipetting and Accutase (Sigma-Aldrich) treatment for 1-2 min To get adherent culture, $5*10^4$ cells were seeded into μ-slides $VI^{0,4}$ (Ibidi), coated with 2 $\mu g/cm^2$ laminin (Sigma-Aldrich) overnight.

4.6. Immunofluorescence staining of NMDAR subunits

LN229 and G1702 cells were stained as described (4.5) and no treatment was applied. The following combinations of primary and secondary antibodies were used (antibody dilutions in brackets).

anti-GluN1 (1:100)	+	donkey anti-rabbit Alexa 488 (1:400)
anti-GluN2A (1:100)	+	donkey anti-mouse Alexa 488 (1:400)
anti-GluN2B (1:200)	+	donkey anti-mouse Alexa 488 (1:400)

The samples were imaged with the inverted epifluorescence microscope Axio Observer Z1 (Zeiss, Oberkochen) using a 20x objective. The images were linearly edited with the *Fiji* software.

4.7. Analysis of 53BP1 and Top2β foci

LN229, U-87 MG and G1702 cells were seeded as described (4.5) and treated directly after seeding as indicated. Next day, the samples were treated with 20 μM EdU for 30 min before fixation. Then the samples were stained according to the general protocol (4.5). After permeabilization, EdU was detected with a Click-iT EdU imaging kit, following the manufacturer instructions (Thermo Fisher Scientific) using Alexa Fluor 594 azide or 647 azide (Thermo Fisher Scientific) and 80 μl reaction buffer/channel. The following combinations of primary and secondary antibodies were used (antibody dilutions in brackets).

anti-53BP1 (1:1000)	+	donkey anti-rabbit Alexa 488 (1:400)
anti-Top2β (1:100)	+	goat anti-mouse Alexa 594 (1:400)

For foci counting the immunofluorescent stained samples were imaged with a 20x objective on the inverted epifluorescence microscope Axio Observer Z1 (Zeiss). Single nuclei were detected by the μManager software based on area size and shape of the Hoechst33342 signal. Then, the integrated density of the Hoechst 33342 signal of single nuclei was measured by the μManager software and blotted against their mean EdU signal. This blot allowed discrimination between G1 phase cells with low Hoechst 33342 and low/no EdU signal, S-phase cells with intermediate Hoechst 33342 and high EdU signal and G2-phase cells with high Hoechst 33342 and low/no EdU signal. For foci counting non-S-phase cells or G1-phase cells were manually gated (see **Figure 7**), depending on the experimental setup. Then, single cells were relocated and foci manually counted using a 63x objective. The foci of at least 40 single cells per condition and experiment were counted and the mean of all single cell values

of all independent experiments were used for statistical analysis. Mann-Whitney-Test (MWT) was used for statistics (GraphPad Prism 7.0, San Diego, U.S.A.).

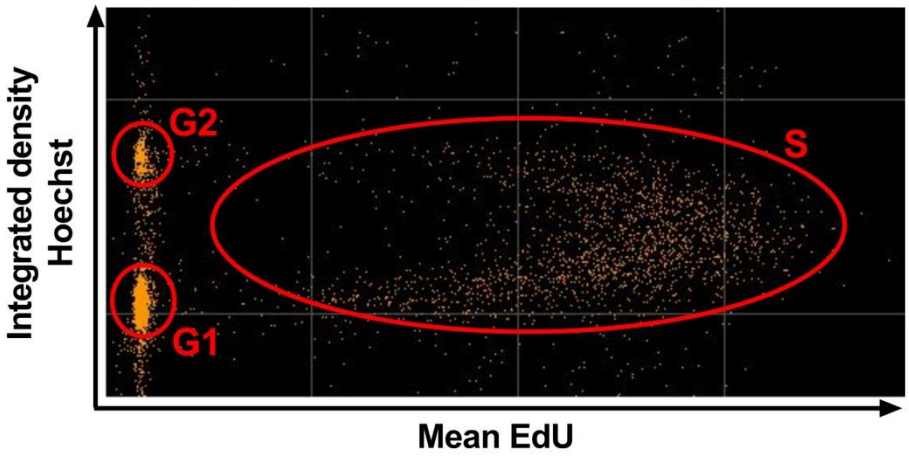

Figure 7: Representative gating of cell cycle phases. The micro-manager software was used to plot the integrated density of the Hoechst signal against the mean EdU signal of a cell. Each yellow point represents the calculated values for one cell. The gates were manually set for each experiment.

4.8. Cell cycle analysis

LN229 cells were seeded as described (4.5) and treated directly after seeding as indicated. Next day, the samples were treated with 20 μM EdU for 30 min. before fixation. Then the samples were stained according to the general protocol (4.5). After permeabilization, EdU was detected with a Click-iT EdU imaging kit, following the manufacturer instructions (Thermo Fisher Scientific) using Alexa Fluor 594 azide (Thermo Fisher Scientific) and 80 μl reaction buffer/channel. The cells were imaged with a 20x objective on an inverted epifluorescence microscope as described (4.7). At least 1000 cells per experiment were gated manually and the cell cycle distribution was calculated. Student´s t-test was used for statistics (GraphPad Prism 7.0).

4.9. High-content microscopy

LN229 cells were stained as described above (4.7) but without staining against Top2β. EdU was labeled with Alexa azide 594. The samples were imaged via the Operetta High-Content Imaging System (PerkinElmer, Waltham, U.S.A.) using a 40x high NA objective. The Harmony analysis software was used to select single nuclei based on the shape and intensity of the Hoechst 33342 signal. The EdU signal was used to exclude S-phase cells and foci were automatically counted in the 53BP1 channel using the “spot analysis” feature. The same thresholds were set for all samples and at least 1500 cells per condition were counted. No statistical analysis was done since only one independent experiment was performed.

4.10. Calcium imaging

$2.5*10^4$ LN229 cells were seeded into 8-well μ-slides (Ibidi). Next day, the cells were treated with the calcium dye Fluo-4 AM (Thermo Fisher Scientific) dissolved in DMSO for 30 min. to a final concentration of 2 μM. The cells were washed once with the imaging buffer and imaged on an epifluorescence microscope (Zeiss). Alterations in fluorescence intensity of Fluo-4 were measured with a GFP filter by taking an image every second. Glutamate and glycine were applied to the cells to an end-concentration of 1 mM and 100 μM respectively after 20 seconds and 10 μM Ionomycin was given after 90 seconds. The image sequences were analyzed for visual inspection and processed by using *Fiji* software by subtracting the mean background of the integrated density of every cell and then normalized all values to the fist and the highest value of every cell. The data were plotted as relative fluorescence intensity scale versus time. Cells which showed an unsteady Fluo-4 signal before application were excluded from analysis. Representative images are displayed in false color to highlight local differences of Fluo-4 fluorescence intensity. The images were linearly edited with the *Fiji* software.

4.11. Western Blot

For western blot analysis $7*10^5$ LN229 cells were seeded in T25 culture flasks (Sarstedt) or $2*10^5$ G1702 cells were seeded in 6-well plates (Starlab, Hamburg) and treated overnight as indicated. On the next day the cells were washed once with ice cold PBS and lysed in 120 μl (T25) or 40 μl (6-well plate) ice cold lysis buffer containing 1 mM pefabloc® (Carl Roth). Protein concentrations were determined using a BCA protein assay kit following the manufacturers protocol (Thermo Fisher Scientific) and ~30-60 μg protein were mixed with 4x SDS-loading buffer containing 100mM DTT, denaturized at 64°C for 10 min. and loaded on 6%-12% gradient gel or 10% continuous gel per lane. A protein ladder with a size of 10-180 kDa (Thermo Fisher Scientific) was used as marker. The proteins were separated in running buffer on ice at constant 120-130 V. A discontinuous approach with separate buffers for anode and cathode was used to transfer the separated proteins to a PVDF membrane (Merck Millipore, Burlington, U.S.A.). The blotting was performed in a semi-dry transfer system (Biorad, Hercules, U.S.A) for 36 min. at constant 15 V. Afterwards, the blots were blocked for 1 h at RT, treated with anti-cFos antibody (1:2000) or anti-Top2β (1:500) and anti-GAPDH (1:2000) diluted in antibody buffer overnight at 4°C. Then the blots were washed 3 times for 10 min. with TBS-T and incubated with anti-mouse/anti rabbit HRP conjugated secondary antibody (1:10000) for 1 h at RT and washed again 3 times for 10 min. Immunoblots were detected using luminol reagent (Thermo Fisher Scientific or Merck Millipore) in the ChemiDoc MP imaging system (BioRad). Quantitative analysis was done with the Image Lab software (BioRad). All band intensities were normalized to the

intensity of the GAPDH band in the same lane and the cFos/GAPDH ratios were normalized to the control treatment of the experiment. For statistics one sample t tests were used (GraphPad Prism 7.0).

Irradiation with X-ray for Western Blot

Western Blot samples were irradiated directly after seeding and treatment with agonists/inhibitors. The samples were irradiated in an X-ray tube with tungsten anode (Philips, Amsterdam, Netherlands) at 33.7 mA and 90 kV with a dose rate of 1.162 Gy/min (Fricke dosimetry) and at 45 cm distance using 1 mm aluminum filter.

4.12. Transfection with siRNA

For siRNA transfection, $6*10^5$ LN229 cells were seeded in T25 flasks (Sarstedt) overnight and transfected with 16μg si-RNA next day (si1 UCGGGCUAGGAAAGAAGUAA(UU); si2 CAGCCGAAAGACCUAAAUACA(UU) (Eurofins Scientific, Luxemburg); sequence described by Kamaci *et al*. 2011 [132]) according to the manufacturers protocol with the K2 transfection System (Biontex, München). As a control, the cells were treated only with K2 transfection reagent, but without siRNA. The transfected cells were used for experiments after 24 h.

4.13. Clonogenic survival

LN229 cells transfected with or without Top2β siRNA were trypsinized and seeded into 6 well plates (Sarstedt) as triplets and treated with 1 mM Glu or 1 mM Glu/20 μM ifenprodil. Untransfected cells were used as an additional control. The number of seeded cells depended on the treatment and X-ray dose as shown in the following table:

Table 3: Number of seeded cells for clonogenic survival assay

Treatment	0 Gy	2 Gy	4 Gy	6 Gy
Glu **Glu/Sham transfected**	500 cells/well	500 cells/well	1000 cells/well	2000 cells/well
Glu/ifenprodil **Glu/siRNA transfected**	750 cells/well	750 cells/well	1500 cells/well	3000 cells/well

The cells were allowed to attach for 3 h and then irradiated in an X-ray tube with tungsten anode (Philips) at 33.7 mA and 90 kV with a dose rate of 1.162 Gy/min (Fricke dosimetry) and at 45 cm distance using 1 mm aluminum filter. Non irradiated cells were placed in the radiation chamber for 100 s without irradiation. Colonies were allowed to form for 8 days, fixated with 70% ethanol and stained with 0.1% crystal violet in 25% ethanol. The colonies with more than 50 cells were manually

counted under a binocular using 65x-150x magnification. The plating efficiencies (*PE*) were determined depending on the number of seeded cells:

$$PE = \frac{Number\ of\ colonies}{Number\ of\ seeded\ cells}$$

The survival fraction (*SF*) was calculated by dividing the *PE* of each dose by the *PE* of the non-irradiated cells. The values of three independent experiments were fitted to a linear quadratic mathematical model by GraphPad Prism software with the equation:

$$SF = e^{(-\alpha D - \beta D^2)}$$

Where (*SF*) is the surviving fraction and (*D*) is the x-ray dose. Additionally, the relative survival ratio was calculated out of the mean value of all three experiments. The relative survival ratio is *SF* of untreated cell divided by *SF* of treated cells. For statistical analysis student´s t-test was used (GraphPad Prism 7).

4.14. BDNF Assay

For the measurement of extracellular BDNF concentrations $2*10^4$ LN229 cells/well were seeded into 24-well plates (Sarstedt) and treated directly after as indicated. Next day the supernatants were collected and centrifuged at 16200 g for 5 min. to remove remaining cells and debris. The BDNF concentration of the supernatants was measured with a human BDNF ELISA Kit (Abcam, ab99978) following the manufacturers protocol. In short, BDNF is bound to immobilized anti-human-BDNF antibody and then coupled to HRP via biotinylated anti-BDNF-antibodies. TMB substrate solution is added and color develops in proportion to the amount of BDNF bound. Then absorbance at 450 nm was measured with a TECAN Infinite M 200 microplate reader (Männedorf, Schweiz). All treatments were done as triplets and the concentration of BDNF was normalized to the mean value of the SAS/Glu treated sample. One sample t-test was done for statistics (GraphPad Prism 7).

Irradiation with X-ray for BDNF-Assay

Samples were irradiated 30 min. after seeding and treatment with agonists/inhibitors inside 24-well plates. The samples were irradiated in an X-ray tube with tungsten anode (Phillips) at 33.7 mA and 90 kV with a dose rate of 1.162 Gy/min (Fricke dosimetry) and at 45 cm distance using 1 mm aluminum filter.

4.15. Electrophysiological measurements of G1702 cells

Electrophysiological measurements of G1702 cells have been performed by M.Sc. Juliane Joswig. For this, ~4*10^5 G1702 cells were seeded into a 35 mm cell culture dish (Sarstedt), coated with 2 μg/cm² laminin (Sigma-Aldrich). Once in following three days, the media was removed and cells were covered external solution for patch clamp recordings. Coated (Sigmacote®, Sigma-Aldrich) borosilicate capillaries (length 10 cm, outer diameter 1.5 mm, inner diameter 1.17 mm) were pulled in two steps with a micropipette Puller PC-10 (Narishige, Tokyo, Japan) to patch-pipettes with a resistance of 6 Ω to 10 Ω, which were filled with internal solution. Cells were measured in whole-cell configuration. For this, the membrane potential was clamped to -70 mV for ~10 s. After ~3 s perfusion systems were manually switched and cells were now perfused with external solution containing 1 mM Glu/100 μM Gly for ~ 3s. After this, perfusion was again switched to external solution for additional ~3 s. Cells which showed a current upon Glu/Gly perfusion which was at least twice as high as the current background noise and which could be washed out with external solution without Glu/Gly were counted as responsive. The maximal (I_{max}) current after Glu/Gly application was analyzed with IGOR (WaveMetrics, Portland, U.S.A.).

5. Results

All figures presented in the chapters "results" and "discussion" have been created by Henrik Lutz. The figures 9, 10(a,b and d), 11, 12, 13, 14, 15a, 16(b-d), 17 (a+b) and 19 have been published in similar or identical form as "*NMDA Receptor Signaling Mediates cFos Expression via Top2beta-Induced DSBs in Glioblastoma Cells"* in *cancers* [133]. Figures 8 and 15 b have been published in similar or identical form as "*NMDA Receptor-Mediated Signaling Pathways Enhance Radiation Resistance, Survival and Migration in Glioblastoma Cells-A Potential Target for Adjuvant Radiotherapy*" in *cancers* [73].

5.1. Glu induces Ca^{2+} transients in NMDAR-expressing LN229 cells

The activation of NMDARs by Glu opens the receptors ion channel, allowing cations to flow into (Na^+, Ca^{2+}) or out (K^+) of the cell. The influx of Ca^{2+} is a crucial step for NMDAR signaling in neurons and cancer cells alike. For this reason the initial step of NMDAR signaling, the entrance of Ca^{2+}, was investigated in GBM cells. We chose to analyze the NMDAR-expressing GBM cell line LN229 which showed Glu-mediated currents in electrophysiological measurements [73].

To validate if Glu also mediates Ca^{2+} currents, we imaged LN229 cells with the non-ratiometric Ca^{2+} indicator Flou-4 AM. The cells were loaded with Flou-4 and sampled with 1 Hz on an epifluorescence microscope. After 20 s 1 mM Glu and 100 μM Gly were applied to the cells and 10 μM Ionomycin after 90 s (**Figure 8a**). The diagram shows the relative intensity of two responding (red) and two non-responding (black) cells over time. The non-responding cells showed a slow, continuous increase of relative intensity, which is likely induced by the imaging process itself, but the intensity of responding cells showed a faster increase after Glu/Gly application (50% of cells responding, n=10). The responding cells displayed a persistent increase of Flou-4 intensity which either stabilized at a certain level or oscillated. Slow oscillation with a high amplitude were caused by changes of the relative intensity inside the nuclear area (**Figure 8b*i*)**, while fast oscillations with low amplitude were caused by local changes of the relative intensity inside cell protrusions (blue arrow; **Figure 8a and b*ii***). These results demonstrate that application of Glu/Gly is able to induce transient Ca^{2+} currents as well as a longer lasting increase of nuclear Ca^{2+} in LN229 cells.

We next analyzed the expression pattern of NMDAR subunits in LN229 cells via immunofluorescence staining. GluN1, GluN2A and GluN2B subunits were expressed in LN229 cells (**Figure 8c**). Remarkably, high amounts of the subunits could be seen in the ER but also in the cells protrusions and lamellipodia (blue arrows). The localization of NMDAR subunits is similar to the localization of fast Ca^{2+} oscillations seen after Glu/Gly application.

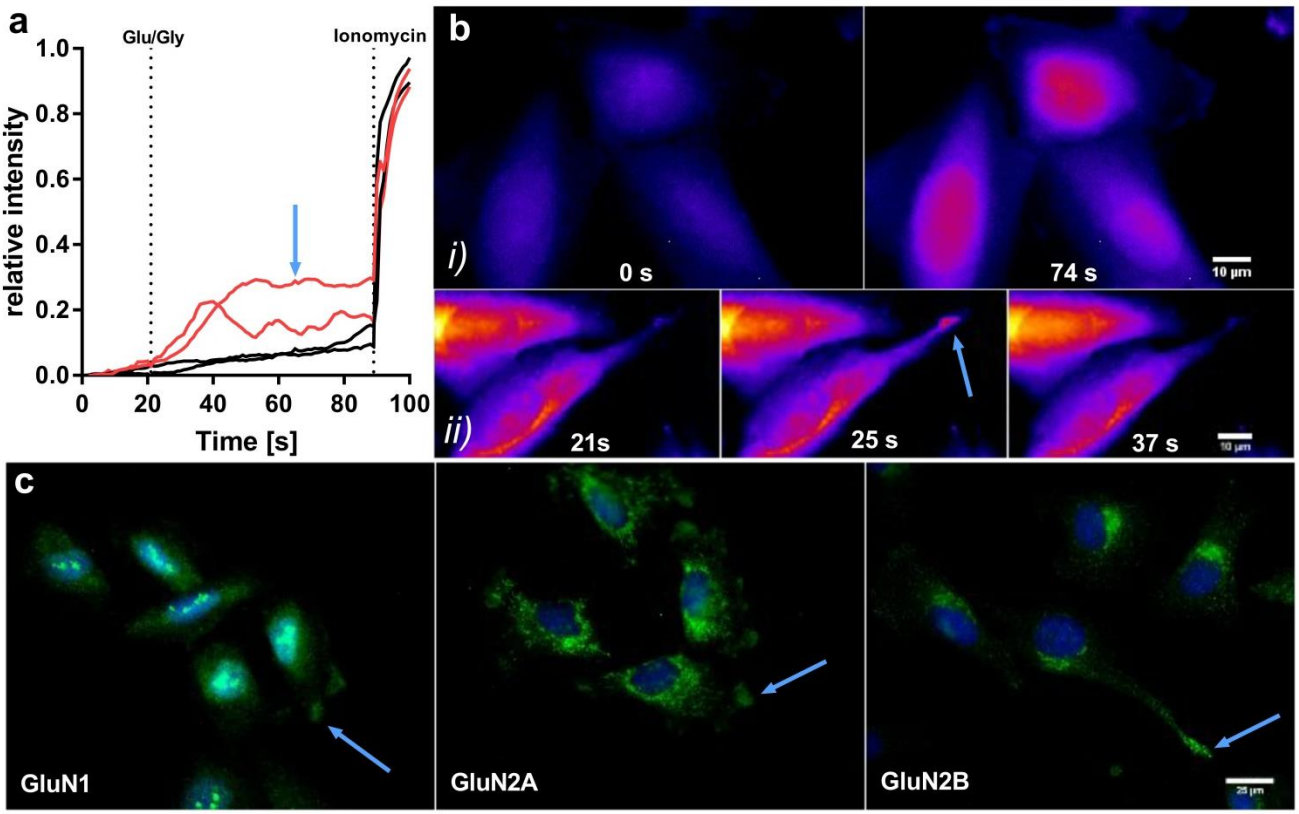

Figure 8: Glu-mediated Ca^{2+} transients and NMDAR expression in LN229 cells. (a) Ca^{2+}-imaging of LN229 cells loaded with Fluo-4 shows an increase of intracellular Ca^{2+} in half of the cells after application of Glu/Gly (n=10). The diagram displays the relative Fluo-4 fluorescence over time of two cells responding (red) and two cells non-responding (black) to the application of 1 mM Glu/100 µM Gly (t=20 s). 10 µM ionomycin were given after 90s as an internal control. Blue arrow indicates a short oscillation with low amplitude. **(b) i)** Representative images of Flou-4 loaded cells before (t=0 s) and after (t=74 s) application of 1 mM Glu/100 µM Gly at t=20 s. The increased fluorescence intensity demonstrates an increased concentration of Ca^{2+} in the nuclear area, with different strong response of individual cells (scalebar: 10 µm). **ii)** Representative images of Flou-4 loaded cells after application of 1 mM Glu/100 µM Gly at t=20 s. Local oscillations of the Ca^{2+}-signal can be observed at cell protrusions (blue arrow; scalebar: 10 µm). **(c)** Immunofluorescence staining of the NMDAR subunits GluN1, GluN2A and GluN2B. All subunits are expressed in LN229 cells, especially at cell protrusions (blue arrows) and also in the ER (Hoechst 33342=blue, NMDAR subunits=green, scalebar: 25 µm).

5.2. Glu induces DSBs upon NMDAR activation in GBM cell lines

As demonstrated in **5.1**, LN229 cells show Glu-mediated Ca^{2+} influx, which represents the initial step of NMDAR signaling. Moving forward, we analyzed if a characteristic step of NMDAR signaling to promote gene expression can be found in LN229 cells: The induction of Glu-dependent DSBs upon NMDAR activation [104].

5.2.1. Glutamate-induced DSBs in LN229 cells

In order to check if LN229 cells use Glu-induced DSBs, the number of DSBs was quantified by immunostaining of 53BP1 foci after Glu treatment. In a first experiment, LN229 cells were treated with 250 μM sulfasalazine (SAS) which inhibits the endogenous release of Glu by the system x_c^- antiporter and the number of 53BP1 foci in non-S-phase cells (EdU negative cells) were counted. SAS treated LN229 cells showed a mean number of 1.9±0.2 53BP1 foci/cell (**Figure 9a**), but cells which were additionally treated with 1 mM Glu showed a significantly increased number of 53BP1 foci (3±0.3; $p<0.0001$; **Figure 9a**) indicating that Glu also induces DSBs in LN229 cells.

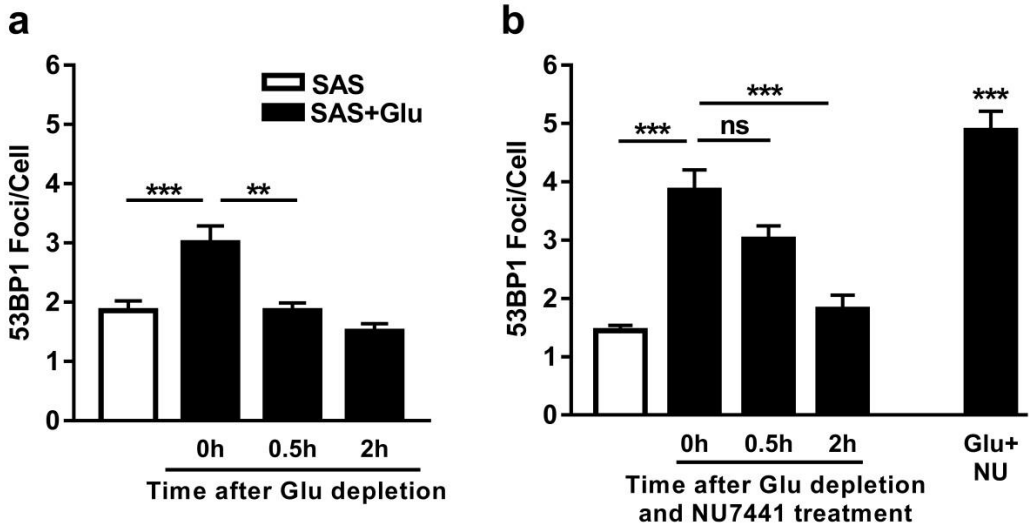

Figure 9: Glu induces transient DSBs in LN229 cells. Experiments included in this figure were performed by Thy Anh Nguyen. **(a)** Overnight treatment with 1 mM Glu increases the mean number of 53BP1 foci/cell in non-S-phase LN229 cells cultivated with 250 µM SAS. Depletion of Glu leads to a reduction of foci to the basal level after 0.5h (n=3; 40 cells/n, error bars show SEM, bar graphs show the mean of all single values). **(b)** The reduction of 53BP1 foci was delayed for 2 h when 1 µM NU7441 was given at the time point of Glu depletion (LN229 cells treated with 250 µM SAS and 1 mM Glu overnight). Overnight treatment with 1 mM Glu and 1 µM NU7441 increased the number of 53BP1 foci compared to Glu treated LN229 cells. (n=3; 40 cells/n; error bars show SEM; bar graphs show the mean of all single values). (Mann-Whitney Test for statistics; p>0.05 (ns), p≤0.05 (*), p≤0.01 (**), p≤0.001 (***))

Next, we wanted to see how persistent Glu-mediated DSBs in GBM cells are. For this LN229 cells were treated with 1 mM Glu/250 μM SAS overnight and Glu was depleted next day. Again, 53BP1 foci were counted in non-S-phase cells. Glu depletion decreased the number of 53BP1 foci to 1.9±0.1 ($p=0.0019$) after 0.5 h, which is similar to the number of SAS treated LN229 cells without Glu treatment (**Figure 9a**) and the number of foci/cell did not increase until 2 h after depletion (1.5±0.1). These results indicate that Glu-mediated DSBs are not persistent in LN229 cells. To check whether 53BP1 foci decrease after Glu depletion is facilitated by classical DNA repair pathways, the same experiment was done again, but additionally the catalytic subunit of the DNA-dependent protein kinase (DNA-PK_{cs}) was inhibited with 1 μM NU7441 at the time point of Glu depletion (**Figure 9b**). DNA-PK_{cs} is required for NHEJ, a repair pathway which occurs in G1-, S- and G2-phase cells. In this experiment the number of 53BP1 foci/cell was again significantly increased when LN229 cells were treated with Glu and SAS (3.9±0.3) compared to cells treated with SAS alone (1.4±0.1; $p<0.0001$). Strikingly, the number of 53BP1 foci was no longer decreased 0.5 h after Glu depletion (3.0±0.2) when NU7441 was added simultaneously. After 2 h a significant decrease to 1.8±0.2 foci/cell ($p<0.001$) was found, indicating that Glu-mediated DSBs are more persistent upon DNA-PK_{cs} inhibition (**Figure 9b**). Additionally, overnight treatment with Glu and NU7441 leads to a significant increase of 53BP1 foci (4.9±0.3; $p<0.001$) compared to cells solely treated with Glu.

5.2.2. Glu induces DSBs in a subpopulation of LN229 cells

Our results could show that the mean number of DSBs, indicated by 53BP1 foci, increases upon Glu treatment in LN229 cells. Interestingly, the number of DSBs within individual LN229 cells highly differed (**Figure 10a**), which led us to the hypothesis that only a fraction of LN229 cells respond to Glu treatment with induction of DSBs. To increase the visibility of subpopulations within the LN229 cells, the induction of 53BP1 foci was analyzed in a high number of cells using automated, high-content microscopy. Therefore, the cells were treated with 250 μM SAS with or without 1 mM Glu or left untreated and 53BP1 foci were automatically counted in at least 1500 non-S-phase cells. Similar to our first results, the number of foci/cell in SAS treated cells was increased from 0.3±0.02 to 1.9±0.1 after Glu treatment (**Figure 10b**). The untreated cells reached a value of 1.7±0.1 foci/cell, which is similar to Glu treated cells, confirming the effectiveness of SAS in reducing the number of 53BP1 foci.
Since a specific number of genomic loci had been identified to be the target of stimulus-induced DSBs upon NMDAR activation in neurons, we ask if Glu also induces a specific number of DSBs in a subpopulation of LN229 cells. The histogram of 53BP1 foci/cell for SAS (red) and SAS/Glu (black) treated cells (**Figure 10c**) shows a shift from zero or low numbers of foci/cell to higher numbers of foci/cell upon Glu treatment. A low peak at 10 foci/cell could be supposed but this assumption could

not be verified since only one experiment was performed. Notably, all numbers of foci between 0-20 could be found in Glu treated LN229 cells, but only four cell had more than 20 foci.

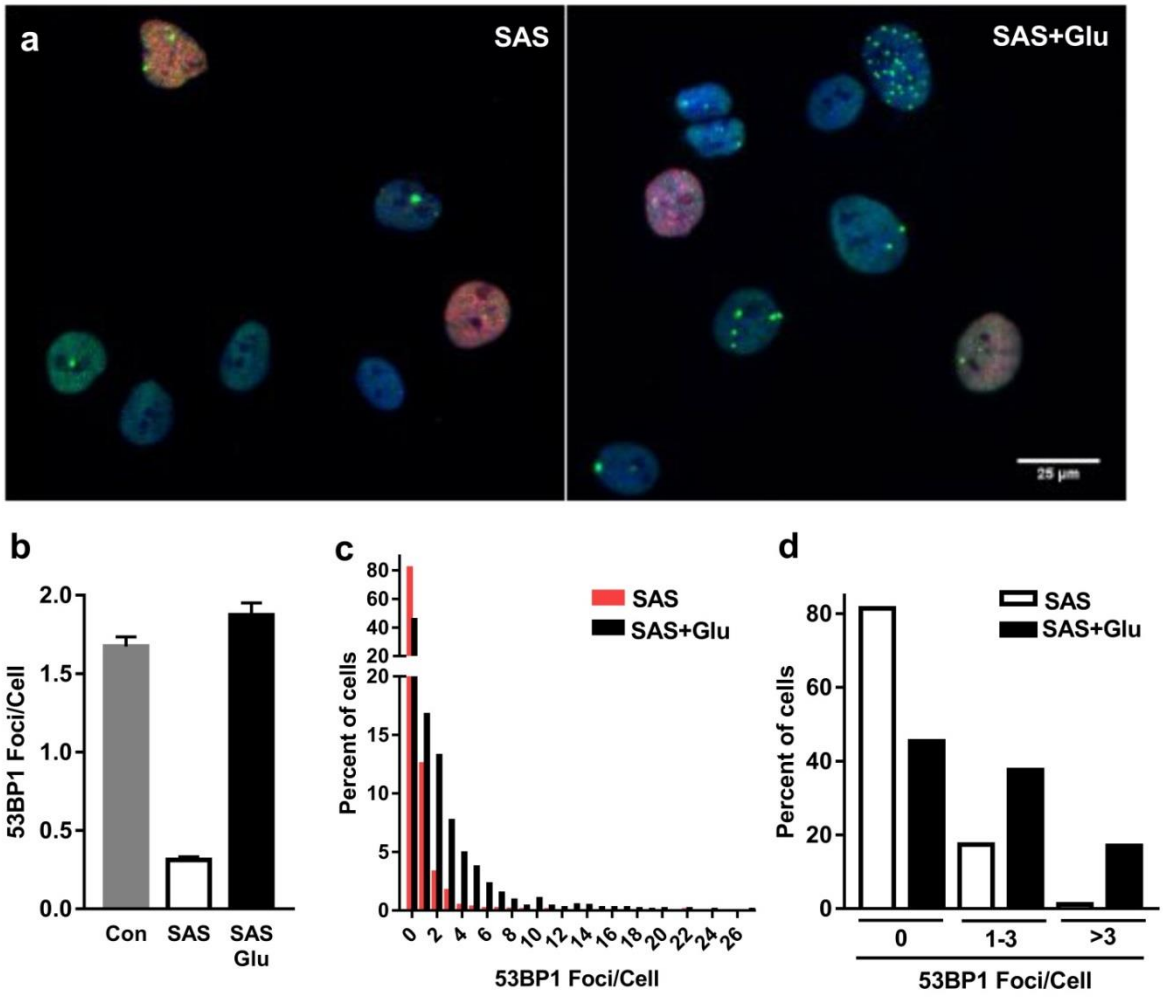

Figure 10: Glu induces DSBs in a subpopulation of LN229 cells. (a) Representative immunofluorescence staining of LN229 cells treated with 250 µM SAS or 250 µM SAS/1 mM Glu (53BP1 = Green, EdU = red, Hoechst = blue). Note that LN229 cells show a heterogeneous distribution of 53BP1 foci after Glu treatment (Scalebar: 25µm). **(b-d)** High throughput counting of 53BP1 foci in LN229 cells treated with 250 µM SAS or 250 µM SAS/1 mM Glu or untreated (n=1; >1500cells/n). **(b)** Cells treated with Glu and untreated cells show a higher number of 53BP1 foci/cell (mean±SEM). **(c)** Histogram of 53BP1 foci/cell for SAS (black) and SAS/Glu (red) treated cells. Glu does not induce a specific number of foci. **(d)** Distribution of 53BP1 foci/cell within the cell population. About 80% of the cells have no foci when treated with SAS but the number of cells without foci decreases in the presence of Glu. Glu treatment increases the low (1-3) and high (>3) numbers of foci in LN229 cells indicating differential response of subpopulations.

However, to characterize how cells respond to Glu with the induction of foci, they were sorted into 3 groups, bearing no, a low number (1-3) or a high number (>3) of 53BP1 foci (**Figure 10d).** 81.4% of all cells treated with SAS had no foci and 17.4% showed between 1 and 3 foci. After Glu treatment 45.4% of all cells showed no foci, indicating that 36% of the cells specifically reacted to Glu by DSB induction. Furthermore, the results demonstrate that nearly half of the cells did not respond to Glu treatment at all. The proportion of cells with 1-3 foci/cell increased to 37.6% for Glu treated cells as

well as the number of cells with higher amounts of DSBs from 1.1% to 17.0%. These results confirm the existence of Glu-mediated DSBs with an automated approach and demonstrate that Glu-mediated DSBs do not occur in all LN229 cells.

5.2.3. DSB induction depends on NMDAR activation

The Glu-mediated induction of DSBs in LN229 cells could be demonstrated, but it is unclear which GluRs contribute to the induction of DSBs. In neurons, induction of DSBs is mediated by NMDARs, suggesting that NMDARs are also needed for the induction in GBM cells [104]. On the other hand, GBM cells show an especially high expression of Ca^{2+}-permeable AMPARs, indicating a dominant role of AMPARs in GBM cells [40].

To find the contribution of NMDARs and AMPARs we analyzed the number of 53BP1 foci after application of the specific agonists AMPA and NMDA. The endogenous release of glutamate was again inhibited with 250 μM SAS, and LN229 cells were treated with 1 mM Glu, 100 μM NMDA or 100 μM AMPA overnight and 53BP1 foci in non-S-phase cells were quantified (**Figure 11a**). First of all, Glu treatment significantly increased the number of 53BP1 foci/cell to 2.3±0.2 compared to cells only treated with SAS (1.3±0.1; $p<0.0001$) which closely matches the number of foci/cell of untreated cells (2.4±0.2). NMDA treatment led to a number of 53BP1 foci (2.3±0.2; $p<0.0001$) which is comparable to Glu treated cells, whereas addition of AMPA showed a significantly lower number of foci compared to NMDA treatment (1.8±0.2; $p=0.016$). To verify the contribution of NMDARs and AMPARs to Glu-mediated induction of DSBs, LN229 cells were treated with Glu in the presence of the specific AMPAR antagonist NBQX (100 μM) or the NMDAR antagonist ifenprodil (20 μM). Addition of ifenprodil resulted in a significant decrease of 53BP1 foci (1.6±0.2; $p<0.001$, **Figure 11a**) compared to sole Glu treatment, whereas addition of NBQX led to a significant lower decrease of 53BP1 foci compared to ifenprodil (1.95±0.16; $p=0.026$). The higher induction of 53BP1 foci upon NMDA compared to AMPA treatment and the significantly higher decrease of foci upon ifenprodil compared to NBQX treatment, lead to the assumption that Glu-mediated DSBs are dominantly induced upon NMDAR activation. Although AMPARs show a minor ability to induce DSBs their contribution to Glu-mediated DSBs was neglected in the succeeding experiments.

In order to proof, that the induction of NMDAR-dependent DSBs is not restricted to LN229 cells, we checked if another NMDAR-expressing cell line also shows induction of DSBs upon NMDAR activation. We therefore analyzed the induction of 53BP1 foci upon Glu treatment in U-87 MG cells, since they showed functional expression of NMDARs in electrophysiological experiments [73]. Again, the endogenous release of glutamate was inhibited with 250 μM SAS, and U-87 MG cells were treated with 1 mM Glu overnight. Glu treatment increased the number of 53BP1 foci/cell significantly to 2.2±0.2

(p<0.001) compared to cells solely treated with SAS (1.3±0.1), demonstrating the existence of Glu-induced DSBs also in U-87 MG cells (**Figure 11b**). To check if the foci induction is dependent on NMDAR activation we treated the cells with NMDA (100 μM), which significantly increased the number of foci/cell to 2.7±0.2 (p<0.001). For validation of the NMDAR-dependent effect, the cells were treated with 1 mM Glu and the NMDAR blocker MK801 (20 μM) and the GluN2B specific inhibitor ifenprodil (20 μM). MK801 significantly decreased the number of foci/cell to 1.8±0.2 (p=0.014), while specific inhibition of NMDAR containing the GluN2B with ifenprodil did not lead to a significant decrease (1.9±0.2; p=0.13). However, these results demonstrate that the induction of NMDAR-dependent DSBs can be observed in the U-87 MG cell line and is not restricted to LN229 cells.

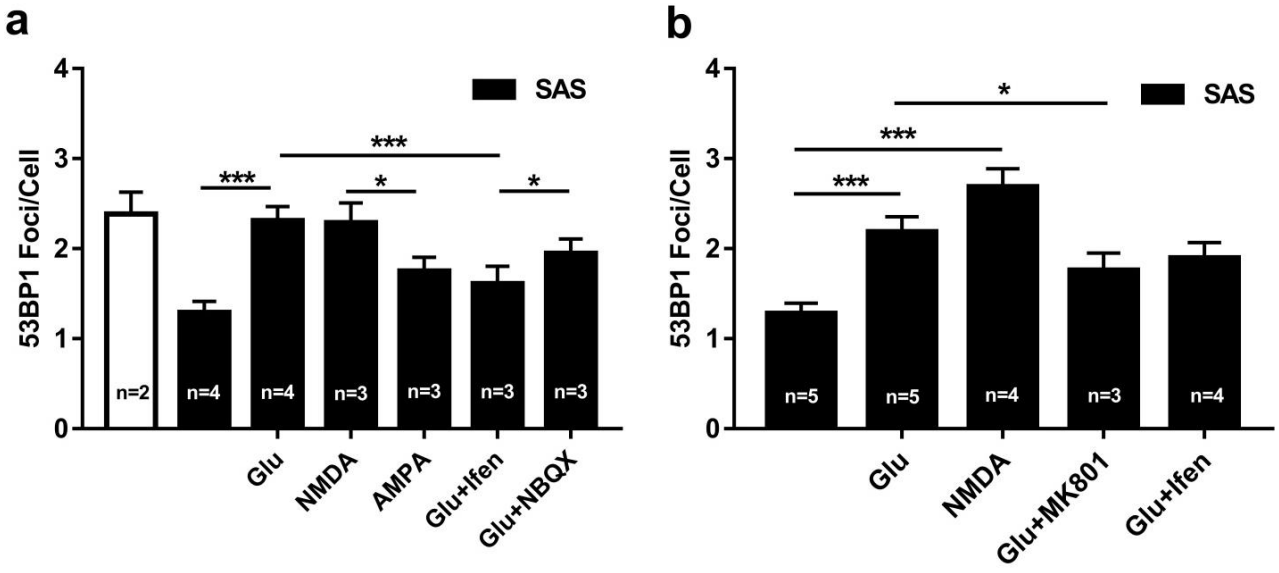

Figure 11: Glu-induced DSBs are mediated by NMDARs. (a) LN229 cells were treated with 250 µM SAS and 1 mM Glu, 100 µM NMDA, 100 µM AMPA, 1 mM Glu/20 µM ifenprodil, 1 mM Glu/100 µM NBQX or kept untreated overnight and 53BP1 foci/cell of non-S-phase cells were counted. The number of 53BP1 foci/cell increased with Glu as well as with NMDA and reach the same level as untreated cells. AMPA induced a significant lower amount of foci than NMDA. Ifenprodil led to a stronger decrease of foci than NBQX. **(b)** U-87 MG cells were treated with 250 µM SAS and 1 mM Glu, 100 µM NMDA, 1 mM Glu/20 µM MK801 or 1 mM Glu/20 µM ifenprodil overnight and 53BP1 foci/cell of non-S-phase cells were counted. Treatment with Glu and NMDA significantly increases the number of 53BP1 foci/cell compared to SAS treated cells while MK801 reduces the number of foci/cell compared to Glu treated cells. Ifenprodil shows no significant decrease of foci. (n indicated in bar diagrams; 50 cell/n; bar graphs show the mean of all single values; error bars show SEM; Mann-Whitney Test; p>0.05 (ns), p≤0.05 (*), p≤0.01 (**), p≤0.001 (***))

5.3. NMDAR-dependent DSBs are associated with Top2 activity in LN229 cells

GBM cells show NMDAR-dependent induction of DSBs. Such DSBs are inflicted by Top2β in neurons in order to promote NMDAR-dependent gene transcription [104]. To check if GBM cells and neurons use the same NMDAR signaling pathway to promote transcription, we analyzed the impact of Top2β on NMDAR-mediated DSB induction and considered the impact of cell cycle progression on DSB induction.

5.3.1. Cell cycle effects on Glu-mediated DSBs

By now, it is unclear how NMDAR activation induces DSBs in GBM cells. One possibility is that NMDAR activation could impact the cells progression through cell cycle and therefore alters the proportion of G1 and G2 phase cells. Since some DSBs, which occur during replication in S-phase, remain unrepaired as cells process through cell cycle, the number of DSBs in G2 phase often is higher than in G1-phase. To rule out the possibility that NMDAR-dependent DSBs are a result of alterations in G1/G2-phase ratio we decided to count 53BP1 foci in a single cell cycle phase. We chose to count 53BP1 foci in G1-phase cells because most transcriptional activity happens in the G1-phase of the cell cycle [134, 135]. Based on the fact that Glu-mediated DSBs have a regulative function in the transcription of several genes in neurons, we expected that Glu-mediated DSBs should be especially present in G1-phase LN229 cells.

Therefore, we treated LN229 cell with 250μM SAS and 1 mM Glu, 100 μM NMDA or 1 mM Glu and 20 μM ifenprodil and counted the number of 53BP1 foci in G1 phase cells only (**Figure 11Figure 12a**). Glu treatment significantly increases the number of foci/cell to 2.8±0.2 ($p<0.001$) compared to cells only treated with SAS (1.8±0.1) which matches the number of foci/cell in untreated cells (2.8±0.3). Treatment with NMDA significantly increased the number of 53BP1 foci to 2.3±0.2 ($p=0.013$). These results show that Glu-mediated DSBs occur in G1-phase LN229 cells. However, inhibition of NMDARs with ifenprodil led to no significant decrease of foci/cell (2.1±0.1; $p=0.08$) compared to Glu treatment.

To rule out other cell cycle-dependent effects on the number of DSBs, we additionally performed a cell cycle analysis in LN229 cells via EdU. When the cells were treated with 250 μM SAS and 1 mM Glu or 100 μM NMDA overnight no changes of the cell cycle could be detected (**Figure 12b**). The percentages of cells in G1 phase were 28.5±2.8%, 28.6±0.6% and 29.6±1.3% after SAS, SAS/Glu and SAS/NMDA treatment, respectively. In the same order the values were 61.2±6.2%, 62.1±4.5% and 60.1±5.9% for S-phase and 10.3±3.8%, 9.3±4.8% and 10.3±4.2% for G2-phase. These results show that the

induction of 53BP1 foci upon Glu treatment does not rely on changes in the cell cycle, but likely is the result of an active DSB induction upon NMDAR activation.

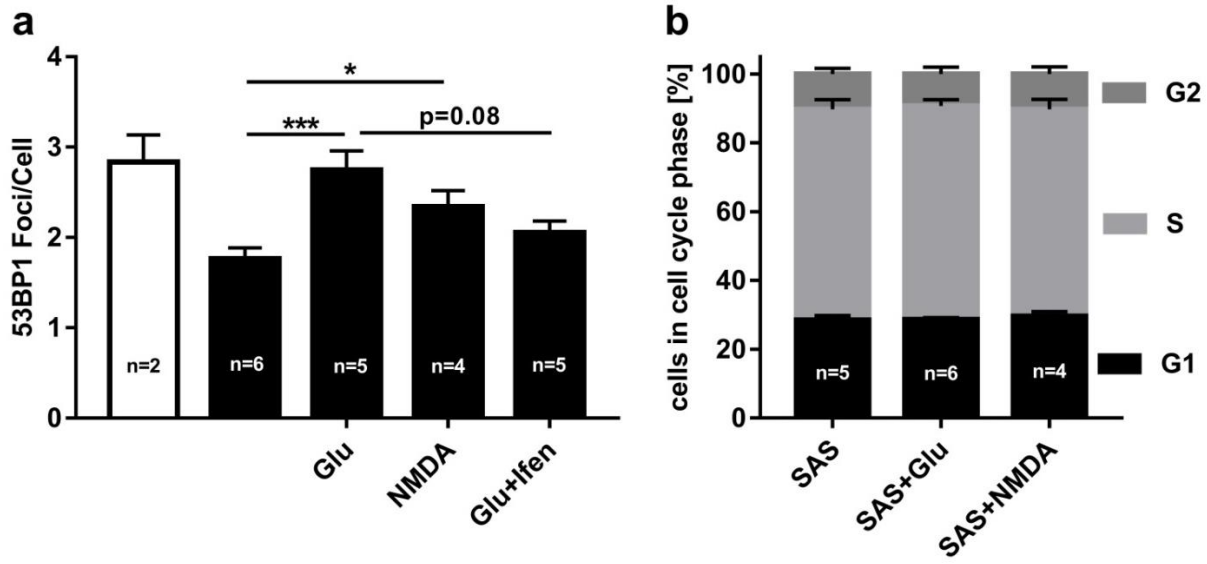

Figure 12: Cell cycle effects on Glu-mediated DSBs. (a) Analysis of 53BP1 foci/cell in G1 phase LN229 cells treated with 250 µM SAS and 100 µM NMDA, 1 mM Glu, 1 mM Glu/20 µM ifenprodil or untreated overnight. Significant increase of 53BP1 foci/cell with NMDA or Glu but no significant reduction with 20 µM ifenprodil compared to Glu treatment. (n indicated in bar diagrams, 50 cell/n, bar graphs show the mean of all single values; error bars show SEM; Mann-Whitney Test). **(b)** Cell cycle analysis of LN229 cells treated with 250 µM SAS and 1 mM Glu or 100 µM NMDA overnight. Treatment with iGluR agonists did not change the cell cycle distribution. Phases were gated by EdU and Hoechst signal. (n indicated in bar diagrams; at least 1000 cells/n; error bars show SEM; students t-test). ($p>0.05$ (ns), $p\leq0.05$ (*), $p\leq0.01$ (**), $p\leq0.001$ (***))

5.3.2. Top2 inhibition prevents NMDAR-dependent DSB induction

The role of Top2 activity for the induction of NMDAR-dependent DSBs was investigated in LN229 cells. Therefore, the cells were treated with 1 mM Glu or with 1 mM Glu and 100 nM ICRF193, an catalytic inhibitor of Top2 [136]. Additionally, samples were treated with 1 mM Glu and 20 μM MK801, a specific NMDAR blocker or 1 mM Glu and 20 μM MK801 and 100 nM ICRF193. All samples were treated overnight and 53BP1 foci were counted in G1-phase cells. Glu treated cells had a mean number of 2.4±0.2 foci/cell, which significantly decreased to 1.7±0.2 ($p=0.003$) when MK801 was added (**Figure 13**). Interestingly, the mean number of foci/cell was 1.8±0.1 after ICRF193 treatment, which is only slightly higher than the number of foci after MK801 treatment (ICRF193: 1.754±0.1358 compared to MK801: 1.733±0.178), but the decrease of foci caused by ICRF193 is statistically not significant ($p=0.12$). Double treatment with ICRF193 and MK801 led to a significant decrease of 53BP1 foci/cell compared to Glu treated cells (1.5±0.1; $p=0.001$), but compared to MK801 or ICRF193 treated cells double treatment showed no significant decrease. Although ICRF193 did not

statistically reduce the number of 53BP1 foci/cell, the amount of 53BP1 foci/cell between MK801 and ICRF193 treated cells are remarkably similar.

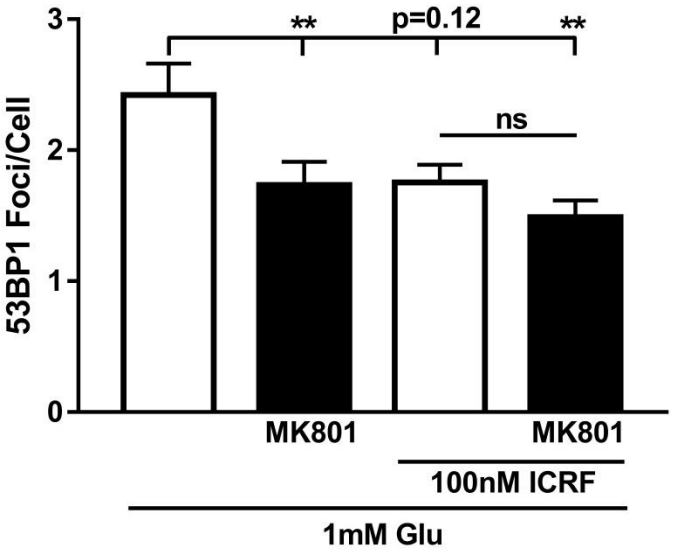

Figure 13: NMDAR-induced DSBs are mediated by Top2. LN229 cells were treated with 1 mM Glu and 20 µM MK801 or 100 nM ICRF193 or 20 µM MK801/100 nM ICRF193 overnight and 53BP1 foci were counted in G1-phase cells. MK801 treatment significantly decreased the number of foci, while ICRF193 showed a similar decrease which is not statistically significant. Combined MK801/ICRF193 treatment did not significantly decrease the amount of 53BP1 foci, indicating a sub-additive effect (n=3; 60 cell/n; bar graphs show the mean of all single values; error bars show SEM; Mann-Whitney Test; p>0.05 (ns), p≤0.05 (*), p≤0.01 (**), p≤0.001 (***)).

5.3.3. Top2β is associated with Glu-mediated DSBs

In neuronal Glu signaling Top2β is recruited to the promoter region of several genes, where it induces DSBs upon NMDAR activation. We checked if Top2β recruitment to gene sites can be observed in immunofluorescence staining. Interestingly, the immunofluorescence staining showed that Top2β forms foci structures inside the nucleus of LN229 cells (**Figure 14a**). Additionally, Top2β foci colocalize with 53BP1 foci, indicating induction of DSBs at sites of high Top2β activity.

To validate the correlation of 53BP1 and Top2β, LN229 cells were treated with 250 μM SAS or 250 μM SAS and 1 mM Glu and the amount of 53BP1 foci and Top2β foci per cell were counted in non-S-phase cells (**Figure 14b**). Glu treatment significantly increased the amount of 53BP1 foci from 1.8±0.2 to 2.4±0.2 (p=0.03) and the number of Top2β foci from 0.9±0.1 to 1.4±0.1 (p=0.01) foci/cell, which demonstrates that Glu induces a similar number of 53BP1 and Top2β foci (0.6 and 0.5 foci/cell respectively) in LN229 cells.

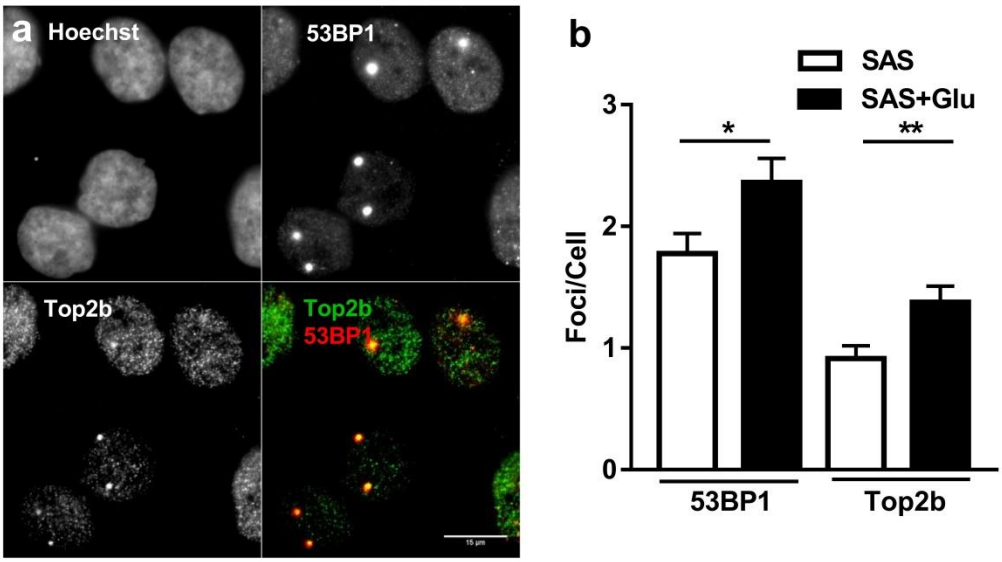

Figure 14: Top2β is accumulated at DSB sites. (a) Representative immunofluorescence staining of LN229 cells treated with 1 mM Glu overnight. The images of the Hoechst staining as well as the 53BP1 and Top2β immunofluorescence staining are displayed as well as a merge image of Top2β (green) and 53BP1 (red). Top2β forms foci structures, which colocalize with 53BP1 foci (scalebar: 15 µM). **(b)** LN229 cells were treated with 250 µM SAS **or** 250 µM SAS and 1 mM Glu and 53BP1 foci and Top2β foci were counted in non-S-phase cells. The number of 53BP1 and Top2β foci significantly increased after Glu treatment. (n=2; 40 cells/n; bar graphs show the mean of all single values; error bars show SEM; Mann-Whitney Test; $p>0.05$ (ns), $p\leq0.05$ (*), $p\leq0.01$ (**), $p\leq0.001$ (***).

5.4. Top2β-mediated NMDAR signaling regulates cFos expression in GBM cells and promotes radioresistance

So far, the results point out that Glu induces NMDAR-dependent DSBs in LN229 and U-87 MG cells, supporting the hypothesis of comparable NMDAR signaling in GBM cells and neurons. As a next step we asked if NMDAR-induced DSBs are capable to regulate gene expression in GBM cells as well. We therefore chose to analyze expression of the ERG *cFos*, which is expressed dependent on NMDAR-induced DSBs in neurons [104] and has also been correlated with GBM radioresistance [98].

5.4.1. cFos and BDNF expression are regulated by NMDAR signaling in LN229 cells

First, NMDAR and AMPAR were inhibited with 20 μM MK801/100 μM NBQX overnight and cFos expression was quantified in LN229 cells by western blot (**Figure 15a)**. The results showed a high variance, reaching from no effect to almost 50% decrease with a mean reduction of cFos expression to 80±20%. Interestingly, the GluN2B specific antagonist ifenprodil (20 μM), significantly reduced the expression of cFos to 75±11% (p=0.02), which indicates the involvement of GluN2B containing NMDARs in cFos regulation in LN229 cells. To validate the impact of NMDAR signaling on cFos expression we next inhibited two key proteins downstream in the NMDARs signaling cascade. First CREB was inhibited with 25 μM KG501, which significantly decreased the relative expression of cFos to 61±12% (p=0.01) **(Figure 15a).** Second, Top2 was inhibited with 1 μM ICRF193, which led to a down regulation of cFos to 80±4% (p=0.001). Hence, in LN229 cells three different proteins of the NMDAR signaling pathway are involved in cFos regulation.

cFos itself is a transcription factor, which regulates the expression of several genes. In neurons, for example, cFos regulates the expression of BDNF, a signaling protein which is important for neuronal survival but which also promotes glioma growth and is correlated with tumor grade [15, 137]. Therefore, the secretion of BDNF into the culturing media was used to find out whether NMDAR signaling is able to regulate the expression of genes downstream of cFos. If Glu release of LN229 cells was inhibited with 250 μM SAS overnight, the amount of BDNF secreted into the media significantly decreased to 52±13% (p=0.01) compared to cells additionally treated with 1 mM Glu (**Figure 15b**). The relative BDNF concentration of untreated cells was similar to cells treated with Glu and SAS (104±9%). These results indicate that BDNF expression is regulated by Glu.

Next, the impact of NMDAR signaling proteins on BDNF expression was checked. LN229 cells were treated with 250 μM SAS/1 mM Glu and NMDARs, CREB or Top2 were inhibited with 20 μM MK801, 25 μM KG501 or 10 μM merbarone, respectively (**Figure 15b**). Compared to Glu treatment alone, NMDAR inhibition with MK801 led to a non-significant decrease to 68±14% (p=0.69) of BDNF in the media, while inhibition of CREB significantly decreased the relative concentration of BDNF to 58±13%

(p=0.02). Inhibition of Top2 endonuclease activity with merbarone led to a mean value of 41±18%. It must be mentioned, that statistical tests have been performed on the triplet values of two independent experiments and for merbarone only a single triplet experiment was performed. Therefore, the validity of the results is improvable. However, the tendency for NMDAR, CREB and Top2β inhibition all indicate that the expression of BDNF is regulated by NMDAR signaling in LN229 cells.

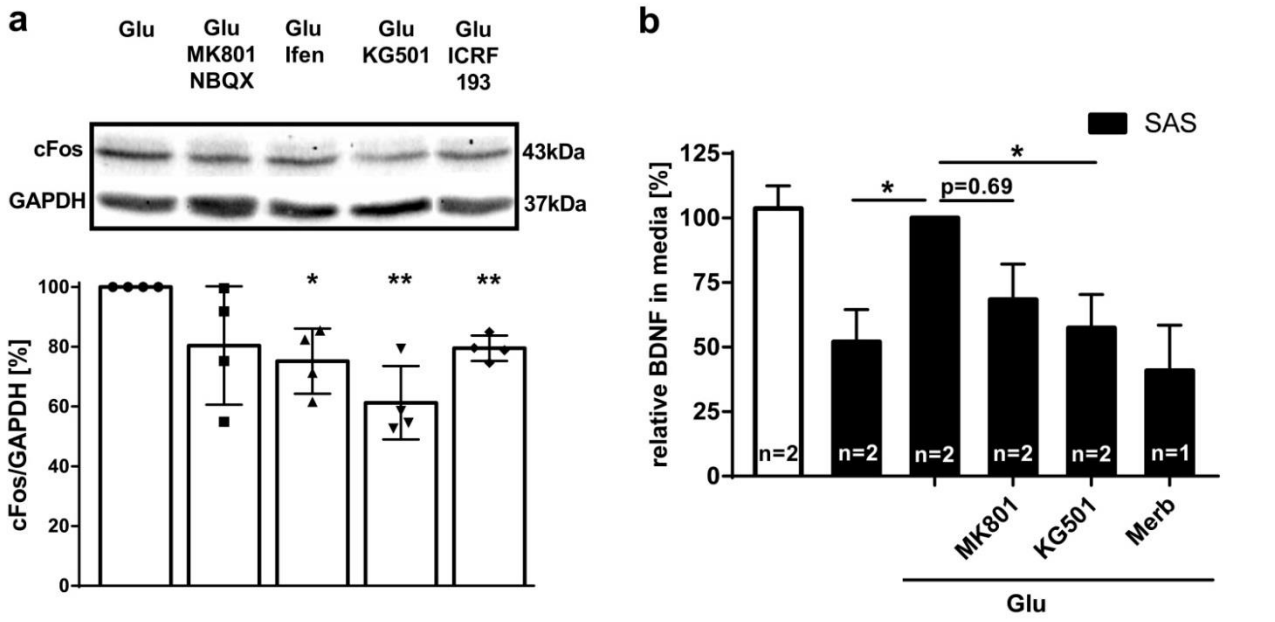

Figure 15: NMDAR signaling regulates expression of cFos and BDNF in LN229 cells. (a) Analysis of cFos expression after specific inhibition of NMDAR signaling proteins by western blot. LN229 cells were treated overnight with 1 mM Glu, 1 mM Glu/20 µM MK801/100 µM NBQX, 1 mM Glu/20 µM ifenprodil, 1 mM Glu/25 µM KG501 or 1 mM Glu/1 µM ICRF193. Representative bands from one experiment are displayed for each treatment and the bar diagram shows the mean intensity of cFos/GAPDH normalized to Glu treatment of all experiments. Inhibition of NMDARs with ifenprodil, inhibition of CREB with KG501 and inhibition of Top2 with ICRF193 all lead to a significant downregulation of cFos. Bar diagrams show the mean±SD of four experiments (one sample t-test; p>0.05 (ns), p≤0.05 (*), p≤0.01 (**), p≤0.001 (***)). **(b)** Analysis of BDNF secretion into the cell culture medium after specific activation and inhibition of NMDAR signaling proteins. LN229 cells were treated overnight with only media or 250 µM SAS, SAS/1 mM Glu, SAS/Glu/20 µM MK801, SAS/Glu/25 µM KG501 or SAS/Glu/10 µM merbarone and BDNF concentrations were measured as triplets with a colorimetric BDNF assay kit and all values were normalized to the mean value of SAS/Glu treated samples of each experiment. Inhibition of Glu release with SAS as well as inhibition of NMDARs with MK801, inhibition of CREB with KG501 and inhibition of Top2 with merbarone lead to lower amounts of BDNF compared to Glu treated samples. Bar diagrams show the mean±SEM of all measured values (n indicated in bar diagrams; one sample t-test; p>0.05 (ns), p≤0.05 (*), p≤0.01 (**), p≤0.001 (***)).

5.4.2. NMDAR signaling regulates cFos expression in primary GBM cells

Immortalized cell lines show relatively stable expression patterns and are useful to investigate specific signaling pathways under controlled conditions. But cancer cell lines do not reflect the properties of primary cancer cells, limiting the transferability of results from cell lines to primary cells. We therefore checked if NMDAR signaling also occurs in the primary GBM cell line G1702.

At first, expression of functional iGluRs was checked by electrophysiological measurements. When patched in whole cell configuration 46% of all measured G1702 cells showed currents upon application of 1 mM Glu and 100 μM Gly with a mean I_{max} of 42.7±14.7 pA, indicating functional iGluRs in primary GBM cells (**Figure 16a**).

We next investigated the expression of NMDAR subunits by immunofluorescence staining. G1702 cells showed expression of GluN1 and GluN2B subunits. Consistently, GluN2B expression could be observed at the end of cellular protrusions (**Figure 16b**), indicating the same special distribution as in LN229 cells (see **Figure 8**).

Further, the colocalisation of Top2β and 53BP1 was checked in G1702 cells treated with 1 mM Glu overnight. As seen before in LN229 cells, immunofluorescence staining revealed that Top2β forms foci which partly colocalized with 53BP1 foci (**Figure 16c** and **Figure 14a**) suggesting Top2β is recruited to Glu-mediated DSBs in G1702 cells.

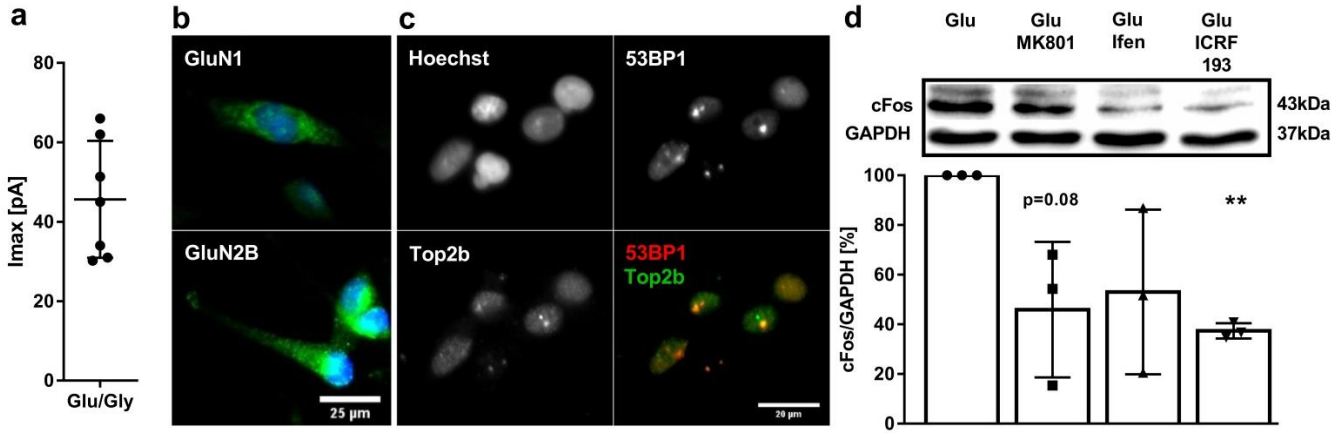

Figure 16: NMDAR signaling in primary G1702 cells. (a) Whole cell patch clamp recordings of G1702 cells were performed by Juliane Joswig. Diagram shows the mean I_{max} of responsive cells after application of 1 mM Glu/100 µM Gly (error bars show SD). **(b)** Immunofluorescence staining of GluN1 and GluN2B subunits of the NMDAR in G1702 cells. Notably GluN2B subunits are localized at the end of cellular protrusions (GluN1/GluN2B=green, Hoechst33342=blue; scalebar: 25 µm). **(c)** Immunofluorescence staining of 53BP1 (red) and Top2β (green) in G1702 cells. Top2β and 53BP1 form foci which partly colocalize (scalebar 20 µm). **(d)** Relative cFos/GAPDH expression in G1702 cells treated with 1 mM Glu and 20 µM MK801, 20 µM ifenprodil or 1 µM ICRF193 overnight and analyzed by western blot. NMDAR inhibition leads to a non-significant decrease of cFos expression while ICRF193 significantly decreases cFos expression (error bars show SD, n=3, One sample t-test, p>0.05 (ns), p≤0.05 (*), p≤0.01 (**), p≤0.001 (***)).

Finally, we analyzed the impact of NMDAR signaling on cFos expression. G1702 cells were treated with 1 mM Glu and NMDARs were inhibited with MK801 (20 μM) or the specific GluN2B inhibitor ifenprodil (20 μM) and cFos expression was quantified by western blot (**Figure 16d**). For MK801 treatment we observed a mean cFos expression of 46±27% compared to Glu treated cells ($p=0.075$). The mean expression of cFos after ifenprodil treatment was 53±33% of the control ($p=0.134$). Although the mean expression of cFos indicates even stronger down regulation than in LN229 cells, high variances do not allow to state significant changes of cFos. In contrast, inhibition of Top2 with 1 μM ICRF193 decreased the mean expression of cFos significantly to 37±3% in G1702 cells ($p<0.001$), underlining the importance of the Top2 on cFos expression in GBM cells.

5.4.3. Top2β-dependent NMDAR signaling promotes radioresistance in LN229 cells

Inhibition of Top2 endonuclease activity impacts the induction of NMDAR-mediated DSBs in LN229 cells and reliably inhibits cFos expression in two GBM cell lines. In addition, immunofluorescence staining indicated that Top2β activity is involved in NMDAR signaling in GBM cells. In neurons, the activity of Top2β mediates NMDAR-dependent gene expression [104].

To proof the specific role of Top2β for NMDAR signaling in GBM cells a knock down of Top2β with two different siRNAs was performed. Western blot analysis of siRNA transfected LN229 cells revealed that both siRNAs successfully down regulated Top2β (**Figure 17a**). Additionally, Top2β knock down significantly decreased the expression of cFos to about 50% compared to cells transfected without RNA (si1 55.7±8.2%, $p=0.012$; si2 53.6±6.1%; $p=0.005$). Remarkably, siRNA knock down of Top2β leads to a stronger decrease of cFos than inhibition of Top2 with ICRF193 (compare **Figure 15a** and **Figure 17a**). Thus, the specific knock down of Top2β with siRNA confirms that cFos regulation in LN229 cells is dependent on Top2β activity.

The discovery of NMDAR-dependent and Top2β-mediated regulation of cFos in GBM cells raises the question if inhibition of this pathway could be used as a therapeutic strategy for GBM patients. cFos overexpression has been correlated with radioresistance in GBM cells [98], suggesting that down regulation of cFos through inhibition of the NMDAR signaling pathway might sensitize GBM cell to irradiation. Therefore, clonogenic survival upon irradiation with X-rays was performed with and without siRNA knock down of Top2β. LN229 cells were transfected with one of two siRNAs (si1; si2) or without RNA (no siRNA) or kept untransfected (c) and all samples were additionally treated with 1 mM Glu. All samples were irradiated with 0 Gy-6 Gy of X-rays and clonogenic survival was determined. The results show that there is no difference between control cells (c) and cells transfected without RNA (no siRNA) (**Figure 17b**). Knock down of Top2β with siRNA2 (si2, red) significantly decreased the clonogenic survival of LN229 cells already at 2 Gy ($p=0.014$), but also at 4 Gy ($p=0.01$)

and 6 Gy (p=0.002) compared to transfection without siRNA. Transfection with siRNA1 led to a less pronounced decrease of the clonogenic survival and only shows a significant decrease at 6 Gy (p=0.035) (**Figure 17b**). However, in LN229 cells Top2β knock-down clearly decreases radioresistance.

Induction of regulative DSBs by Top2β is a later event of the NMDAR signaling pathway. To validate the specific role of NMDAR signaling on radioresistance we decided to inhibit the initial step of the NMDAR signaling pathway with the GluN2B specific antagonist ifenprodil. For this, LN229 cells were treated with 1 mM Glu or 1 mM Glu/20 μM ifenprodil, irradiated with 0 Gy-6 Gy X-rays and clonogenic survival was determined. Inhibition of NMDAR with ifenprodil significantly decreases the clonogenic survival at 2 Gy (p=0.009), 4 Gy (p=0.009) and 6 Gy (p=0.02) (**Figure 17c**). The relative survival ratio for therapeutic dose of 2 Gy is 1.7 for ifenprodil treatment and 1.4 for siRNA2, indicating a similar potency of both treatments to decrease survival upon irradiation. Hence, inhibition of NMDAR signaling at two different steps sensitizes LN229 cells to X-ray treatment, confirming the impact of NMDAR activity for GBM radioresistance.

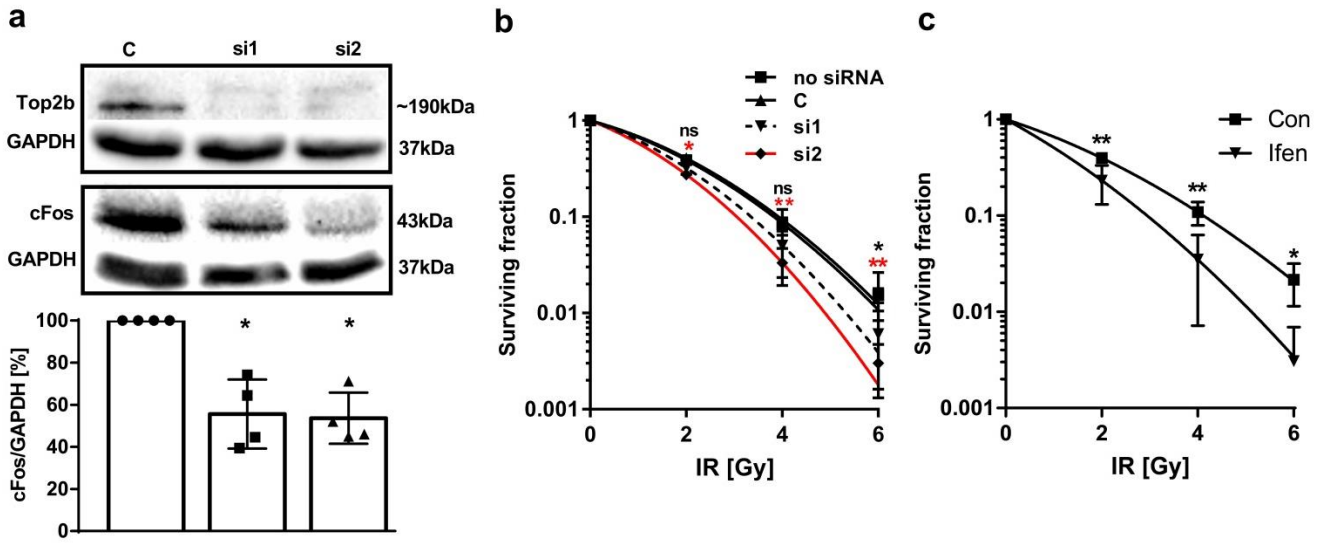

Figure 17: Inhibition of NMDARs and siRNA knock down of Top2β sensitizes LN229 cells to X-ray treatment. (a) Successful knock-down of Top2β with two different siRNAs after overnight treatment with 1 mM Glu led to a significant down regulation of cFos. Relative cFos/GAPDH expression was analyzed by western blot (n=4; error bars show SD; One sample t-test). **(b)** Clonogenic survival of LN229 cells treated with 1 mM Glu and transfected with two different siRNAs against Top2β or transfected without RNA and irradiated with 0, 2, 4 and 6 Gy X-ray. Diagram shows fitted data. siRNA2 significantly reduces the survival starting at 2 Gy. siRNA1 shows an intermediate effect (n=3, each experiment was performed as triplet; error bars show SD; student´s t-test). **(c)** Clonogenic survival of LN229 cells treated with 1 mM Glu or 1 mM Glu/20 µM ifenprodil and irradiated with 0, 2, 4 and 6 Gy X-ray. Diagram shows fitted data. Ifenprodil significantly reduces the survival starting at 2 Gy (n=3, each experiment was performed as triplet; error bars show SD; student´s t-test). (p>0.05 (ns), p≤0.05 (*), p≤0.01 (**), p≤0.001 (***))

5.5. NMDAR signaling impacts IR activated gene expression in GBM cells

IR activates CREB through phosphorylation at Ser133 in GBM cells and induces the expression of cFos in neurons [73, 138]. This raises the question if NMDAR signaling interplays the IR activated gene expression in GBM cells. We therefore decided to check the relations of NMDAR-dependent gene regulation and irradiation induced gene activation on the secretion of BDNF. At first, LN229 cells were treated without or with 250 μM SAS or additionally with 1 mM Glu and irradiated with 2 Gy X-rays or sham and all values were normalized to SAS treated cells. Since only one independent experiment was done it cannot be stated if differences are significant or not. If not treated with SAS, BDNF increased to 134±16% compared to SAS treated samples and irradiation further increased the amount of BDNF to 219±30% (**Figure 18a**). Interestingly, the amount of BDNF only increased to 106±7% upon irradiation when treated with SAS. Glu treatment increased BDNF to 127±7% and when samples were additionally irradiated BDNF further increased to 241±59%. Thus, Glu treated samples and control samples without SAS show a high secretion of BDNF upon irradiation while SAS treated samples did not.

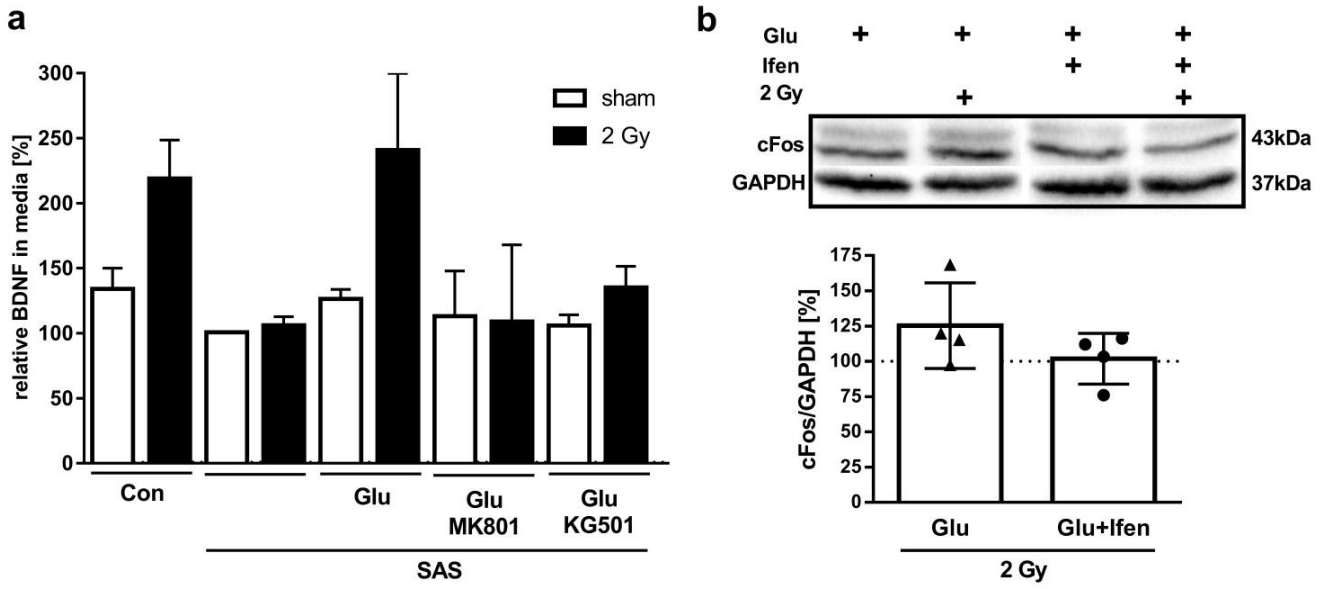

Figure 18: Impact of IR on BDNF and cFos expression upon NMDAR activation. (a) BDNF secretion in LN229 cells after treatment without or with 250 µM SAS and/or additionally 1 mM Glu, 1 mM Glu/20 µM MK801 or 1 mM Glu/25 µM KG501. The cells were irradiated with 2 Gy X-rays directly after treatment or sham irradiated and BDNF concentration in the media was measured next day with an antibody based assay kit. All values are normalized to SAS treated, sham irradiated cells. The lack of SAS or additional treatment with Glu caused a high increase of BDNF after irradiation while treatment with MK801 or KG501 blocked the increase of BDNF upon irradiation (n=1, bar diagrams show the mean value of triplets, error bars show SEM, no statistical test was done since n=1). **(b)** Radiation-induced cFos expression. LN229 cells were treated with 1 mM Glu or 1 mM Glu/20 µM ifenprodil and irradiated with 2 Gy X-rays or sham. Next day the relative amount of cFos was measured by western blot. The graphs show the relative change of cFos expression after irradiation. cFos seems to be upregulated after irradiation when treated with Glu but inhibition of NMDARs with ifenprodil seems to negate radiation-induced cFos expression. All results are tendencies; no significant chances can be stated (p=4; student´s t-test; one sample t-test).

Additionally, we checked if Glu- and radiation-dependent regulation of BDNF is mediated by NMDAR signaling proteins. For this, LN229 cells were treated with 1 mM Glu/250 μM SAS and NMDARs or CREB were inhibited with 20 μM MK801 or with 25 μM KG501 respectively. MK801 decreased the amount of BDNF compared to Glu treatment (113±35%% to 127±7%) and irradiation notably failed to increase BDNF upon MK801 treatment (109±59%) indicating that NMDAR-activation is needed for radiation-induced BDNF expression. CREB inhibition decreased the amount of BDNF compared to Glu treatment as well (106±8% to 127±7%) and irradiation led to a minor increase of BDNF (135±16%) compared to Glu treatment (241±59%) confirming the role of NMDAR signaling on LN229 radiation response.

To validate the role of NMDARs for radio response, the expression of cFos upon radiation and NMDAR inhibition was investigated. LN229 cells were treated with 1 mM Glu or 1 mM Glu/20 μM ifenprodil and irradiated with 2 Gy X-rays or sham irradiated. **Figure 18b** shows relative amount cFos in irradiated cell compared to sham irradiated cells. When treated with Glu the mean amount of cFos was increased to 125±15% after irradiation, while cells additionally treated with ifenprodil did not show an increase of cFos (102±9%) upon irradiation. However, neither the induction of cFos upon irradiation nor the reduction upon ifenprodil ($p=0.23$) treatment is statistically significant.

6. Discussion

GBM, one of the most lethal cancers, is incurable due to its high heterogeneity, radioresistance and invasive growth [8, 9, 76]. GBM cells use autocrine secreted Glu to promote their growth, survival and invasion upon activation of Ca^{2+}-permeable iGluRs [41]. The high Ca^{2+}-conductance and impact among several cancers brought NMDARs into the focus of Glu-induced malignancy in GBM [48-50, 52, 53]. Although the effects of NMDAR activation in GBM cells are well studied, the signaling pathways behind NMDAR-mediated survival and growth are unknown [50, 73, 75, 131]. We hypothesized that GBM cells use NMDAR-dependent regulation of ERGs analogous to neurons.

NMDAR-dependent expression of ERGs is a hallmark for the development and plasticity of our brain and cognitive functions like learning and memory [33, 34, 64]. The expression of these genes, which are in part also implicated in tumor malignancy, is controlled by NMDAR activity triggered induction of DSBs within their promoter regions [98-100, 104, 105]. Here, we investigated whether this particular step of neuronal signaling, the NMDAR-dependent Top2β-induced DSBs, exists analogous in GBM and thus might be a new challenging aspect for cancer therapy. Our data reveal that beyond the basal function of NMDARs in excitatory neurotransmission and synaptic plasticity, these receptors play indeed a prominent role in the malignancy of human tumors. The presented results demonstrate the increased expression of ERGs upon NMDAR activation and the implication of these genes in mediating tumor survival and radioresistance.

6.1. Role of spatial and temporal NMDAR-mediated Ca^{2+} transients in GBM physiology

To investigate NMDAR signaling in GBM cells we used the LN229 GBM cell line and first validated expression of NMDARs as well as Glu-mediated Ca^{2+} conductance (**Figure 8**).

Activation of NMDARs by Glu and subsequent channel opening and Ca^{2+}-influx are the initial steps of NMDAR signaling in neurons [79]. In LN229 cells, application of Glu/Gly transiently increased the intensity of the Ca^{2+} sensitive dye Fluo-4 in cell protrusions demonstrating Ca^{2+} transients through the membrane. The increase of intracellular Ca^{2+} showed a cell compartment specific kinetic, the nuclear area reveals a slow Ca^{2+} oscillation with high amplitudes while the faster Ca^{2+} oscillations with lower amplitudes were observed in the cellular protrusions (**Figure 8a/b**).

Immunofluorescence staining of the NMDAR subunits showed that GluN1, GluN2A and GluN2B were expressed along the membrane and especially in cell protrusions. The accumulation of NMDAR subunits inside the membrane of protrusions indicates a specialized localization of NMDAR in the membrane likely through binding of intracellular proteins (**Figure 8c**). The Glu/Gly-mediated Ca^{2+} transients in the cell protrusions fit the localization of NMDAR subunits observed in immunofluorescence staining, which suggests functional NMDARs in LN229 cells.

In neurons the binding of NMDARs to proteins of the postsynaptic density are crucial for functional NMDAR signaling [75, 79]. The specific localization of NMDARs suggests that NMDAR binding proteins might also be present in LN229 cells.

Local Ca^{2+} pules control lamellipodia retraction in migrating cells [139] and NMDAR-mediated Ca^{2+} oscillation promote neuronal migration upon CaMKII activation [90, 140]. The finding, that Glu/Gly induces local Ca^{2+} transients within lamellipodia of LN229 cells, fits to the observation that NMDARs promote migration in GBM cells [50, 73, 75] and suggest that migration is similar regulated in GBM cells and neurons.

NMDAR-mediated Ca^{2+} oscillation also control gene expression [141]. As shown, Glu/Gly treatment increased the intensity of Flou-4 inside the nuclear area (**Figure 8b**), which is likely caused by increased nuclear Ca^{2+} concentrations. Nuclear Ca^{2+} is a main mediator of NMDAR-dependent gene expression through activation of nuclear CaMKIV and CREB [61, 142]. Hence, Glu-mediated increase of nuclear Ca^{2+} in LN229 cells further suggests functional NMDAR signaling similar to neurons.

50% of the tested LN229 cells responded to Glu/Gly treatment with increased nuclear Ca^{2+}. Hence, Glu-mediated Ca^{2+} signaling is no uniform property of LN229 cells but occurs in a subpopulation of cells (**Figure 8a**), representing GBMs heterogenic nature [8]. The observation, that only a subpopulation of LN229 cells responded to Glu/Gly during Ca^{2+}-imaging, fits the results from electrophysiological measurements of LN229 cells, where Glu/Gly-induced currents in ~40% of all cells and is also supported by the finding that GBM tumors do not show homogeneous NMDAR-expression *in vivo* [50, 73].

Repeated Ca^{2+} influx does not cause an overall increase of cytoplasmic Ca^{2+} in LN229 cells (**Figure 8b**), which would be an initial mediator of excitotoxic apoptosis in neurons [77, 78]. The lack of cytoplasmic Ca^{2+} increase therefore confirms the non-toxic role of NMDARs in GBM cells [50, 73].

In sum, NMDAR expression and Glu-mediated Ca^{2+} transients at cell protrusions and lamellipodia as well as increased Ca^{2+} concentration in the nuclear area of LN229 cells indicate functional NMDAR signaling, similar to neurons. Thus, LN229 cells are a suitable cell system to investigate NMDAR signaling in GBM cells.

6.2. NMDAR activation induces DSBs in a GBM subpopulation

As described in chapter **3.3.**, the induction of DSBs into the TSS of ERGs is required for the activity-dependent expression of these genes in neurons [104]. To verify if NMDAR-mediated DSB induction is also present in GBM cells, we quantified 53BP1 foci in LN229 cells with and without Glu treatment. 53BP1 is a DNA repair protein, which accumulates at DSB site during DNA damage response and is a broadly used DSB marker which may persist after DSB repair [143].

Inhibition of Glu release via system X^-_c with SAS led to relatively low numbers of 53BP1 foci, while simulations treatment with Glu revealed significantly more 53BP1 foci in LN229 cells. Together with the rapid disappearance of 53BP1 foci already 30 min after Glu depletion, these results demonstrate Glu specific induction of 53BP1 foci in LN229 cells (**Figure 9a**). We could verify that the 53BP1 foci indeed represent DSBs by inhibiting the NHEJ DNA repair pathway (**Figure 9b**). Inhibition of DNA-PK_{cs} with NU7441 prevented the fast disappearance of 53BP1 foci upon Glu depletion. This clearly demonstrates that 53BP1 foci represent DSBs induced by Glu, which are rapidly repaired via DNA-PK_{cs}-dependent NHEJ.

DNA-PK_{cs} inhibition led to a prolonged activation of neuronal genes which are regulated via DSB induction and has been proposed to facilitate the repair of Glu-induced DSBs in neurons [104]. Furthermore, DNA-PK has been closely linked to DSB-regulated transcription in other cells [122, 123]. Unlike to neurons, in MCF-7 breast cancer cells DNA-PK_{cs} activity is supposed to be needed for the induction of regulatory DSBs rather than for repair. Pre-incubation with NU7441 prevents estrogen receptor α dependent induction of γH2AX foci in MCF-7 cells, indicating a role of DNA-PK_{cs} in the induction of DSBs or at least in the phosphorylation of γH2AX [123]. In LN229 cells, overnight treatment with NU7441 and Glu significantly increased the number of 53BP1 foci compared to Glu treatment alone (**Figure 9b**). Hence, the results from LN229 cells are comparable to the results found in neurons, where DNA-PK_{cs} mediates the repair of Glu-dependent DSBs.

Individual LN229 cells differently responded to Glu treatment with the induction of DSBs. While some cells had high numbers 53BP1 foci, other cells showed no or few foci (**Figure 10a**). To estimate how the number of DSBs is distributed among LN229 cells, we performed a high-content automatic quantification of 53BP1 foci, which confirmed the Glu-dependent induction of DSBs in LN229 cells (**Figure 10b**). The histogram of the 53BP1 foci/cell number shows a general shift from low numbers of foci in SAS treated cells to higher numbers of foci in SAS/Glu treated cells (**Figure 10c**). In neurons, NMDAR-dependent induction of DSBs was identified within 20 genes [104], suggesting that Glu induces DSBs in a specific number of genes in LN229 cell as well, which might be displayed by a specific number of 53BP1 foci. The histogram indicates a small peak at 10 foci/cell but the limited sample size does not allow a statistical validation of this increase (**Figure 10c**).

The separation of LN229 cells into three classes bearing no, one to three or more than three 53BP1 foci/cell revealed that the percentage of LN229 cells without 53BP1 foci decreases from 81.4% to 45.4% upon Glu treatment, indicating that at least 36% of all LN229 cells reacted to Glu with the induction of DSBs (**Figure 9d**). Most responding cells showed a low increase of 53BP1 foci (20 percent of all cells) but 16% of all cells also displayed a high increase of 53BP1 foci after Glu treatment (**Figure 9d)**, indicating similar induction of high and low number of DSBs in LN229 cells. Hence,

53BP1 foci counting did not reveal any preference in the number of Glu-induced DSBs in LN229 GBM cells.

The finding that at least 36% of all LN229 cells did and 45.4% did not respond to Glu treatment with the induction of 53BP1 foci (**Figure 9d**) is in line with the inhomogeneous expression of iGluRs in the LN229 cell population. Interestingly, the fraction of cells which respond to Glu with the induction of DSBs fairly matches the percentages of Glu/Gly responsive LN229 cells in Fluo-4 imaging (50%) (**Figure 8**) and in electrophysiological measurements (~40%) [73]. This suggests that LN229 cells expressing functional iGluRs also respond to Glu with the induction of DSBs.

The seemingly random induction of 53BP1 foci upon Glu treatment may be caused by a high variance (**Figure 10c)**. During the catalytic cycle Top2β-mediated DSBs are normally religated after T-segment transition (**Figure 6**) without activation of DNA damage response proteins [110]. Top2β-induced DSBs should therefore be undetectable by DSBs markers like 53BP1 and γH2AX. Nevertheless, Top2β activity has been shown to induce γH2AX and 53BP1 foci in order to start transcription [104, 122, 123]. The reason for this atypical functioning is not understood. Pommier *et al*. proposed that long-lived transcriptional DSBs might be induced stochastically upon Top2β activity or may depend on temporary blockage of Top2β religation for example through acute tensions within the G-segment [106, 109]. In consequence only a part of Top2β-induced DSBs are long-lived enough to induce DNA damage response which can be detected with DSB markers. This idea is also supported by the results of Madabhushi and colleges in 2015. They demonstrated that phosphorylation of H2AX results from Top2β-mediated DSB induction in at least 20 genes, but the number of γH2AX foci in NMDA treated neurons was below that number, the shift between the induced DSBs and the number in foci indicates that Top2β-induced DSBs do not necessarily provoke a detectable DNA damage response [104].

The stochastic variation of the detectable DSBs might provide a reason for the highly variable number of 53BP1 foci observed upon Glu treatment in LN229 cells. In addition, the overnight treatment with Glu likely leads to repeated induction and repair of Glu-induced DSBs. As a result, the analysis of 53BP1 foci includes cells which are in different stages of DSB induction and repair, leading to highly variant 53BP1 foci number. Following these thoughts, the actual amount of Glu-induced DSBs cannot be detected in most cells, while the rest of the cells show lower numbers of 53BP1 foci. Interestingly, all numbers of 53BP1 foci/cell between 0-20 could be observed in LN229 cells while only four out of 1514 cells showed more than 20 53BP1 foci. In analogy with the results observed in neurons, this may hint that NMDARs also promotes the expression of up to 20 genes upon DSB induction in LN229 cells [104].

Anyhow, counting DSB markers like 53BP1 and γH2AX is no reliable way to determine the total number of DSBs induced by Glu. DSB markers can be used to analyze the overall increase in DSBs and therefore are a useful tool to analyze Glu-induced DSBs. To analyze how many and where Glu-

dependent DSBs are induced in GBM cells other methods like chromatin immunoprecipitation DNA-sequencing (Chip-Seq) of γH2AX [104] should be used.

Activation of synaptic iGluRs upon neuronal activity leads to the induction of regulatory DSBs in neurons and NMDAR-dependent Ca^{2+} currents have been shown to mediate the DSB induction [104]. In GBM cells Ca^{2+} permeable AMPARs and NMDARs have been shown to impact cell survival and migration [40, 46, 144]. Since LN229 cells functionally express NMDARs and AMPARs [144] we analyzed the contribution of NMDAR and AMPAR activation to the induction of DSBs in LN229 cells. NMDARs activation induced the same number of 53BP1 foci as Glu, while activation of AMPARs led to a decreased number of foci (**Figure 11a**). Similar, inhibition of NMDARs with ifenprodil led to stronger decrease of 53BP1 foci in Glu treated LN229 cells than inhibition of AMPARs with NBQX (**Figure 11a**). Taken together, activation and inhibition of NMDARs and AMPARs clearly show that Glu-dependent DSBs are mainly mediated by NMDARs in LN229 cells.

However, AMPAR activation increased the number of 53BP1 foci/cell as well, indicating that AMPARs are capable to induce DSBs in LN229 cells. Similar to NMDARs, AMPARs bind to synaptic scaffold proteins, leading to a colocalization of AMPARs and NMDARs in neurons [145]. This suggests that AMPARs and NMDARs colocalize in LN229 cells as well. In contrast to most neuronal AMPARs, those AMAPRs expressed in GBM cells have been reported to be permeable for Ca^{2+} [45, 46]. This specific Ca^{2+} permeability and the putative colocalization with NMDARs might enable AMPARs to activate typical NMDAR-dependent signaling pathways, like the induction of DSBs, in GBM cells.

However, NMDARs have been identified to be the main mediator of Glu-dependent DSBs in LN229 cells. In addition to LN229 cells, NMDARs also mediate Glu-dependent induction of DSBs in the GBM cell line U-87 MG, which has been shown to express functional NMDARs [73]. Notably, NMDA treatment induced more 53BP1 foci than Glu treatment in U-87 MG cells (**Figure 11b**). LN229 cells and U-87 MG cells both secrete Glu via system X^-_c [40, 144] which has been inhibited during the experiments with SAS. But unlike other GBM cells lines [36] U-87 MG cells express the Glu transporter EAAT2, which imports extracellular Glu [146]. Combined system X^-_c inhibition and EAAT2 expression might lead to a continuous decrease of extracellular Glu but not NMDA in the media of U-87 MG cells during the experiments. The lower Glu concentration could lead to a partial activation of iGluRs and a decreased response. In contrast, LN229 cells showed slow increase of extracellular Glu even with SAS treatment, indicating no Glu uptake via EAAT2 [73].

The NMDAR blocker MK801 significantly reduced the number of 53BP1 foci in Glu treated U-87 MG, while specific inhibition of GluN2B bearing NMDARs with ifenprodil showed no significant reduction of 53BP1 foci (**Figure 11b**). The mean values of 53BP1 foci/cell were 1.8±0.2 for MK801 and 1.9±0.2 for ifenprodil treated U-87 MG cells, suggesting that an increased sample size might resolve the statistical insignificance of the ifenprodil treatment. The almost equal potency of ifenprodil and MK801 to reducing Glu included DSB suggests that even most NMDARs which contribute to DSB induction

contain GluN2B subunits. Combined with the distinct effect of ifenprodil in LN229 cells (**Figure 11a**), these results confirm the explicit role of GluN2B in NMDAR signaling of GBM cells which has been proposed in previous studies [50, 73].
In sum, we could identify Glu-mediated DSBs in a subpopulation of GBM cells. These DSBs depend on NMDAR activation and are repaired by NHEJ, which points out that the induction and repair of Glu-mediated DSBs in GBM cells is equally regulated as in neurons [104].

6.3. NMDAR-dependent DSBs are associated with Top2β activity

To address the question how Glu-dependent DSBs are induced in GBM cells, we analyzed the role of cell cycle progression of NMDAR-mediated DSBs. Replicational stress leads to the induction of DSBs during S-phase and some of these breaks remain unrepaired during cell cycle progression, leading to a higher number of DSBs in G2-phase cells than in G1-phase cells [147]. Since Glu-induced DSBs have been counted in G1- and G2-phase cells, a shift of the G1 to G2 ratio would also shift the determined mean of 53BP1 foci/cell.
Analysis of 53BP1 foci shows that Glu and NMDA induce DSBs in G1-phase cells, indicating that Glu-dependent induction of DSBs is independent of cell cycle progression (**Figure 12a**). Additionally, the EdU cell cycle assay revealed that Glu and NMDA treatment do not alter cell cycle progression of LN229 cells (**Figure 12b**), clearly demonstrating that DSB induction upon NMDAR activation is not caused by cell cycle distortions.
Glu-dependent DSBs are required to start the transcription of ERGs in neurons [104]. We expected Glu-induced DSBs to regulate gene expression in LN229 cells as well and transcriptional activity is highest during G1-phase [134, 135]. Thus, Glu-dependent DSB induction in G1-phase cells supports the idea of a transcriptional role of Glu-induced DSBs in LN229 cells. The Glu-dependent induction of DSBs in G1- phase cells, might additionally hint that Glu-induced DSBs are mediated by Top2β, since Top2α has been shown to be mainly expressed during S- and G2-phase, while Top2β is constantly expressed during all cell cycle phases [109, 118].
In neurons, NMDAR-dependent induction of DSBs is mediated by Top2β. Catalytic inhibition of Top2 with ICRF193 and simulations Glu treatment did not significantly decrease the number of 53BP1 foci in LN229 cells compared to Glu treated cells but reached almost the exact value of MK801 treated LN229 cells (**Figure 13**), suggesting that Top2 inhibition would reveal a significant reduction of 53BP1 foci upon repeated testing. Double treatment with MK801 and ICRF193 did lead to a slight and non-significant decrease which indicates a sub-additive effect of NMDAR and Top2 inhibition and suggests that NMDAR and Top2 are part of the same signaling pathway (**Figure 13**).

Our results show that Top2 activity likely induces NMDAR-dependent DSBs in LN229 cells, but it is not clear which Top2 isotype is responsible for the induction. ICRF193 has been reported to be more potent against Top2β than Top2α [148] and to avoid Top2 poisoning only 100 nM ICRF193 were used, suggesting a predominant inhibition of Top2β. However, a higher sensitivity of Top2α to ICRF193 has been reported as well, forbidding to state a specific inhibition [149].

In expectation that Top2β mediates Glu-induced of LN229 cells, we performed a immunofluorescence staining against Top2β, which revealed a focal accumulation of Top2β as well as colocalization with 53BP1 foci, indicating high Top2β activity at DSB sites (**Figure 14a**). Glu treatment significantly increased the number of Top2β foci in LN229 cells to a similar extent as 53BP1 foci (**Figure 14b**).
The increased number of Top2β foci upon Glu treatment suggests that Top2β is activated by Glu in LN229 cells. The colocalization of Top2β and 53BP1 as well as the simultaneous increase in Top2β and 53BP1 foci points out that increased Top2β activity correlates with DSBs induction in LN229 cells.
Top2β activity promotes the induction of DSBs in neurons [104] but Top2β has also been implicated in DNA damage repair of GBM cells [150], indicating that Top2β foci are the consequence of DSB induction rather than their cause. The reduced number of DSBs upon ICRF193 treatment (**Figure 13**) shows that Top2β is not involved in the repair of Glu-induced DSBs in LN229 cells, since a decreased Top2β-mediated repair upon ICRF193 treatment should lead to an increased number of DSBs.
Taken together, decreased DSB induction upon Top2 inhibition and induction of Top2β foci upon Glu treatment demonstrate that Top2β activity likely induces Glu-dependent DSBs in LN229 cells. The Top2β-dependent induction of DSBs suggests that LN229 cells use the same NMDAR signaling pathway, which regulates the expression of ERGs in neurons [104].

6.4. Implications of NMDAR-mediated DSB formation for the expression of ERGs

We checked if Top2-mediated NMADR signaling is indeed capable to promote transcription of the ERG *cFos* in LN229 cells (**Figure 15**). The results show, that cFos expression is downregulated upon inhibition of NMDARs with ifenprodil as well as inhibition of CREB with KG501 and Top2 with ICRF193 (**Figure 15a**). The decreased cFos expression upon inhibition of three different proteins in the NMDAR signaling pathway clearly demonstrate that cFos is regulated upon NMDAR activation in LN229 cells. The Top2 dependence of cFos expression in particular shows that cFos expression is mediated by the induction of regulatory DSBs, and therefore shows that NMDAR signaling in neurons and GBM cells both use the induction of DSBs to promote gene transcription of *cFos*.
Notably, the simultaneous inhibition of NMDARs with MK801 and AMAPRs with NBQX did not lead to a significant decrease of cFos but showed highly variant results (**Figure 15a**). MK801 should at least

have the same effect as ifenprodil since MK801 blocks all NMDARs. According to Choo *et al.*, the differential activation of signaling pathways by NMDARs with different subunit compositions might be one reason for the different effects of MK801 and ifenprodil on cFos expression [84]. Another reason for the high variability of MK801 provides the fact that MK801 is quite unstable under cell culture conditions, with a half-life of ~1 h [151]. We used 20 μM MK801, which should be sufficient to fully block NMDARs, but rapid degradation might result in a minor or even no block. The need for high MK801 concentrations is also demonstrated by other publications where up to 700 μM MK801 were used [53]. However, ifenprodil treatment reliably inhibited cFos expression demonstrated the impact of NMDARs on cFos expression and confirmed the important role of GluN2B for GBM cells at the same time [50].

NMDAR and Top2β inhibition caused a similar decrease of cFos expression but CREB inhibition lead to a stronger downregulation of cFos (**Figure 15a**). Phosphorylation of CREB at Ser 133 upon Glu treatment was demonstrated by Müller-Längle *et al.* [73], but CREB phosphorylation is promoted by many other factors including growth factor FGF-2 and neurotrophins [88, 152]. This suggests that CREB inhibition interferes with additional pathways which regulate CREB-dependent cFos expression in LN229 cells. In turn, the similar inhibition of cFos by ifenprodil and ICRF193 suggest that Top2β does not regulate cFos expression beside the NMDAR signaling pathway.

The transcription factor cFos is known to be important for brain development [153] and also a proto-oncogene [100, 105]. In order to estimate the impact of impaired cFos expression we analyzed the expression of BDNF, a gene which is regulated by cFos [154] and also is a prominent promoter of glioma growth [13, 15, 137, 155].

Our results show that BDNF secretion of LN229 cells increases upon Glu treatment (**Figure 15b**). The inhibition of NMDARs with MK801 revealed a non-significant ($p=0.07$) decrease, while CREB inhibition led to a stronger and significant downregulation of BDNF. Additionally, inhibition of catalytic activity of Top2 with merbarone results in downregulation of BDNF, indicated by a single experiment.

Although the decrease of BDNF secretion upon MK801 treatment is not significant, the result ($n=2$) indicates that additional data may show a significant decrease. In analogy to cFos expression, inhibition of CREB shows the strongest decrease of BDNF secretion. BDNF is regulated by nine promoter and various transcription factors, beside others also directly by CREB [156]. This might suggest that BDNF expression is not regulated by cFos in LN229 cells at all, but directly by NMDAR-mediated CREB activation. However, the downregulation of BDNF by merbarone indicates a cFos-dependent regulation of BDNF in LN229 cells. Madabhushi and colleges demonstrated that Top2β regulates the expression of cFos and explicitly showed that Top2β does not regulate the expression of BDNF [104], indicating that merbarone-mediated downregulation of BDNF depends on cFos.

In summary our results revealed functional NMDAR signaling in LN229 cells, which is capable to regulate gene expression. The Top2-dependent expression of cFos shows that LN229 cells use the induction of regulatory DSBs to promote the expression of an ERG, which demonstrates that LN229 cells use the same regulatory pathway for ERG expression as neurons [104]. Furthermore, the NMDAR-dependent expression of cFos and BDNF demonstrates that NMDAR signaling may have high impact on the malignancy of GBM cells, since cFos and BDNF promote radioresistance and tumor growth and have been shown to correlate with poor prognosis in glioma [13, 15, 98, 137, 155].

The investigation of NMDAR signaling in LN229 cells revealed the impact of NMDAR-dependent and Top2β-mediated induction of DSBs. We used the primary GBM cell line G1702, which was grown as spheroid culture, to check if our findings in GBM cell lines also reflect the situation in primary GBM. Whole cell patch clamp recording showed Glu/Gly-induced currents in 46% of the cells, demonstrating functional iGluR expression (**Figure 16a**). Immunofluorescence staining of GluN1 and GluN2B revealed a similar localization pattern as in LN229 cells (**Figure 16b** and **Figure 8c**), indicating similar binding to intracellular proteins and therefore similar signaling. In additional analogy to LN229 cells, G1702 cells show Glu-induced 53BP1 foci which colocalize with Top2β foci, indicating Top2β-mediated induction of DSBs (**Figure 16c** and **Figure 14a**). Last, NMDAR inhibition with MK801 and ifenprodil led to a highly variable and therefore non-significant decrease of cFos, while inhibition of Top2β significantly decreased the expression of cFos in G1702 cells (**Figure 16d**).
These results demonstrate that the primary GBM cell line G1702 shows similar signaling properties as LN229 cells. The expression of iGluR in 46% of all G1702 cell and 40% of all LN229 cells [73], the similar expression of NMDAR subunits and the colocalization of 53BP1 and Top2β foci upon Glu treatment demonstrate a similar subpopulation of Glu responsive cells in both cell lines. However, the observation of patch clamp recording and immunofluorescence staining might not fully reflect the situation of the spheroid culture since G1702 cells were grown as adherent cultures on laminin for these experiments.
The analysis of cFos expression in G1702 cells revealed a similar high variance upon MK801 treatment as in LN229 cells, which might as well be caused be the relative instability of MK801 [151]. Unexpectedly, in G1702 cell ifenprodil treatment led to a similar high variance in cFos expression as MK801, suggesting variant expression of GluN2B containing NMDARs. Interestingly, in tumor samples high GluN2B expression has been shown at the tumor margin but not inside the tumor mass [50], suggesting that the relative number of GluN2B expression cells changes with the size of the tumor. This observation might also be true for spheroid cultures. If GluN2B expression is restricted to the edge of the spheroid, the spheroid size would determine the percentage of GluN2B-expressing cells. For our experiments we did not use spheroids of controlled size, which might have led to the high variances in

the percentage of GluN2B-expressing cells and consequently in cFos expression upon ifenprodil treatment.

Despite the high variances, both NMDAR inhibitors show the potency to reduce cFos expression in G1702 even more than in LN229 cells. This is also supported by the fact, that Top2 inhibition decreases cFos expression to 37% in G1702 compared to 80% in LN229 cells (**Figure 15a** and **Figure 16d**). Interestingly, Top2 inhibition leads to a very reliable reduction of cFos expression with might indicate that NMDARs signaling can be effectively shut down upon Top2 inhibition in G1702 cells, although the results cannot exclude that Top2 activity might regulate cFos expression through additional pathways.

Taken together, the primary G1702 cell line reveals several properties of functional NMDAR signaling, which shows a high potential in the regulation of cFos expression in this cells. This demonstrates together with our results from LN229 and U-87 MG cells that NMDAR signaling might be broadly used among GBMs. Additionally the results confirm the potential benefit of Top2 inhibition in order to control cFos expression in GBM therapy.

GBM cells use Top2β-dependent NMDAR signaling to regulate genes which have been shown to promote GBM growth, survival and radioresistance [13, 15, 98, 137, 155]. Especially inhibition of Top2 has been shown reliably decrease the expression of cFos in LN229 and G1702 cells. We therefore tested if Top2 inhibition can be used to impair NMDAR-mediated survival in GBM cells [73]. First we assured that impaired cFos expression upon ICRF193 treatment actually depends on the inhibition of Top2β. The specific knock-down of Top2β with two different siRNAs significantly reduces cFos expression in LN229 cells (**Figure 17a**), demonstrating Top2β specific cFos regulation. To validate the impact of Top2β-mediated gene expression the clonogenic survival of LN229 cells with Top2β knock-down were irradiated with increasing doses of X-rays (**Figure 17b**). Top2β siRNA2 significantly decreased the clonogenic survival of LN229 cells already at 2 Gy while siRNA1 shows a lower decrease of clonogenic survival which still was significant at 6 Gy. This clearly shows that Top2β expression promotes radioresistance in LN229 cells. Interestingly, inhibition of NMDARs with ifenprodil reduced the clonogenic survival of LN229 cells to a similar extent as Top2β inhibition, with a relative survival ratio of 1.7 for ifenprodil treatment and 1.4 for siRNA2 for the therapeutic dose of 2 Gy (**Figure 17c**).

The different radiosensitizing of siRNA1 and siRNA2 is surprising, since both siRNA similarly reduced the expression of cFos. The effectiveness of the siRNA to reduce the cologenic survival strongly depends on the transfection efficiency. siRNA1 already showed a higher variance in the reduction of cFos (**Figure 17a**), maybe caused by slow RNA degradation, and the lower transfection efficiency subsequently resulted in a reduced effect during the cologenic survival assay.

The limited effectiveness of siRNA knock-down might also provide a reason why Top2β knock-down was slightly less effective to reduce the radioresistance in LN229 cells than ifenprodil treatment.

Additionally, NMDAR activation led to a faster repair of DSBs upon IR [73] which might also contribute to the radiosensitizing effect of NMDAR inhibition and suggests that NMDARs operates through additional pathways as the Top2β-mediated induction of ERGs in GBM cells.
The striking effect of GluN2B specific inhibition with ifenprodil on NMDAR-dependent induction of DSBs and cFos expression as well as its radiosensitizing effect demonstrates the GluN2B containing NMDARs play an outstanding role in Glu-mediated gene expression and radioresistance of GBM cells. Together with the finding that GluN2B promotes the migration and invasion of GBM cells, our results show that GluN2B-expressing subpopulations promote GBM malignancy [50, 73, 75]. The highly invasive growth and radioresistance are challenging GBM therapy and inhibition of GluN2B therefore might provide a promising enhancement to current GBM therapies.

6.5. IR enhances NMDAR signaling in GBM cells

Adriana Längle demonstrates in her PhD thesis that both, NMDAR activation and IR phosphorylate CREB at Ser133 in LN229 cells and proposed an interplay of NMDAR signaling and IR damage response [144]. Interestingly, cFos expression is also promoted upon IR in the brain [138], suggesting that IR might promote the expression of genes which are regulated by NMDAR signaling. To investigate a potential interplay the secretion of BDNF upon radiation and NMDAR activation was measured in a single experiment (**Figure 18a**). IR increased the amount of BDNF only upon simultaneous Glu treatment but not upon inhibition of NMDARs or CREB. Although no statistical test could be performed these results indicate the NMDAR-mediated activation of CREB increases IR activated gene expression and therefore confirm the idea of a NMDAR-IR interplay. Further, IR potentially increases the expression of cFos upon Glu treatment, which is negated by simultaneous block of NMDARs with ifenprodil (**Figure 18b**).
These results support the idea of NMDAR- and IR signaling interplay and suggest that NMDAR-mediated radioresistance in GBM cells is enhanced by the link of NMDAR- and IR signaling pathways [73] (**Figure 17b/c**).
In fact Adriana Längle suggested that in addition to phosphorylation of CREB at Ser133, IR might lead to phosphorylation of Thr100, Ser111 and Ser121, which deactivate CREB and reduce CREB-dependent transcription [144]. In contrast, our results suppose an amplifying effect of IR on NMDAR-mediated transcription. IR can activate MAPK pathways including the ERK1/2 signaling pathway [157]. IR generated reactive oxygen species are known to participate in ERK1/2 activation [158]. In addition, IR promoted the secretion of TGFα in A431 squamous carcinoma cells and MDA-MB-231 mammary carcinoma cells, which induced EGFR-dependent ERK1/2 activation and increased the cells survival and proliferation [159].

However, ERK1/2 activation alone does not promote CREB-dependent gene transcription in neurons [160]. As described in **Figure 4a,** different signaling pathways contribute to the activation of NMDAR-mediated gene transcription. NMDAR-dependent activation of ERK1/2 needs the increase of cytosolic Ca^{2+} near NMDARs to phosphorylate CREB at Ser133 [86]. Although phosphorylation of CREB at Ser133 is a commonly used marker for CREB activation it is not sufficient to activate CREB-mediated gene transcription [152]. To fully activate NMDAR-mediated gene expression the increase of nuclear Ca^{2+} is needed [141, 142]. Chawla and colleges demonstrated, that increased nuclear Ca^{2+} mediates CaMKIV-dependent phosphorylation of the CREB cofactor CBP at Ser301, which activates CBP and promotes transcription [160]. While nuclear Ca^{2+} increase is sufficient to promote CREB-mediated transcription, activation of ERK1/2 has been shown to enhance CREB-mediated transcription [160] and is thought to be needed for sustained CREB-mediated transcription upon NMDAR activation [86].

The enhancing effect of ERK1/2 activation on NMDAR-mediated gene transcription suggests that strong IR-mediated ERK1/2 activation might lead to the increased expression of cFos and BDNF upon NMDAR activation in GBM cells. In turn, ERK1/2 activation upon IR cannot promote cFos expression, because CBP is not activated through the increase of nuclear Ca^{2+}. Interestingly, Ca^{2+} increases the catalytic activity of Top2β [161], suggesting that NMDAR-mediated increase of nuclear calcium might directly contribute to Top2β activation.

The synergy of IR and NMDAR activation on the transcription of cFos and BDNF may explain the high impact of NMDAR signaling on GBM radioresistance and provides further evidence that inhibition of NMDAR signaling is a potential target for adjuvant radiotherapy.

7. Conclusion

The results presented in this work demonstrate that GBM cells use Top2β-dependent NMDAR signaling to promote the transcription of the ERG cFos resulting in increased radioresistance. Based on our findings and results from other groups [40, 73] we propose how Glu mediates ERG expression in GBM cells (**Figure 19**). Glu secreted via system X^-_c activates NMDARs in GBM cells, which leads to Ca^{2+} transients over the membrane and increases free nuclear Ca^{2+}. While local Ca^{2+} increase at the membrane activates the ERK1/2 pathway, the nuclear Ca^{2+} increase activates CaMKIV which both lead to phosphorylation of CREB at Ser133. Additionally, CBP is activated by CaMKIV and Top2β gets activated either through not identified kinases or directly by increased Ca^{2+} concentration inside the nucleus. Top2β then induces a DSB in the promoter region of cFos allowing enhancer and promoter interaction. Together, Top2β-mediated DSB induction and phosphorylation of CREB and CBP initiate transcription of cFos and subsequently BDNF, which promote survival and radioresistance.

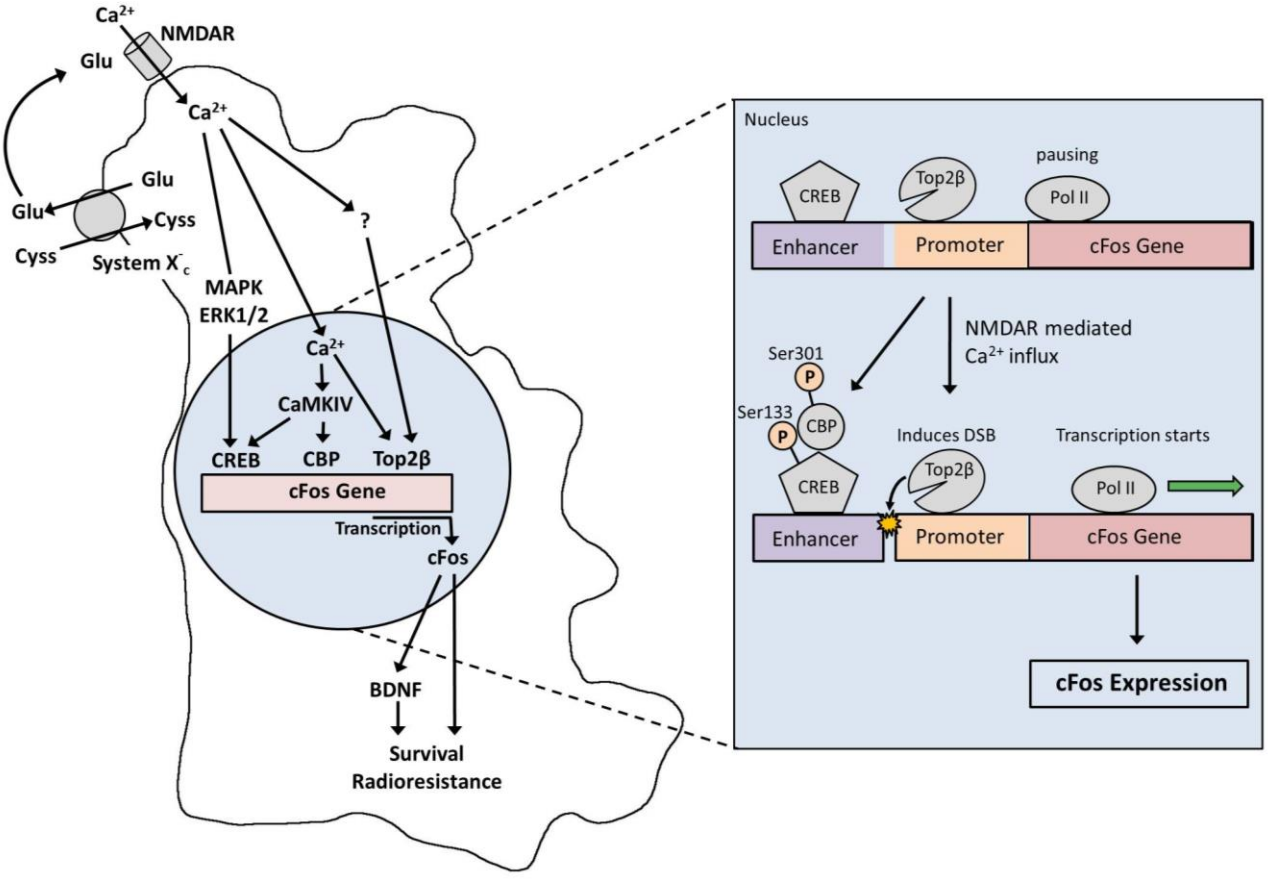

Figure 19: Schematic model of NMDAR-mediated ERG transcription in GBM cells. Glu secreted by system X^-_c accumulates and activates NMDARs in the lamellipodia and cell protrusions of GBM cells. NMDAR channel opening allows Ca^{2+} transients lead to the activation of ERK1/2 and increase free nuclear Ca^{2+}, likely released by intracellular Ca^{2+} stores. ERK1/2 facilitates the phosphorylation of CREB at Ser133. The increased nuclear Ca^{2+} allows CaMKIV to phosphorylate CREB and CBP at Ser133 and Ser301 and increases Top2β catalytic activity. Additionally, Top2β may be activated by nuclear Ca^{2+} and/or unknown kinases. Upon activation, Top2β inflicts a single DSB into the TSS of the *cFos* gene, which enables promoter-enhancer interaction. This interaction, together with CREB and CBP activation, allows the pausing Pol II to start transcription. cFos promotes the expression of BDNF and both, cFos and BDNF, promote survival and radioresistance in GBM cells.

The identification of Top2β-mediated, regulatory DSBs upon NMDAR activation show that GBM cells use a neuronal signaling pathway in order to promote their own survival and radioresistance [104]. Further, the usage of similar signaling pathways of GBM cells and neurons demonstrate that efficient NMDAR-mediated transcription of ERGs does not need the highly complex architecture of synapses. This indicates that limited requirements are needed for functional NMDAR signaling, although NMDAR signaling in neurons may be more complex, allowing fine-tuning of the NMDAR response during synaptic transmission [79].

NMDARs are expressed among several cancer types, which use NMDARs to promote survival and growth [52-54, 72, 89]. Additionally, Top2β-mediated gene expression is also used by different cancer cell lines upon activation of estrogen and androgen receptors [117], which suggests that other cancer types than GBM may meet the requirements for NMDAR-dependent and Top2β-mediated gene transcription. Thus, the mechanism identified by us in GBM cells, might also promote radioresistance in other NMDAR-expressing cancer cells.

We also found, that NMDAR expression and NMDAR-mediated induction of DSB is no uniform property of GBM cells, but occur in a subpopulation of cells. Interestingly, high expression of Ca^{2+} permeable iGluRs and Top2β has been demonstrated in GBM TICs [150, 162] and NMDAR expression of GBM cells promotes invasive growth and correlated with poor prognosis [50]. In addition, NMDARs and cFos have been suggested as predictive markers for poor prognosis in other cancer types as well [49, 53, 99, 101], suggesting that inhibition of NMDAR signaling affects a subpopulation of cells, which is highly relevant for therapy.

The high impact of NMDAR signaling on the clonogenic survival of GBM cells supports this idea. The radiosensitizing effect of ifenprodil and Top2β knock-down provides a rationality to inhibit NMDARs and Top2β in adjuvant radiotherapy. The explicit role of GluN2B containing NMDARs in migration and invasive growths of GBM cells has been reported by others [50, 73, 75]. The radiosensitizing effect as well as the prominent reduction of Glu-mediated DSBs and cFos expression by ifenprodil expands the impact of GluN2B on GBM cells. Hence, specific targeting of GluN2B containing NMDARs in GBM therapy should be considered. Notably, in some countries ifenprodil is an approved drug used to prevent brain damage during cerebral infarction or hemorrhage. Ifenprodil has limited side effects and clinical trials currently test if ifenprodil might be useful for other applications as well [163, 164]. Thus, the use of ifenprodil appears to be a promising way to improve GBM therapy.

Additionally, Top2 inhibitors are broadly used in cancer treatment and therefore several approved drugs with known side effects are available. Most therapeutic strategies which aim at Top2 in cancer use Top2 poisons to induce DNA damage and apoptosis [112]. In this line, the targeted activation of Top2β-mediated transcription in cancer cells combined with Top2 poisoning has been proposed [117]. However, a general disadvantage of Top2 poisons is that the induction of DSBs endangers genomic integrity and promotes secondary malignancies [114, 115].

Knock-down of Top2β with siRNA in GBM cells and the resulting radiosensitization demonstrate that DSB induction is not needed for a Top2β targeted therapy. Our results indicate that catalytic Top2 inhibitors like ICRF193 and merbarone, which stop Top2β-mediated transcription, might be useful in adjuvant radiotherapy of NMDAR-expressing tumors. The usage of catalytic Top2 inhibitors is thought to be less toxic than Top2 poisons and therefore may help to reduce the side effects of cancer therapy [110].

In summary, the results presented in this thesis confirms the striking role of NMDARs and especially the GluN2B subunit on GBM cells and provides rationality to inhibit Top2β-dependent NMDAR signaling in cancer therapy.

8. Literature

1. Kleihues, P., D.N. Louis, B.W. Scheithauer, L.B. Rorke, G. Reifenberger, P.C. Burger, and W.K. Cavenee, *The WHO classification of tumors of the nervous system.* J Neuropathol Exp Neurol, 2002. **61**(3): p. 215-25; discussion 226-9.
2. Tamimi, A.F. and M. Juweid, *Epidemiology and Outcome of Glioblastoma*, in *Glioblastoma*, S. De Vleeschouwer, Editor 2017, : The Authors.: Brisbane AU.
3. Wen, P.Y. and S. Kesari, *Malignant gliomas in adults.* N Engl J Med, 2008. **359**(5): p. 492-507.
4. Stupp, R., M.E. Hegi, W.P. Mason, M.J. van den Bent, M.J. Taphoorn, R.C. Janzer, S.K. Ludwin, A. Allgeier, B. Fisher, K. Belanger, P. Hau, A.A. Brandes, J. Gijtenbeek, C. Marosi, C.J. Vecht, K. Mokhtari, P. Wesseling, S. Villa, E. Eisenhauer, T. Gorlia, M. Weller, D. Lacombe, J.G. Cairncross, and R.O. Mirimanoff, *Effects of radiotherapy with concomitant and adjuvant temozolomide versus radiotherapy alone on survival in glioblastoma in a randomised phase III study: 5-year analysis of the EORTC-NCIC trial.* Lancet Oncol, 2009. **10**(5): p. 459-66.
5. van den Bent, M.J., A.A. Brandes, R. Rampling, M.C. Kouwenhoven, J.M. Kros, A.F. Carpentier, P.M. Clement, M. Frenay, M. Campone, J.F. Baurain, J.P. Armand, M.J. Taphoorn, A. Tosoni, H. Kletzl, B. Klughammer, D. Lacombe, and T. Gorlia, *Randomized phase II trial of erlotinib versus temozolomide or carmustine in recurrent glioblastoma: EORTC brain tumor group study 26034.* J Clin Oncol, 2009. **27**(8): p. 1268-74.
6. Geraldo, L.H.M., C. Garcia, A.C.C. da Fonseca, L.G.F. Dubois, E.S.T.C.L. de Sampaio, D. Matias, E.S. de Camargo Magalhaes, R.F. do Amaral, B.G. da Rosa, I. Grimaldi, F.S. Leser, J.M. Janeiro, L. Macharia, C. Wanjiru, C.M. Pereira, V. Moura-Neto, C. Freitas, and F.R.S. Lima, *Glioblastoma Therapy in the Age of Molecular Medicine.* Trends Cancer, 2019. **5**(1): p. 46-65.
7. Weller, M., N. Butowski, D.D. Tran, L.D. Recht, M. Lim, H. Hirte, L. Ashby, L. Mechtler, S.A. Goldlust, F. Iwamoto, J. Drappatz, D.M. O'Rourke, M. Wong, M.G. Hamilton, G. Finocchiaro, J. Perry, W. Wick, J. Green, Y. He, C.D. Turner, M.J. Yellin, T. Keler, T.A. Davis, R. Stupp, and J.H. Sampson, *Rindopepimut with temozolomide for patients with newly diagnosed, EGFRvIII-expressing glioblastoma (ACT IV): a randomised, double-blind, international phase 3 trial.* Lancet Oncol, 2017. **18**(10): p. 1373-1385.
8. Sottoriva, A., I. Spiteri, S.G. Piccirillo, A. Touloumis, V.P. Collins, J.C. Marioni, C. Curtis, C. Watts, and S. Tavare, *Intratumor heterogeneity in human glioblastoma reflects cancer evolutionary dynamics.* Proc Natl Acad Sci U S A, 2013. **110**(10): p. 4009-14.
9. Kelley, K., J. Knisely, M. Symons, and R. Ruggieri, *Radioresistance of Brain Tumors.* Cancers (Basel), 2016. **8**(4).
10. Bao, S., Q. Wu, R.E. McLendon, Y. Hao, Q. Shi, A.B. Hjelmeland, M.W. Dewhirst, D.D. Bigner, and J.N. Rich, *Glioma stem cells promote radioresistance by preferential activation of the DNA damage response.* Nature, 2006. **444**(7120): p. 756-60.
11. Stupp, R., W.P. Mason, M.J. van den Bent, M. Weller, B. Fisher, M.J. Taphoorn, K. Belanger, A.A. Brandes, C. Marosi, U. Bogdahn, J. Curschmann, R.C. Janzer, S.K. Ludwin, T. Gorlia, A. Allgeier, D. Lacombe, J.G. Cairncross, E. Eisenhauer, and R.O. Mirimanoff, *Radiotherapy plus concomitant and adjuvant temozolomide for glioblastoma.* N Engl J Med, 2005. **352**(10): p. 987-96.
12. Wild-Bode, C., M. Weller, A. Rimner, J. Dichgans, and W. Wick, *Sublethal irradiation promotes migration and invasiveness of glioma cells: implications for radiotherapy of human glioblastoma.* Cancer Res, 2001. **61**(6): p. 2744-50.
13. Wang, X., B.C. Prager, Q. Wu, L.J.Y. Kim, R.C. Gimple, Y. Shi, K. Yang, A.R. Morton, W. Zhou, Z. Zhu, E.A.A. Obara, T.E. Miller, A. Song, S. Lai, C.G. Hubert, X. Jin, Z. Huang, X. Fang, D. Dixit, W. Tao, K. Zhai, C. Chen, Z. Dong, G. Zhang, S.M. Dombrowski, P. Hamerlik, S.C. Mack, S. Bao, and J.N. Rich, *Reciprocal Signaling between Glioblastoma Stem Cells and Differentiated Tumor Cells Promotes Malignant Progression.* Cell Stem Cell, 2018. **22**(4): p. 514-528 e5.
14. Mann, J., R. Ramakrishna, R. Magge, and A.G. Wernicke, *Advances in Radiotherapy for Glioblastoma.* Front Neurol, 2017. **8**: p. 748.

15. Xiong, J., L. Zhou, Y. Lim, M. Yang, Y.H. Zhu, Z.W. Li, F.H. Zhou, Z.C. Xiao, and X.F. Zhou, *Mature BDNF promotes the growth of glioma cells in vitro.* Oncol Rep, 2013. **30**(6): p. 2719-24.
16. Jiapaer, S., T. Furuta, S. Tanaka, T. Kitabayashi, and M. Nakada, *Potential Strategies Overcoming the Temozolomide Resistance for Glioblastoma.* Neurol Med Chir (Tokyo), 2018. **58**(10): p. 405-421.
17. Erickson, L.C., *The role of O-6 methylguanine DNA methyltransferase (MGMT) in drug resistance and strategies for its inhibition.* Semin Cancer Biol, 1991. **2**(4): p. 257-65.
18. Dean, M., T. Fojo, and S. Bates, *Tumour stem cells and drug resistance.* Nat Rev Cancer, 2005. **5**(4): p. 275-84.
19. Vescovi, A.L., R. Galli, and B.A. Reynolds, *Brain tumour stem cells.* Nat Rev Cancer, 2006. **6**(6): p. 425-36.
20. Singh, S.K., C. Hawkins, I.D. Clarke, J.A. Squire, J. Bayani, T. Hide, R.M. Henkelman, M.D. Cusimano, and P.B. Dirks, *Identification of human brain tumour initiating cells.* Nature, 2004. **432**(7015): p. 396-401.
21. Eramo, A., L. Ricci-Vitiani, A. Zeuner, R. Pallini, F. Lotti, G. Sette, E. Pilozzi, L.M. Larocca, C. Peschle, and R. De Maria, *Chemotherapy resistance of glioblastoma stem cells.* Cell Death Differ, 2006. **13**(7): p. 1238-41.
22. Kawamura, Y., J. Takouda, K. Yoshimoto, and K. Nakashima, *New aspects of glioblastoma multiforme revealed by similarities between neural and glioblastoma stem cells.* Cell Biol Toxicol, 2018. **34**(6): p. 425-440.
23. Ma, D.K., M.A. Bonaguidi, G.L. Ming, and H. Song, *Adult neural stem cells in the mammalian central nervous system.* Cell Res, 2009. **19**(6): p. 672-82.
24. Lee, J.H., J.E. Lee, J.Y. Kahng, S.H. Kim, J.S. Park, S.J. Yoon, J.Y. Um, W.K. Kim, J.K. Lee, J. Park, E.H. Kim, W.S. Chung, Y.S. Ju, S.H. Park, J.H. Chang, and S.G. Kang, *Human glioblastoma arises from subventricular zone cells with low-level driver mutations.* Nature, 2018. **560**(7717): p. 243-247.
25. Verhaak, R.G., K.A. Hoadley, E. Purdom, V. Wang, Y. Qi, M.D. Wilkerson, C.R. Miller, L. Ding, T. Golub, J.P. Mesirov, G. Alexe, M. Lawrence, M. O'Kelly, P. Tamayo, B.A. Weir, S. Gabriel, W. Winckler, S. Gupta, L. Jakkula, H.S. Feiler, J.G. Hodgson, C.D. James, J.N. Sarkaria, C. Brennan, A. Kahn, P.T. Spellman, R.K. Wilson, T.P. Speed, J.W. Gray, M. Meyerson, G. Getz, C.M. Perou, and D.N. Hayes, *Integrated genomic analysis identifies clinically relevant subtypes of glioblastoma characterized by abnormalities in PDGFRA, IDH1, EGFR, and NF1.* Cancer Cell, 2010. **17**(1): p. 98-110.
26. Phillips, H.S., S. Kharbanda, R. Chen, W.F. Forrest, R.H. Soriano, T.D. Wu, A. Misra, J.M. Nigro, H. Colman, L. Soroceanu, P.M. Williams, Z. Modrusan, B.G. Feuerstein, and K. Aldape, *Molecular subclasses of high-grade glioma predict prognosis, delineate a pattern of disease progression, and resemble stages in neurogenesis.* Cancer Cell, 2006. **9**(3): p. 157-73.
27. Beier, D., J.B. Schulz, and C.P. Beier, *Chemoresistance of glioblastoma cancer stem cells--much more complex than expected.* Mol Cancer, 2011. **10**: p. 128.
28. Lee, J., S. Kotliarova, Y. Kotliarov, A. Li, Q. Su, N.M. Donin, S. Pastorino, B.W. Purow, N. Christopher, W. Zhang, J.K. Park, and H.A. Fine, *Tumor stem cells derived from glioblastomas cultured in bFGF and EGF more closely mirror the phenotype and genotype of primary tumors than do serum-cultured cell lines.* Cancer Cell, 2006. **9**(5): p. 391-403.
29. Marcus, H.J., K.L. Carpenter, S.J. Price, and P.J. Hutchinson, *In vivo assessment of high-grade glioma biochemistry using microdialysis: a study of energy-related molecules, growth factors and cytokines.* J Neurooncol, 2010. **97**(1): p. 11-23.
30. Takano, T., J.H. Lin, G. Arcuino, Q. Gao, J. Yang, and M. Nedergaard, *Glutamate release promotes growth of malignant gliomas.* Nat Med, 2001. **7**(9): p. 1010-5.
31. Seidlitz, E.P., M.K. Sharma, Z. Saikali, M. Ghert, and G. Singh, *Cancer cell lines release glutamate into the extracellular environment.* Clin Exp Metastasis, 2009. **26**(7): p. 781-7.
32. Yelamanchi, S.D., S. Jayaram, J.K. Thomas, S. Gundimeda, A.A. Khan, A. Singhal, T.S. Keshava Prasad, A. Pandey, B.L. Somani, and H. Gowda, *A pathway map of glutamate metabolism.* J Cell Commun Signal, 2016. **10**(1): p. 69-75.

33. McEntee, W.J. and T.H. Crook, *Glutamate: its role in learning, memory, and the aging brain.* Psychopharmacology (Berl), 1993. **111**(4): p. 391-401.
34. Lau, C.G., K. Takeuchi, A. Rodenas-Ruano, Y. Takayasu, J. Murphy, M.V. Bennett, and R.S. Zukin, *Regulation of NMDA receptor Ca2+ signalling and synaptic plasticity.* Biochem Soc Trans, 2009. **37**(Pt 6): p. 1369-74.
35. Moots, P.L., R.J. Maciunas, D.R. Eisert, R.A. Parker, K. Laporte, and B. Abou-Khalil, *The course of seizure disorders in patients with malignant gliomas.* Arch Neurol, 1995. **52**(7): p. 717-24.
36. Ye, Z.C., J.D. Rothstein, and H. Sontheimer, *Compromised glutamate transport in human glioma cells: reduction-mislocalization of sodium-dependent glutamate transporters and enhanced activity of cystine-glutamate exchange.* J Neurosci, 1999. **19**(24): p. 10767-77.
37. Lo, M., Y.Z. Wang, and P.W. Gout, *The x(c)- cystine/glutamate antiporter: a potential target for therapy of cancer and other diseases.* J Cell Physiol, 2008. **215**(3): p. 593-602.
38. Robert, S.M. and H. Sontheimer, *Glutamate transporters in the biology of malignant gliomas.* Cell Mol Life Sci, 2014. **71**(10): p. 1839-54.
39. Chung, W.J., S.A. Lyons, G.M. Nelson, H. Hamza, C.L. Gladson, G.Y. Gillespie, and H. Sontheimer, *Inhibition of cystine uptake disrupts the growth of primary brain tumors.* J Neurosci, 2005. **25**(31): p. 7101-10.
40. Lyons, S.A., W.J. Chung, A.K. Weaver, T. Ogunrinu, and H. Sontheimer, *Autocrine glutamate signaling promotes glioma cell invasion.* Cancer Res, 2007. **67**(19): p. 9463-71.
41. de Groot, J. and H. Sontheimer, *Glutamate and the biology of gliomas.* Glia, 2011. **59**(8): p. 1181-9.
42. Neant, I., J. Haiech, M.C. Kilhoffer, F.J. Aulestia, M. Moreau, and C. Leclerc, *Ca(2+)-Dependent Transcriptional Repressors KCNIP and Regulation of Prognosis Genes in Glioblastoma.* Front Mol Neurosci, 2018. **11**: p. 472.
43. Hansen, K.B., F. Yi, R.E. Perszyk, H. Furukawa, L.P. Wollmuth, A.J. Gibb, and S.F. Traynelis, *Structure, function, and allosteric modulation of NMDA receptors.* J Gen Physiol, 2018. **150**(8): p. 1081-1105.
44. Dingledine, R., K. Borges, D. Bowie, and S.F. Traynelis, *The glutamate receptor ion channels.* Pharmacol Rev, 1999. **51**(1): p. 7-61.
45. Ishiuchi, S., Y. Yoshida, K. Sugawara, M. Aihara, T. Ohtani, T. Watanabe, N. Saito, K. Tsuzuki, H. Okado, A. Miwa, Y. Nakazato, and S. Ozawa, *Ca2+-permeable AMPA receptors regulate growth of human glioblastoma via Akt activation.* J Neurosci, 2007. **27**(30): p. 7987-8001.
46. Ishiuchi, S., K. Tsuzuki, Y. Yoshida, N. Yamada, N. Hagimura, H. Okado, A. Miwa, H. Kurihara, Y. Nakazato, M. Tamura, T. Sasaki, and S. Ozawa, *Blockage of Ca(2+)-permeable AMPA receptors suppresses migration and induces apoptosis in human glioblastoma cells.* Nat Med, 2002. **8**(9): p. 971-8.
47. Stepulak, A., H. Luksch, C. Gebhardt, O. Uckermann, J. Marzahn, M. Sifringer, W. Rzeski, C. Staufner, K.S. Brocke, L. Turski, and C. Ikonomidou, *Expression of glutamate receptor subunits in human cancers.* Histochem Cell Biol, 2009. **132**(4): p. 435-45.
48. Deutsch, S.I., A.H. Tang, J.A. Burket, and A.D. Benson, *NMDA receptors on the surface of cancer cells: target for chemotherapy?* Biomed Pharmacother, 2014. **68**(4): p. 493-6.
49. Abdul, M. and N. Hoosein, *N-methyl-D-aspartate receptor in human prostate cancer.* J Membr Biol, 2005. **205**(3): p. 125-8.
50. Li, L. and D. Hanahan, *Hijacking the neuronal NMDAR signaling circuit to promote tumor growth and invasion.* Cell, 2013. **153**(1): p. 86-100.
51. Mittelbronn, M., P. Harter, A. Warth, A. Lupescu, K. Schilbach, H. Vollmann, D. Capper, B. Goeppert, K. Frei, H. Bertalanffy, M. Weller, R. Meyermann, F. Lang, and P. Simon, *EGR-1 is regulated by N-methyl-D-aspartate-receptor stimulation and associated with patient survival in human high grade astrocytomas.* Brain Pathol, 2009. **19**(2): p. 195-204.
52. North, W.G., G. Gao, A. Jensen, V.A. Memoli, and J. Du, *NMDA receptors are expressed by small-cell lung cancer and are potential targets for effective treatment.* Clin Pharmacol, 2010. **2**: p. 31-40.

53. North, W.G., G. Gao, V.A. Memoli, R.H. Pang, and L. Lynch, *Breast cancer expresses functional NMDA receptors.* Breast Cancer Res Treat, 2010. **122**(2): p. 307-14.
54. Watanabe, K., T. Kanno, T. Oshima, H. Miwa, C. Tashiro, and T. Nishizaki, *The NMDA receptor NR2A subunit regulates proliferation of MKN45 human gastric cancer cells.* Biochem Biophys Res Commun, 2008. **367**(2): p. 487-90.
55. Laube, B., J. Kuhse, and H. Betz, *Evidence for a tetrameric structure of recombinant NMDA receptors.* J Neurosci, 1998. **18**(8): p. 2954-61.
56. Kleckner, N.W. and R. Dingledine, *Requirement for glycine in activation of NMDA-receptors expressed in Xenopus oocytes.* Science, 1988. **241**(4867): p. 835-7.
57. Ahmadi, S., U. Muth-Selbach, A. Lauterbach, P. Lipfert, W.L. Neuhuber, and H.U. Zeilhofer, *Facilitation of spinal NMDA receptor currents by spillover of synaptically released glycine.* Science, 2003. **300**(5628): p. 2094-7.
58. Wang, J.Q., M.L. Guo, D.Z. Jin, B. Xue, E.E. Fibuch, and L.M. Mao, *Roles of subunit phosphorylation in regulating glutamate receptor function.* Eur J Pharmacol, 2014. **728**: p. 183-7.
59. Hansen, K.B., H. Brauner-Osborne, and J. Egebjerg, *Pharmacological characterization of ligands at recombinant NMDA receptor subtypes by electrophysiological recordings and intracellular calcium measurements.* Comb Chem High Throughput Screen, 2008. **11**(4): p. 304-15.
60. Kuner, T. and R. Schoepfer, *Multiple structural elements determine subunit specificity of Mg2+ block in NMDA receptor channels.* J Neurosci, 1996. **16**(11): p. 3549-58.
61. Zhang, S.J., M.N. Steijaert, D. Lau, G. Schutz, C. Delucinge-Vivier, P. Descombes, and H. Bading, *Decoding NMDA receptor signaling: identification of genomic programs specifying neuronal survival and death.* Neuron, 2007. **53**(4): p. 549-62.
62. Ikonomidou, C., F. Bosch, M. Miksa, P. Bittigau, J. Vockler, K. Dikranian, T.I. Tenkova, V. Stefovska, L. Turski, and J.W. Olney, *Blockade of NMDA receptors and apoptotic neurodegeneration in the developing brain.* Science, 1999. **283**(5398): p. 70-4.
63. Jiang, H., W. Jiang, J. Zou, B. Wang, M. Yu, Y. Pan, Y. Lin, Y. Mao, and Y. Wang, *The GluN2B subunit of N-methy-D-asparate receptor regulates the radial migration of cortical neurons in vivo.* Brain Res, 2015. **1610**: p. 20-32.
64. Cull-Candy, S., S. Brickley, and M. Farrant, *NMDA receptor subunits: diversity, development and disease.* Curr Opin Neurobiol, 2001. **11**(3): p. 327-35.
65. Inagaki, N., H. Kuromi, T. Gonoi, Y. Okamoto, H. Ishida, Y. Seino, T. Kaneko, T. Iwanaga, and S. Seino, *Expression and role of ionotropic glutamate receptors in pancreatic islet cells.* FASEB J, 1995. **9**(8): p. 686-91.
66. Gu, Y., P.G. Genever, T.M. Skerry, and S.J. Publicover, *The NMDA type glutamate receptors expressed by primary rat osteoblasts have the same electrophysiological characteristics as neuronal receptors.* Calcif Tissue Int, 2002. **70**(3): p. 194-203.
67. Chen, J., Y. Zheng, H. Xiong, and Y. Ou, *NMDA receptors are involved in the regulation of BMP4-mediated survival in rat cochlear epithelial cells.* Neurosci Lett, 2014. **566**: p. 275-9.
68. Morhenn, V.B., M. Murakami, T. O'Grady, J. Nordberg, and R.L. Gallo, *Characterization of the expression and function of N-methyl-D-aspartate receptor in keratinocytes.* Exp Dermatol, 2004. **13**(8): p. 505-11.
69. Gonzalez-Cadavid, N.F., I. Ryndin, D. Vernet, T.R. Magee, and J. Rajfer, *Presence of NMDA receptor subunits in the male lower urogenital tract.* J Androl, 2000. **21**(4): p. 566-78.
70. Seeber, S., K. Becker, T. Rau, T. Eschenhagen, C.M. Becker, and M. Herkert, *Transient expression of NMDA receptor subunit NR2B in the developing rat heart.* J Neurochem, 2000. **75**(6): p. 2472-7.
71. Stepulak, A., R. Rola, K. Polberg, and C. Ikonomidou, *Glutamate and its receptors in cancer.* J Neural Transm (Vienna), 2014. **121**(8): p. 933-44.
72. Rzeski, W., L. Turski, and C. Ikonomidou, *Glutamate antagonists limit tumor growth.* Proc Natl Acad Sci U S A, 2001. **98**(11): p. 6372-7.

73. Müller-Längle, A., H. Lutz, S. Hehlgans, F. Rodel, K. Rau, and B. Laube, *NMDA Receptor-Mediated Signaling Pathways Enhance Radiation Resistance, Survival and Migration in Glioblastoma Cells-A Potential Target for Adjuvant Radiotherapy.* Cancers (Basel), 2019. **11**(4).
74. Kim, M.S., K. Yamashita, J.H. Baek, H.L. Park, A.L. Carvalho, M. Osada, M.O. Hoque, S. Upadhyay, M. Mori, C. Moon, and D. Sidransky, *N-methyl-D-aspartate receptor type 2B is epigenetically inactivated and exhibits tumor-suppressive activity in human esophageal cancer.* Cancer Res, 2006. **66**(7): p. 3409-18.
75. Li, L., Q. Zeng, A. Bhutkar, J.A. Galvan, E. Karamitopoulou, D. Noordermeer, M.W. Peng, A. Piersigilli, A. Perren, I. Zlobec, H. Robinson, M.L. Iruela-Arispe, and D. Hanahan, *GKAP Acts as a Genetic Modulator of NMDAR Signaling to Govern Invasive Tumor Growth.* Cancer Cell, 2018. **33**(4): p. 736-751 e5.
76. Lefranc, F., E. Le Rhun, R. Kiss, and M. Weller, *Glioblastoma quo vadis: Will migration and invasiveness reemerge as therapeutic targets?* Cancer Treat Rev, 2018. **68**: p. 145-154.
77. Dong, X.X., Y. Wang, and Z.H. Qin, *Molecular mechanisms of excitotoxicity and their relevance to pathogenesis of neurodegenerative diseases.* Acta Pharmacol Sin, 2009. **30**(4): p. 379-87.
78. Giorgi, C., F. Baldassari, A. Bononi, M. Bonora, E. De Marchi, S. Marchi, S. Missiroli, S. Patergnani, A. Rimessi, J.M. Suski, M.R. Wieckowski, and P. Pinton, *Mitochondrial Ca(2+) and apoptosis.* Cell Calcium, 2012. **52**(1): p. 36-43.
79. Hardingham, G.E. and H. Bading, *Synaptic versus extrasynaptic NMDA receptor signalling: implications for neurodegenerative disorders.* Nat Rev Neurosci, 2010. **11**(10): p. 682-96.
80. Waxman, E.A. and D.R. Lynch, *N-methyl-D-aspartate receptor subtypes: multiple roles in excitotoxicity and neurological disease.* Neuroscientist, 2005. **11**(1): p. 37-49.
81. Kim, E., S. Naisbitt, Y.P. Hsueh, A. Rao, A. Rothschild, A.M. Craig, and M. Sheng, *GKAP, a novel synaptic protein that interacts with the guanylate kinase-like domain of the PSD-95/SAP90 family of channel clustering molecules.* J Cell Biol, 1997. **136**(3): p. 669-78.
82. Akazawa, C., R. Shigemoto, Y. Bessho, S. Nakanishi, and N. Mizuno, *Differential expression of five N-methyl-D-aspartate receptor subunit mRNAs in the cerebellum of developing and adult rats.* J Comp Neurol, 1994. **347**(1): p. 150-60.
83. Loftis, J.M. and A. Janowsky, *The N-methyl-D-aspartate receptor subunit NR2B: localization, functional properties, regulation, and clinical implications.* Pharmacol Ther, 2003. **97**(1): p. 55-85.
84. Choo, A.M., D.M. Geddes-Klein, A. Hockenberry, D. Scarsella, M.N. Mesfin, P. Singh, T.P. Patel, and D.F. Meaney, *NR2A and NR2B subunits differentially mediate MAP kinase signaling and mitochondrial morphology following excitotoxic insult.* Neurochem Int, 2012. **60**(5): p. 506-16.
85. Zhou, X., Q. Ding, Z. Chen, H. Yun, and H. Wang, *Involvement of the GluN2A and GluN2B subunits in synaptic and extrasynaptic N-methyl-D-aspartate receptor function and neuronal excitotoxicity.* J Biol Chem, 2013. **288**(33): p. 24151-9.
86. Hardingham, G.E., F.J. Arnold, and H. Bading, *A calcium microdomain near NMDA receptors: on switch for ERK-dependent synapse-to-nucleus communication.* Nat Neurosci, 2001. **4**(6): p. 565-6.
87. Joyal, J.L., D.J. Burks, S. Pons, W.F. Matter, C.J. Vlahos, M.F. White, and D.B. Sacks, *Calmodulin activates phosphatidylinositol 3-kinase.* J Biol Chem, 1997. **272**(45): p. 28183-6.
88. Peltier, J., A. O'Neill, and D.V. Schaffer, *PI3K/Akt and CREB regulate adult neural hippocampal progenitor proliferation and differentiation.* Dev Neurobiol, 2007. **67**(10): p. 1348-61.
89. Stepulak, A., M. Sifringer, W. Rzeski, S. Endesfelder, A. Gratopp, E.E. Pohl, P. Bittigau, U. Felderhoff-Mueser, A.M. Kaindl, C. Buhrer, H.H. Hansen, M. Stryjecka-Zimmer, L. Turski, and C. Ikonomidou, *NMDA antagonist inhibits the extracellular signal-regulated kinase pathway and suppresses cancer growth.* Proc Natl Acad Sci U S A, 2005. **102**(43): p. 15605-10.
90. Strack, S., R.B. McNeill, and R.J. Colbran, *Mechanism and regulation of calcium/calmodulin-dependent protein kinase II targeting to the NR2B subunit of the N-methyl-D-aspartate receptor.* J Biol Chem, 2000. **275**(31): p. 23798-806.

91. Liu, Z., G. Han, Y. Cao, Y. Wang, and H. Gong, *Calcium/calmodulindependent protein kinase II enhances metastasis of human gastric cancer by upregulating nuclear factorkappaB and Aktmediated matrix metalloproteinase9 production.* Mol Med Rep, 2014. **10**(5): p. 2459-64.
92. Chi, M., H. Evans, J. Gilchrist, J. Mayhew, A. Hoffman, E.A. Pearsall, H. Jankowski, J.S. Brzozowski, and K.A. Skelding, *Phosphorylation of calcium/calmodulin-stimulated protein kinase II at T286 enhances invasion and migration of human breast cancer cells.* Sci Rep, 2016. **6**: p. 33132.
93. Chen, W., P. An, X.J. Quan, J. Zhang, Z.Y. Zhou, L.P. Zou, and H.S. Luo, *Ca(2+)/calmodulin-dependent protein kinase II regulates colon cancer proliferation and migration via ERK1/2 and p38 pathways.* World J Gastroenterol, 2017. **23**(33): p. 6111-6118.
94. Steven, A. and B. Seliger, *Control of CREB expression in tumors: from molecular mechanisms and signal transduction pathways to therapeutic target.* Oncotarget, 2016. **7**(23): p. 35454-65.
95. Chhabra, A., H. Fernando, G. Watkins, R.E. Mansel, and W.G. Jiang, *Expression of transcription factor CREB1 in human breast cancer and its correlation with prognosis.* Oncol Rep, 2007. **18**(4): p. 953-8.
96. Melnikova, V.O., A.S. Dobroff, M. Zigler, G.J. Villares, R.R. Braeuer, H. Wang, L. Huang, and M. Bar-Eli, *CREB inhibits AP-2alpha expression to regulate the malignant phenotype of melanoma.* PLoS One, 2010. **5**(8): p. e12452.
97. Tan, X., S. Wang, B. Yang, L. Zhu, B. Yin, T. Chao, J. Zhao, J. Yuan, B. Qiang, and X. Peng, *The CREB-miR-9 negative feedback minicircuitry coordinates the migration and proliferation of glioma cells.* PLoS One, 2012. **7**(11): p. e49570.
98. Liu, Z.G., G. Jiang, J. Tang, H. Wang, G. Feng, F. Chen, Z. Tu, G. Liu, Y. Zhao, M.J. Peng, Z.W. He, X.Y. Chen, H. Lindsay, Y.F. Xia, and X.N. Li, *c-Fos over-expression promotes radioresistance and predicts poor prognosis in malignant glioma.* Oncotarget, 2016. **7**(40): p. 65946-65956.
99. Mahner, S., C. Baasch, J. Schwarz, S. Hein, L. Wolber, F. Janicke, and K. Milde-Langosch, *C-Fos expression is a molecular predictor of progression and survival in epithelial ovarian carcinoma.* Br J Cancer, 2008. **99**(8): p. 1269-75.
100. Miller, A.D., T. Curran, and I.M. Verma, *c-fos protein can induce cellular transformation: a novel mechanism of activation of a cellular oncogene.* Cell, 1984. **36**(1): p. 51-60.
101. Volm, M., P. Drings, and W. Wodrich, *Prognostic significance of the expression of c-fos, c-jun and c-erbB-1 oncogene products in human squamous cell lung carcinomas.* J Cancer Res Clin Oncol, 1993. **119**(9): p. 507-10.
102. Muhammad, N., S. Bhattacharya, R. Steele, N. Phillips, and R.B. Ray, *Involvement of c-Fos in the Promotion of Cancer Stem-like Cell Properties in Head and Neck Squamous Cell Carcinoma.* Clin Cancer Res, 2017. **23**(12): p. 3120-3128.
103. Cole, A.J., D.W. Saffen, J.M. Baraban, and P.F. Worley, *Rapid increase of an immediate early gene messenger RNA in hippocampal neurons by synaptic NMDA receptor activation.* Nature, 1989. **340**(6233): p. 474-6.
104. Madabhushi, R., F. Gao, A.R. Pfenning, L. Pan, S. Yamakawa, J. Seo, R. Rueda, T.X. Phan, H. Yamakawa, P.C. Pao, R.T. Stott, E. Gjoneska, A. Nott, S. Cho, M. Kellis, and L.H. Tsai, *Activity-Induced DNA Breaks Govern the Expression of Neuronal Early-Response Genes.* Cell, 2015. **161**(7): p. 1592-605.
105. Healy, S., P. Khan, and J.R. Davie, *Immediate early response genes and cell transformation.* Pharmacol Ther, 2013. **137**(1): p. 64-77.
106. Kim, T.K., M. Hemberg, J.M. Gray, A.M. Costa, D.M. Bear, J. Wu, D.A. Harmin, M. Laptewicz, K. Barbara-Haley, S. Kuersten, E. Markenscoff-Papadimitriou, D. Kuhl, H. Bito, P.F. Worley, G. Kreiman, and M.E. Greenberg, *Widespread transcription at neuronal activity-regulated enhancers.* Nature, 2010. **465**(7295): p. 182-7.
107. Nitiss, J.L., *DNA topoisomerase II and its growing repertoire of biological functions.* Nat Rev Cancer, 2009. **9**(5): p. 327-37.
108. West, A.E. and M.E. Greenberg, *Neuronal activity-regulated gene transcription in synapse development and cognitive function.* Cold Spring Harb Perspect Biol, 2011. **3**(6).

109. Pommier, Y., Y. Sun, S.N. Huang, and J.L. Nitiss, *Roles of eukaryotic topoisomerases in transcription, replication and genomic stability.* Nat Rev Mol Cell Biol, 2016. **17**(11): p. 703-721.
110. Larsen, A.K., A.E. Escargueil, and A. Skladanowski, *Catalytic topoisomerase II inhibitors in cancer therapy.* Pharmacol Ther, 2003. **99**(2): p. 167-81.
111. Liu, L.F., *DNA topoisomerase poisons as antitumor drugs.* Annu Rev Biochem, 1989. **58**: p. 351-75.
112. Nitiss, J.L., *Targeting DNA topoisomerase II in cancer chemotherapy.* Nat Rev Cancer, 2009. **9**(5): p. 338-50.
113. Marinello, J., M. Delcuratolo, and G. Capranico, *Anthracyclines as Topoisomerase II Poisons: From Early Studies to New Perspectives.* Int J Mol Sci, 2018. **19**(11).
114. Felix, C.A., *Secondary leukemias induced by topoisomerase-targeted drugs.* Biochim Biophys Acta, 1998. **1400**(1-3): p. 233-55.
115. Azarova, A.M., Y.L. Lyu, C.P. Lin, Y.C. Tsai, J.Y. Lau, J.C. Wang, and L.F. Liu, *Roles of DNA topoisomerase II isozymes in chemotherapy and secondary malignancies.* Proc Natl Acad Sci U S A, 2007. **104**(26): p. 11014-9.
116. Haffner, M.C., M.J. Aryee, A. Toubaji, D.M. Esopi, R. Albadine, B. Gurel, W.B. Isaacs, G.S. Bova, W. Liu, J. Xu, A.K. Meeker, G. Netto, A.M. De Marzo, W.G. Nelson, and S. Yegnasubramanian, *Androgen-induced TOP2B-mediated double-strand breaks and prostate cancer gene rearrangements.* Nat Genet, 2010. **42**(8): p. 668-75.
117. Haffner, M.C., A.M. De Marzo, A.K. Meeker, W.G. Nelson, and S. Yegnasubramanian, *Transcription-induced DNA double strand breaks: both oncogenic force and potential therapeutic target?* Clin Cancer Res, 2011. **17**(12): p. 3858-64.
118. Bakshi, R.P., S. Galande, and K. Muniyappa, *Functional and regulatory characteristics of eukaryotic type II DNA topoisomerase.* Crit Rev Biochem Mol Biol, 2001. **36**(1): p. 1-37.
119. Yang, X., W. Li, E.D. Prescott, S.J. Burden, and J.C. Wang, *DNA topoisomerase IIbeta and neural development.* Science, 2000. **287**(5450): p. 131-4.
120. Lyu, Y.L., C.P. Lin, A.M. Azarova, L. Cai, J.C. Wang, and L.F. Liu, *Role of topoisomerase IIbeta in the expression of developmentally regulated genes.* Mol Cell Biol, 2006. **26**(21): p. 7929-41.
121. Lyu, Y.L. and J.C. Wang, *Aberrant lamination in the cerebral cortex of mouse embryos lacking DNA topoisomerase IIbeta.* Proc Natl Acad Sci U S A, 2003. **100**(12): p. 7123-8.
122. Ju, B.G., V.V. Lunyak, V. Perissi, I. Garcia-Bassets, D.W. Rose, C.K. Glass, and M.G. Rosenfeld, *A topoisomerase IIbeta-mediated dsDNA break required for regulated transcription.* Science, 2006. **312**(5781): p. 1798-802.
123. Williamson, L.M. and S.P. Lees-Miller, *Estrogen receptor alpha-mediated transcription induces cell cycle-dependent DNA double-strand breaks.* Carcinogenesis, 2011. **32**(3): p. 279-85.
124. Trotter, K.W., H.A. King, and T.K. Archer, *Glucocorticoid Receptor Transcriptional Activation via the BRG1-Dependent Recruitment of TOP2beta and Ku70/86.* Mol Cell Biol, 2015. **35**(16): p. 2799-817.
125. Darby, M.K., B. Schmitt, J. Jongstra-Bilen, and H.P. Vosberg, *Inhibition of calf thymus type II DNA topoisomerase by poly(ADP-ribosylation).* EMBO J, 1985. **4**(8): p. 2129-34.
126. Ju, B.G. and M.G. Rosenfeld, *A breaking strategy for topoisomerase IIbeta/PARP-1-dependent regulated transcription.* Cell Cycle, 2006. **5**(22): p. 2557-60.
127. Canitrot, Y., G. de Murcia, and B. Salles, *Decreased expression of topoisomerase IIbeta in poly(ADP-ribose) polymerase-deficient cells.* Nucleic Acids Res, 1998. **26**(22): p. 5134-8.
128. Nakazawa, N., O. Arakawa, M. Ebe, and M. Yanagida, *Casein kinase II-dependent phosphorylation of DNA topoisomerase II suppresses the effect of a catalytic topo II inhibitor, ICRF-193, in fission yeast.* J Biol Chem, 2019. **294**(10): p. 3772-3782.
129. Joo, J.Y., B.W. Kim, J.S. Lee, J.Y. Park, S. Kim, Y.J. Yun, S.H. Lee, H. Rhim, and H. Son, *Activation of NMDA receptors increases proliferation and differentiation of hippocampal neural progenitor cells.* J Cell Sci, 2007. **120**(Pt 8): p. 1358-70.

130. Ellison, G., *The N-methyl-D-aspartate antagonists phencyclidine, ketamine and dizocilpine as both behavioral and anatomical models of the dementias.* Brain Res Brain Res Rev, 1995. **20**(2): p. 250-67.
131. Ramaswamy, P., N. Aditi Devi, K. Hurmath Fathima, and N. Dalavaikodihalli Nanjaiah, *Activation of NMDA receptor of glutamate influences MMP-2 activity and proliferation of glioma cells.* Neurol Sci, 2014. **35**(6): p. 823-9.
132. Kamaci, N., T. Emnacar, N. Karakas, G. Arikan, K. Tsutsui, and S. Isik, *Selective silencing of DNA topoisomerase IIbeta in human mesenchymal stem cells by siRNAs (small interfering RNAs).* Cell Biol Int Rep (2010), 2011. **18**(1): p. e00010.
133. Lutz, H., T.A. Nguyen, J. Joswig, K. Rau, and B. Laube, *NMDA Receptor Signaling Mediates cFos Expression via Top2beta-Induced DSBs in Glioblastoma Cells.* Cancers (Basel), 2019. **11**(3).
134. Yonaha, M., T. Chibazakura, S. Kitajima, and Y. Yasukochi, *Cell cycle-dependent regulation of RNA polymerase II basal transcription activity.* Nucleic Acids Res, 1995. **23**(20): p. 4050-4.
135. Bertoli, C., J.M. Skotheim, and R.A. de Bruin, *Control of cell cycle transcription during G1 and S phases.* Nat Rev Mol Cell Biol, 2013. **14**(8): p. 518-28.
136. Tanabe, K., Y. Ikegami, R. Ishida, and T. Andoh, *Inhibition of topoisomerase II by antitumor agents bis(2,6-dioxopiperazine) derivatives.* Cancer Res, 1991. **51**(18): p. 4903-8.
137. Xiong, J., L.I. Zhou, Y. Lim, M. Yang, Y.H. Zhu, Z.W. Li, D.L. Fu, and X.F. Zhou, *Mature brain-derived neurotrophic factor and its receptor TrkB are upregulated in human glioma tissues.* Oncol Lett, 2015. **10**(1): p. 223-227.
138. Hong, J.H., C.S. Chiang, J.R. Sun, H.R. Withers, and W.H. McBride, *Induction of c-fos and junB mRNA following in vivo brain irradiation.* Brain Res Mol Brain Res, 1997. **48**(2): p. 223-8.
139. Tsai, F.C. and T. Meyer, *Ca2+ pulses control local cycles of lamellipodia retraction and adhesion along the front of migrating cells.* Curr Biol, 2012. **22**(9): p. 837-42.
140. Komuro, H. and T. Kumada, *Ca2+ transients control CNS neuronal migration.* Cell Calcium, 2005. **37**(5): p. 387-93.
141. Hardingham, G.E., S. Chawla, C.M. Johnson, and H. Bading, *Distinct functions of nuclear and cytoplasmic calcium in the control of gene expression.* Nature, 1997. **385**(6613): p. 260-5.
142. Hardingham, G.E., F.J. Arnold, and H. Bading, *Nuclear calcium signaling controls CREB-mediated gene expression triggered by synaptic activity.* Nat Neurosci, 2001. **4**(3): p. 261-7.
143. Wang, H., S. Adhikari, B.E. Butler, T.K. Pandita, S. Mitra, and M.L. Hegde, *A Perspective on Chromosomal Double Strand Break Markers in Mammalian Cells.* Jacobs J Radiat Oncol, 2014. **1**(1).
144. Längle, A.G., *Ionotrope Glutamatrezeptoren als Targetstrukturen zur Modulation der Strahlenwirkung bei Glioblastomzellen* 2014.
145. Anggono, V. and R.L. Huganir, *Regulation of AMPA receptor trafficking and synaptic plasticity.* Curr Opin Neurobiol, 2012. **22**(3): p. 461-9.
146. Ye, X., Y. Zhang, Q. Xu, H. Zheng, X. Wu, J. Qiu, Z. Zhang, W. Wang, Y. Shao, and H.Q. Xing, *HIV-1 Tat inhibits EAAT-2 through AEG-1 upregulation in models of HIV-associated neurocognitive disorder.* Oncotarget, 2017. **8**(24): p. 39922-39934.
147. Mehta, A. and J.E. Haber, *Sources of DNA double-strand breaks and models of recombinational DNA repair.* Cold Spring Harb Perspect Biol, 2014. **6**(9): p. a016428.
148. Huang, K.C., H. Gao, E.F. Yamasaki, D.R. Grabowski, S. Liu, L.L. Shen, K.K. Chan, R. Ganapathi, and R.M. Snapka, *Topoisomerase II poisoning by ICRF-193.* J Biol Chem, 2001. **276**(48): p. 44488-94.
149. Perrin, D., B. van Hille, and B.T. Hill, *Differential sensitivities of recombinant human topoisomerase IIalpha and beta to various classes of topoisomerase II-interacting agents.* Biochem Pharmacol, 1998. **56**(4): p. 503-7.
150. Kenig, S., V. Faoro, E. Bourkoula, N. Podergajs, T. Ius, M. Vindigni, M. Skrap, T. Lah, D. Cesselli, P. Storici, and A. Vindigni, *Topoisomerase IIbeta mediates the resistance of glioblastoma stem cells to replication stress-inducing drugs.* Cancer Cell Int, 2016. **16**: p. 58.

151. Wegener, N., J. Nagel, R. Gross, C. Chambon, S. Greco, M. Pietraszek, A. Gravius, and W. Danysz, *Evaluation of brain pharmacokinetics of (+)MK-801 in relation to behaviour.* Neurosci Lett, 2011. **503**(1): p. 68-72.
152. Bonni, A., D.D. Ginty, H. Dudek, and M.E. Greenberg, *Serine 133-phosphorylated CREB induces transcription via a cooperative mechanism that may confer specificity to neurotrophin signals.* Mol Cell Neurosci, 1995. **6**(2): p. 168-83.
153. Velazquez, F.N., B.L. Caputto, and F.D. Boussin, *c-Fos importance for brain development.* Aging (Albany NY), 2015. **7**(12): p. 1028-9.
154. Dong, M., Y. Wu, Y. Fan, M. Xu, and J. Zhang, *c-fos modulates brain-derived neurotrophic factor mRNA expression in mouse hippocampal CA3 and dentate gyrus neurons.* Neurosci Lett, 2006. **400**(1-2): p. 177-80.
155. Lawn, S., N. Krishna, A. Pisklakova, X. Qu, D.A. Fenstermacher, M. Fournier, F.D. Vrionis, N. Tran, J.A. Chan, R.S. Kenchappa, and P.A. Forsyth, *Neurotrophin signaling via TrkB and TrkC receptors promotes the growth of brain tumor-initiating cells.* J Biol Chem, 2015. **290**(6): p. 3814-24.
156. Zheng, F., X. Zhou, C. Moon, and H. Wang, *Regulation of brain-derived neurotrophic factor expression in neurons.* Int J Physiol Pathophysiol Pharmacol, 2012. **4**(4): p. 188-200.
157. Dent, P., A. Yacoub, P.B. Fisher, M.P. Hagan, and S. Grant, *MAPK pathways in radiation responses.* Oncogene, 2003. **22**(37): p. 5885-96.
158. Son, Y., S. Kim, H.T. Chung, and H.O. Pae, *Reactive oxygen species in the activation of MAP kinases.* Methods Enzymol, 2013. **528**: p. 27-48.
159. Dent, P., D.B. Reardon, J.S. Park, G. Bowers, C. Logsdon, K. Valerie, and R. Schmidt-Ullrich, *Radiation-induced release of transforming growth factor alpha activates the epidermal growth factor receptor and mitogen-activated protein kinase pathway in carcinoma cells, leading to increased proliferation and protection from radiation-induced cell death.* Mol Biol Cell, 1999. **10**(8): p. 2493-506.
160. Chawla, S., G.E. Hardingham, D.R. Quinn, and H. Bading, *CBP: a signal-regulated transcriptional coactivator controlled by nuclear calcium and CaM kinase IV.* Science, 1998. **281**(5382): p. 1505-9.
161. Osheroff, N. and E.L. Zechiedrich, *Calcium-promoted DNA cleavage by eukaryotic topoisomerase II: trapping the covalent enzyme-DNA complex in an active form.* Biochemistry, 1987. **26**(14): p. 4303-9.
162. Oh, M.C., J.M. Kim, M. Safaee, G. Kaur, M.Z. Sun, R. Kaur, A. Celli, T.M. Mauro, and A.T. Parsa, *Overexpression of calcium-permeable glutamate receptors in glioblastoma derived brain tumor initiating cells.* PLoS One, 2012. **7**(10): p. e47846.
163. Sugaya, N., Y. Ogai, Y. Aikawa, Y. Yumoto, M. Takahama, M. Tanaka, A. Haraguchi, M. Umeno, and K. Ikeda, *A randomized controlled study of the effect of ifenprodil on alcohol use in patients with alcohol dependence.* Neuropsychopharmacol Rep, 2018. **38**(1): p. 9-17.
164. Kotajima-Murakami, H., A. Takano, Y. Ogai, S. Tsukamoto, M. Murakami, D. Funada, Y. Tanibuchi, H. Tachimori, K. Maruo, T. Sasaki, T. Matsumoto, and K. Ikeda, *Study of effects of ifenprodil in patients with methamphetamine dependence: Protocol for an exploratory, randomized, double-blind, placebo-controlled trial.* Neuropsychopharmacol Rep, 2019.

9. Figure and Table directory

10. List of Abbreviations

(+)-MK801	5R,10S)-(+)-5-methyl-10,11-dihydro-5H-dibenzo[a,d]cyclohepten-5,10-imine
ABD	Agonist binding domain
ADP	Adenosine diphosphate
AIF	Apoptosis inducing factor
AMPA	α-amino-3-hydroxy-5-methyl-4-isoxazolepropionic acid
AMPAR	α-amino-3-hydroxy-5-methyl-4-isoxazolepropionic acid receptor
ATD	Amino-terminal domain
ATP	Adenosine triphosphate
ATRX	ATP-dependent helicase
BCA	Bicinchoninic acid
BDNF	Brain derived neurotrophic factor
Bim	Bcl2-interacting mediator of cell death
CaMK	Ca^{2+}/calmodulin kinase
cAMP	Cyclic adenosine monophosphate
CBP	CREB-binding protein
CNS	Central nervous system
CREB	cAMP response element-binding protein
CTD	Carboxyl-terminal domain
Cyss	Cystine
DMEM	Dulbecco's Modified Eagle Medium
DMSO	Dimethyl sulfoxide
DNA	Deoxyribonucleic acid
DNA-PK	DNA-dependent protein kinase
DNA-PK_{cs}	Catalytic subunit of the DNA-dependent protein kinase
DSB	DNA double-strand break
DTT	Dithiothreitol
EAAT	Excitatory amino acid transporter
EC_{50}	Concentration for half maximal activation
EDTA	Ethylenediaminetetraacetic acid
EdU	5-ethynyl-2'-deoxyuridine
EGF	Epidermal growth factor
EGFR	Epidermal growth factor receptor
EGTA	Ethylene glycol-bis(β-aminoethyl ether)-N,N,N′,N′-tetraacetic acid
ER	Endoplasmic reticulum

ERG	Early response gene
ERK	Extracellular signal-regulated kinases
Fasl	Fas ligand
FCS	Fetal calf serum
FGF2	Fibroblast growth factor 2
FOXO	Forkhead box protein O
GBM	Glioblastoma multiforme
GDP	Guanosine diphosphate
GFP	Green fluorescent protein
GKAP	Guanylate kinase-associated protein
Glu	Glutamate
GluA	AMAPR subunit
GluN	NMDAR subunit
GluR	Glutamate receptor
Gly	Glycine
GSC	Glioma stem cells
GSH	Glutathione
GTP	Guanosine triphosphate
H	Hour
HEPES	4-(2-hydroxyethyl)-1-piperazineethanesulfonic acid
HRP	Horseradish peroxidase
ICRF193	4,4'-(1,2-Dimethyl-1,2-ethanediyl)bis-2,6-piperazinedione
IDH1	Isocitrate dehydrogenase 1
Ifenprodil	4-[2-(4-benzylpiperidin-1-yl)-1-hydroxypropyl]phenol
iGluR	Ionotropic glutamate-receptor
I_{max}	Maximal inducible current
IR	Ionizing radiation
Jacob	Juxtasynaptic attractor of caldendrin on dendritic boutons protein
kDa	Kilo Dalton
KG501	Naphthol AS-E phosphate
MAGUK	Membrane-associated guanylate kinases
Merbarone	5-(N-Phenylcarbamoyl)-2-thiobarbituric acid
mGluR	Metabotropic glutamate receptor
MGMT	O_6-methylguanine DNA methyltransferase
Min	Minute
mRNA	Messenger RNA

MWT	Mann-Whitney-Test
n.s.	not significant
NBQX	2,3-dihydroxy-6-nitro-7-sulfamoyl-benzo[f]quinoxaline
NHEJ	Non-homologues end joining
NMDA	N-Methyl-D-aspartate
NMDAR	N-Methyl-D-aspartate-receptor
NSC	Neural stem cell
NU7441	8-(4-Dibenzothienyl)-2-(4-morpholinyl)-4H-1-benzopyran-4-one
PARP	Poly(ADPribose)polymerase
PBS	Phosphate-buffered saline
PFA	Paraformaldehyde
PI3K	Phosphoinositide-3-kinase
PolII	DNA dependent RNA polymerase II
PVDF	Polyvinylidene fluoride
qPCR	Real-time quantitative PCR
RNA	Ribonucleic acid
RT	Room temperature
SAS	Sulfasalazine
SDS	Sodium dodecyl sulfate
Ser	Serine
siRNA	Small interfering RNA
TBS	Tris-buffered saline
TIC	Tumor initiating cell
TMB	3,3′,5,5′-Tetramethylbenzidin
TMD	Transmembrane domain
TMZ	Temozolomide
Top2	Topoisomerase II
Top2β	Topoisomerase IIβ
TORC	Transducer of regulated CREB activity
Tris	Tris(hydroxymethyl)aminomethane
TSS	Transcription start site
Txnip	Thioredoxin-interacting protein
Tyr	Tyrosine
WHO	World Health Organization

11. Curriculum vitae

Name: Henrik Lutz
Date of Birth: 06.11.1988
Place of Birth: Büdingen
Nationality: German

Education:

11/2014-03/2019:

Doctoral candidate at TU Darmstadt in the group of Prof. Dr. Bodo Laube, department of "Neurophysiology and Neurosensory Systems". Scholarship in the DFG funded Graduate school (GRK 1657) "Molecular and cellular responses of ionizing radiation" (2014-2018).

10/2012-09/2014:

Master of Science "Technische Biologie" at TU-Darmstadt

Thesis: "Charakterisierung der modulatorischen Effekte von Gephyrin und Collybistin auf inhibitorische ligandengeteuerte Ionenkanäle" in the group of Prof. Dr. Bodo Laube, department of "Neurophysiology and Neurosensory Systems"

10/2009 - 09/2012:

Bachelor of Science „Biologie" at TU-Darmstadt

Thesis: "Einfluss von Sterolen auf die CO_2-Permeabilität von Lipiddoppelmembranen" in the group of Prof. Dr. Ralf Kaldenhoff, department of "Applied Plant Sciences"

2008:

Abitur at Wolfgang-Ernst Gymnasium, Büdingen

Poster and Publications:

2019	Paper: "NMDA Receptor Signaling Mediates cFos Expression via Top2beta-Induced DSBs in Glioblastoma Cells" *Cancers (Basel)*
2015/2018	Poster presentation at the „Gesellschaft für Biologische Strahlenforschung e.V." annual conference in Dresden und Frankfurt am Main
2016	Poster presentation at the „Society for Neuroscience" annual conference in San Diego

12. Danksagung

Zuallererst möchte ich Prof. Dr. Bodo Laube dafür danken, dass er es mir ermöglicht hat ein so interessantes Thema zu erforschen und dafür, dass er mir die richtigen Anstöße gegeben hat, wenn ich mich in eine gedankliche Sackgasse manövriert hatte.

Ich danke Prof. Dr. Gerhard Thiel dafür, dass er sich als Zweigutachter für meine Dissertation zur Verfügung gestellt hat.

Außerdem möchte ich meinen Prüfern, Prof. Dr. Franz Rödel und Prof. Dr. Alexander Löwer danken.

Ich danke auch der DFG und dem GRK1657 für mein Stipendium und somit der Möglichkeit diese Dissertation zu erstellen.

Ich danke im besonderen Kiki, die mit mir die Täler des GRKs im Kleinwalsertal durchschritten hat und mir dabei half, mich so wenig verrückt als irgend möglich zu machen. Außerdem danke ich Basti, der obwohl seine eigene Promotion schon lange her ist, sich sehr gut in die Probleme eines Doktoranden einfühlen kann und mit einem offenen Ohr oft geholfen hat.

Ich danke außerdem Katja, Michi, Axel, Kai, Gabi, Max, Raj, Selina, Juliane und Kirsten, für eine unvergessliche Zeit in der AG Laube. Ich werde die lauten Gespräche am Mittagstisch genauso in Erinnerung behalten, wie das gefräßige Schweigen am Donnerstag. Es hat mir viel Spaß gemacht mit euch.

Ich bedanke mich bei meinen Freunden, die mich die letzten Monate fast nicht zu Gesicht bekommen haben. Ich bin schon gespannt, was alles so passiert ist in der Welt.

Ein besonderer Dank gilt meiner Familie. Meinen Eltern, die mich, wie es so schön heißt, immer unterstützt haben. Aber es stimmt und ich könnte nicht glücklicher darüber sein. Ich danke aber auch meinen Schwiegereltern, die auch unter meiner Arbeit gelitten und viele Stunden Kinderbetreuung geleistet haben, um mir Luft zum Schreiben zu geben.

Vielen Dank liebe Clara und Pauline, dass es euch gibt und es tut mir leid, wie wenig Zeit ich manchmal für euch beide hatte. Ihr seid mein unerschöpflicher Quell der Freude.

Zu aller Letzt und am allermeisten danke ich meiner Frau. Janina, ohne dich hätte ich diese Arbeit nicht schreiben können. Du hast dafür gesorgt, dass meine Welt in den letzten Monaten nicht ganz zusammengebrochen ist. Du hast mich aufgebaut, dich gekümmert und auch gelitten. Ich liebe dich.